Experimental study of the thermal and rheological behaviour of paraffin-in-water emulsions used as a secondary refrigerants

Virginia Vasile

N°d'ordre NNT : 2019LYSEI056

THESE de DOCTORAT DE L'UNIVERSITE DE LYON

opérée au sein de

INSA Lyon

en cotutelle internationale avec

Université POLITEHNICA de Bucarest

École Doctorale N° 162

Mécanique, Énergétique, Génie Civil, Acoustique (MEGA)

Spécialité de doctorat : Thermique et Énergétique

Soutenue publiquement le 26/07/2019, par :

Virginia VASILE

Experimental study of the thermal and rheological behaviour of paraffin-in-water emulsions used as a secondary refrigerants

Devant le jury composé de :

DARIE George	Professeur (Université POLITEHNICA de Bucarest)	Président
SIROUX Monica	Professeur (INSA Strasbourg)	Rapporteur
FISCHER Ludger J.	Professeur (Université de Lucerne)	Rapporteur
FRUNZULICA Rodica	Professeur (Université Technique de Construction Bucarest)	Examinateur
POPESCU Daniela	Professeur (Université Technique "Gheorghe Asachi " de Iasi)	Examinateur
BADEA Adrian	Professeur (Université POLITEHNICA de Bucarest)	Directeur de thèse
BONJOUR Jocelyn	Professeur (INSA Lyon)	Directeur de thèse
REVELLIN Rémi	Professeur (INSA Lyon)	Co-directeur de thèse
HABERSCHILL Philippe	Maître de Conférences HDR Émérite	Invité
NECULA Horia	Professeur (Université POLITEHNICA de Bucarest)	Invité

Département FEDORA – INSA Lyon - Ecoles Doctorales – Quinquennal 2016-2020

SIGLE	ECOLE DOCTORALE	NOM ET COORDONNEES DU RESPONSABLE
CHIMIE	**CHIMIE DE LYON** http://www.edchimie-lyon.fr Sec. : Renée EL MELHEM Bât. Blaise PASCAL, 3e étage secretariat@edchimie-lyon.fr INSA : R. GOURDON	M. Stéphane DANIELE Institut de recherches sur la catalyse et l'environnement de Lyon IRCELYON-UMR 5256 Equipe CDFA 2 Avenue Albert EINSTEIN 69 626 Villeurbanne CEDEX directeur@edchimie-lyon.fr
E.E.A.	**ÉLECTRONIQUE, ELECTROTECHNIQUE, AUTOMATIQUE** http://edeea.ec-lyon.fr Sec. : M.C. HAVGOUDOUKIAN ecole-doctorale.eea@ec-lyon.fr	M. Gérard SCORLETTI École Centrale de Lyon 36 Avenue Guy DE COLLONGUE 69 134 Ecully Tél : 04.72.18.60.97 Fax 04.78.43.37.17 gerard.scorletti@ec-lyon.fr
E2M2	**ÉVOLUTION, ÉCOSYSTÈME, MICROBIOLOGIE, MODELISATION** http://e2m2.universite-lyon.fr Sec. : Sylvie ROBERJOT Bât. Atrium, UCB Lyon 1 Tél : 04.72.44.83.62 INSA : H. CHARLES secretariat.e2m2@univ-lyon1.fr	M. Philippe NORMAND UMR 5557 Lab. d'Ecologie Microbienne Université Claude Bernard Lyon 1 Bâtiment Mendel 43, boulevard du 11 Novembre 1918 69 622 Villeurbanne CEDEX philippe.normand@univ-lyon1.fr
EDISS	**INTERDISCIPLINAIRE SCIENCES-SANTE** http://www.ediss-lyon.fr Sec. : Sylvie ROBERJOT Bât. Atrium, UCB Lyon 1 Tél : 04.72.44.83.62 INSA : M. LAGARDE secretariat.ediss@univ-lyon1.fr	Mme Emmanuelle CANET-SOULAS INSERM U1060, CarMeN lab, Univ. Lyon 1 Bâtiment IMBL 11 Avenue Jean CAPELLE INSA de Lyon 69 621 Villeurbanne Tél : 04.72.68.49.09 Fax : 04.72.68.49.16 emmanuelle.canet@univ-lyon1.fr
INFOMATHS	**INFORMATIQUE ET MATHEMATIQUES** http://edinfomaths.universite-lyon.fr Sec. : Renée EL MELHEM Bât. Blaise PASCAL, 3e étage Tél : 04.72.43.80.46 infomaths@univ-lyon1.fr	M. Luca ZAMBONI Bât. Braconnier 43 Boulevard du 11 novembre 1918 69 622 Villeurbanne CEDEX Tél : 04.26.23.45.52 zamboni@maths.univ-lyon1.fr
Matériaux	**MATÉRIAUX DE LYON** http://ed34.universite-lyon.fr Sec. : Stéphanie CAUVIN Tél : 04.72.43.71.70 Bât. Direction ed.materiaux@insa-lyon.fr	M. Jean-Yves BUFFIÈRE INSA de Lyon MATEIS - Bât. Saint-Exupéry 7 Avenue Jean CAPELLE 69 621 Villeurbanne CEDEX Tél : 04.72.43.71.70 Fax : 04.72.43.85.28 jean-yves.buffiere@insa-lyon.fr
MEGA	**MÉCANIQUE, ÉNERGÉTIQUE, GENIE CIVIL, ACOUSTIQUE** http://edmega.universite-lyon.fr Sec. : Stéphanie CAUVIN Tél : 04.72.43.71.70 Bât. Direction mega@insa-lyon.fr	M. Jocelyn BONJOUR INSA de Lyon Laboratoire CETHIL Bâtiment Sadi-Carnot 9, rue de la Physique 69 621 Villeurbanne CEDEX jocelyn.bonjour@insa-lyon.fr
ScSo	**ScSo*** http://ed483.univ-lyon2.fr Sec. : Véronique GUICHARD INSA : J.Y. TOUSSAINT Tél : 04.78.69.72.76 veronique.cervantes@univ-lyon2.fr	M. Christian MONTES Université Lyon 2 86 Rue Pasteur 69 365 Lyon CEDEX 07 christian.montes@univ-lyon2.fr

*ScSo : Histoire, Géographie, Aménagement, Urbanisme, Archéologie, Science politique, Sociologie, Anthropologie

« The important thing is to not stop questioning. Curiosity has its own reason for existing. »

Albert EINSTEIN

Acknowledgements

"No duty is more urgent than that of returning thanks." – James Allen

I discovered during this doctoral thesis what passion means and I could not have done it without the people who were close to me. Undertaking this PhD work has been a truly life-changing experience for me and I would like to express my gratitude to all those who were there for me.

This PhD Thesis was carried out at the Centre for Energy and Thermal Sciences of Lyon (CETHIL UMR5008) and Doctoral School of the Faculty of Power Engineering within University POLITEHNICA of Bucharest, under the direction of Professor Jocelyn Bonjour, Professor Remi Revellin from CETHIL and Professor Adrian Badea, Professor Horia Necula from UPB. All the traineeships performed in France were financed by the French Institute in Bucharest through a grant for which I am very grateful.

I would like to first start with the two people that made this possible. It is a great pleasure for me to thank my supervisors Professor Adrian Badea, he is the person who persuaded me in doing a PhD. I feel the need to mention that I was not sure I was capable of such a work until Professor Adrian Badea told me that everything is possible if we just want it to be.

I have no words to thank Professor Phillippe Haberschill, the person who presented me with the nebula of this field of research, who introduced me to this world and who passed to me all his knowledge. I thank him for all the answers, for all the teachings and specifically for all the french-style expressions.

For their wise advice and support they have provided me throughout these years, I warmly thank my supervisors Professor Jocelyn Bonjour and Professor Rémi Revellin. I have most appreciated the trust and autonomy that they gave me during this work. They gave me the motivation that I needed to want more, gain more and do more.

Jocelyn, I greatly appreciate the help for the administration problems encountered, for making everything look easy. I would like to thank you deeply for the rigour, the support, the feedback, understanding, time sparing and energy invested in working with me, for always being there when in need.

Remi I gratefully thank you for the trust, the advices and motivation you gave me. You were always so helpful and provided me with your assistance without which this work would not have been possible.

My sincere gratitude goes to my forever supervisor, professor Horia Necula. I cannot thank you enough for your mentorship over the years. You have been such an integral part of my career. I hope one day to inspire others as you have inspired me. Accept my heartfelt gratitude for your time, support, and patience.

I greatly appreciate the support received through the collaborative work undertaken with the Lucerne University of Applied Sciences and Arts in Switzerland. I would like to share my deeply thanks to the entire team from The Lucerne University, starting with Fischer Ludger, Silvan von Arx and Worlitschek Jörg for their time investment and knowledge sharing.

Special mention goes to all the administrative and technical staff of the laboratory from CETHIL to whom the success of this project owes a lot. I thank the first of all the team (old and current) of the secretary office. I think more particularly in Florence former Administrative Manager, Marilyne, Christine and Silas. A big thank you also goes to the workshop team, notably to Christophe, Nicolas, Joël and Xavier for the help and realization of parts intended for the experimental setup.

I would of course like to thank my doctoral and post-doctoral colleagues thanks to whom the working atmosphere was extremely pleasant at CETHIL. Many thanks to all my romanian colleagues at the Power Engineering Faculty and University POLITEHNICA of Bucharest for encouraging me, for listening to me and for being there when in need for help. I especially thank Professor Sanda Carmen Georgescu for the time spent with me, for the energy, for always encouraging me during this work. Special thanks also go to Professor Corneliu Balan for the careful guidance throughout my first rheology measurements.

Sincere appreciations and thanks go to Professor George Darie for all the support, guidance, trust and interest in my success.

Finally, I want to address a few words to my relatives, my family and my friends.

I would especially like to express my gratitude to my friends who have always been supportive and listened to me when in difficult moments, without complaining. I am very grateful for the support of my family; I would have never finished this PhD thesis without their encouragements and kind words.

I express my deep sense love to my mother *Vasile Nicoleta* and my father *Vasile Tudorache* for their infinite love, understanding, patience, moral support and encouragement without whom, I would have never found the courage to overcome all the difficulties during these past years. They were my everyday strength and I will forever be really indebted to them.

I shall conclude these thanks by dedicating this manuscript to my special person, my aunt *Vasile Elena*. Thank you for being a role model and loving me no matter what. I wish I could repay you for everything you have done for me, but there is no possible way.

I will never forget your almost everyday morning salute *« Did you work on your PhD yesterday? »*

Abstract

A phase change material emulsion (PCME) is a fluid consisting of an emulsion of a phase change material (PCM), such as paraffin, dispersed in a carrier fluid (continuous phase), often water of an aqueous solution of surfactant. PCMEs can be considered as potential high performance thermal fluids (used as secondary refrigerants or as heat transport fluids) owing to their latent heat involved in the fusion of crystallization of the PCM.

This thesis reports experimental results concerning the thermo-rheological behavior of different versions of a PCME (30%wt. paraffin concentration in various aqueous solutions of surfactant) over the temperature range [0 – 20 °C]. The thermophysical properties of the PCMEs were determined. Then, an experimental study of forced convection heat transfer during laminar flow was carried out. The convective heat transfer coefficient of the PCMEs during cooling was determined in an experimental configuration mocking up applications in plate heat exchangers. The configuration mainly consists of two 1 m long rectangular channels (80 x 6 mm^2). Correlations were developed for the prediction of the (local and overall) heat transfers coefficients, based on the Nussel, Reynolds and Prandtl numbers. A specific test bench was also used to analyze the rheological behavior of the PCMEs. Tests were carried out using a viscometer at different temperatures. The stability of the emulsion was examined under various thermo-mechanical loads. Experiments revealed a pseudoplastic behavior for all tested versions of the PCME.

All these results show that PCMEs are an attractive candidate for their applications in the field of air conditioning.

Keywords: *Paraffin emulsion; Laminar flow; Heat transfer; Rheology, Correlation; Thermophysical properties.*

Résumé

Une émulsion à changement de phase (PCME: phase-change matériel émulsion) est un fluide consistant en une émulsion d'un matériau à changement de phase (PCM, phase change matériel), comme de la paraffine, dispersé dans un fluide porteur (phase continue), souvent de l'eau ou une solution aqueuse de surfactant. Les PCME peuvent être envisagés comme fluides à haute performance thermique (frigoporteurs ou caloporteurs) en raison de leur potentiel de transport de chaleur latente (cristallisation ou fusion du PCM).

Cette thèse présente des résultats expérimentaux concernant le comportement thermo-rhéologique des différentes versions de PCME (émulsions de paraffine dans différentes solutions aqueuses de surfactant, avec une concentration massique en paraffine égale à 30 %) sur une plage de température de 0 - 20 °C. Les propriétés thermophysiques des émulsions ont été déterminées. Ensuite, une étude expérimentale du transfert de chaleur par convection forcée laminaire a été effectuée. Le coefficient de transfert de chaleur convectif de l'émulsion pendant le refroidissement a été déterminé dans une configuration expérimentale proche de celle pouvant être rencontrée dans des échangeurs thermiques à plaques. La configuration se compose principalement de deux canaux rectangulaires (80 x 6 mm²) de longueurs égale à 1 m. Des corrélations utiles pour évaluer les coefficients d'échange thermique (locaux ou globaux) ont été établies entre les nombres de Nusselt, de Reynolds et de Prandtl. Un banc d'essais spécifique a également été utilisé pour analyser le comportement rhéologique des PCME. Des essais ont été effectués à l'aide d'un viscosimètre à différentes températures. La stabilité des émulsions a été examinée sous diverses charges thermomécaniques. Les expériences ont révélé un comportement rheofluidisant.

L'ensemble de ces résultats montre que les PCME sont des candidats prometteurs pour les applications à la climatisation.

Mots-clés : *Émulsion de paraffine ; Écoulement laminaire ; Transfert de chaleur ; Rhéologie ; Corrélation ; Propriétés thermophysiques.*

Nomenclature

Latin letters

a	width of the channel	m
	thermal diffusivity	$m^2.s^{-1}$
A	surface	m^2
b	channel height	m
c_m	mass fraction of particles	
c_p	specific heat capacity at constant pressure	$J.kg^{-1}.K^{-1}$
d	diameter of the droplet	m
D	diameter	m
D_h	hydraulic diameter	m
e	tickness of the plate	m
f	friction coefficient	
g	gravitational acceleration	$m.s^{-2}$
G	Gibb's free energy	$J.mol^{-1}$
h	specific enthalpy	$J.kg^{-1}$
	convective heat transfer coefficient	$W.m^{-2}.K^{-1}$
K	consistency coefficient	$Pa.s^n$
L	length	m
L^*	dimensionless length	
m	mass	kg
$\dot{m}$	mass flow	$kg.s^{-1}$
n	degree of the non-Newtonian behaviour	
p	pressure	Pa
$\dot{Q}$	heat transfer rate	W
r	radius of a droplet	m
S	heat transfer area	m^2
t	time	s
T	temperature	K
u	velocity	$m.s^{-1}$
V	separation speed	$m.s^{-1}$
x	axial position	m
x*	dimensionless axial position	
X	weight fraction	%

Greek letters

φ	heat flux	$W.m^{-2}$
$\dot{\gamma}$	shear rate	s^{-1}
λ	thermal conductivity	$W.m^{-1}.K^{-1}$
μ	dynamic viscosity	Pa.s
ρ	density	$kg.m^{-3}$
τ	shear stress	Pa
τ_o	minimal shear stress	Pa
Δh	total heat capacity	$J.K^{-1}$
Δp	pressure loss	Pa
ΔH	enthalpy	J

ΔT	temperature difference	K

Dimensionless numbers

Gz	Graetz number	$Gz = \frac{D_h Pe_{D_h}}{x}$
J	Colburn number	$J = \frac{Nu}{\mathrm{Re}^{1/3}}$
Nu	Nusselt number	$Nu = \frac{hD_h}{\lambda}$
Pe	Peclet number	$Pe = \mathrm{RePr}$
Re	Reynolds number	$\mathrm{Re} = \frac{\rho u_d D_h}{\mu}$
Ste	Stefan number	$Ste = \frac{c_p \Delta T}{\Delta h}$

Non-dimensional numbers

H	$H = \frac{h_{PCME}}{h_w}$
N	$N = \frac{NTU_{PCME}}{NTU_w}$

Abbreviations

HLB	Hydrophile-Lipophile Balance
CMC	Critical micelle concentration
EIP	Emulsion Inversion Point
LFTF	Latent functional thermal fluids
MPCS	Microencapsulated phase change slurry
O/O	oil-in-oil
O/W	oil-in-water
PCM	Phase Change Material
PCS	Phase Change Slurry
PIT	Phase Inversion Temperature
V1	Version 1
V2	Version 2
V3	Version 3
W/O	water-in-oil

Lower Indices

app	apparent
c	continuous phase
crit	critical
e	emulsion
f	fusion
m	melting
PCM	Phase Change Material
PCME	phase change material emulsion
w	Wall

Contents

List of Figures

List of Tables

General Introduction

The International Energy Agency (IEA) published in 2018 the World Energy Outlook (WEO) 2018, a report which presents the evolution of all energy sectors and their projections until 2040.

According to the New Policies Scenario, the global energy demand will increase by more than a quarter to 2040, mostly coming from developing economies led by India. Around 2000, more than 40 % of the global energy demand was assigned to Europe and North America. Developing countries in Asia accounted only for 20 %. According to IEA, by 2040, the world is going to witness a profound shift in energy consumption. Because of the major energy trade flows absorbed by Asia from across the Middle East, Russia, Canada, Brazil and United States, the global energy is suffering changes in different ways.

Even though overall global consumption remains flat with declines in China, Europe and North America offset by rises in India and Southeast Asia, still requires additional measures to assure the full potential of energy supply in respect to climate goals. Worldwide, energy related problems, power efficiency, sustainable development and climate changes are closely linked.

In this context, on 28 November 2018, the European Commission presented a strategic long-term vision for climate-neutral economy by 2050 – A Clean Planet for All. The goal of this strategy is to find realistic technological solutions, to empower citizens and to connect industrial sectors, finance sectors and research sectors to a common vision, a climate –neutral future. Seven strategic areas for the long term strategy to achieving a climate neutral economy are defined: energy efficiency; deployment of renewables; clean, safe and connected mobility, competitive industry and circular economy, infrastructure and interconnections, bio-economy and natural carbon sinks, carbon capture and storage to address remaining emissions. The long-term vision is in accordance with all EU policies and in line with the objective of the Paris Agreement, to keep the global temperature increase below 2°C and pursue efforts to keep it to 1.5°C. The Montreal Protocol on substances that deplete the ozone layer (coolants fridges, CFCS) was agreed in 1987. The objective of the protocol was to reduce the production and consumption of ozone depleting substances. Furthermore, in 2016, the second most significant landmark agreement on the environment, the Kigali Amendment was signed by 196 countries. This treaty is focusing on greenhouse gas reduction and climate change by downsizing hydrofluorocarbons (HFCs).

In this general context of energy efficiency for air conditioning, TES (thermal energy storage) is often viewed as a promising solution. But beyond energy density, the ability to deliver a high power is crucial. Phase Change Slurries (PCS) are viewed as an emerging technology in the field of comfort cooling having the ability to the deliver this power. When thermal power comes to high performance fluids, e.g. PCSs, the power delivery results in the need of high heat transfer coefficients. Often the heat transfer coefficients are limited by the thermophysical properties of the PCSs. Phase Change Material Emulsions (PCMEs) became a subject of research because of their interest for comfort cooling applications as they perfectly fit with the required range of temperatures (0-20°C) owing to the use of paraffin. In addition, this type of fluid is specifically studied, because paraffin is chemically inert and stable and considered safe and reliable (Sharma *et al*., 2009). Furthermore, PCMEs, compared with other fluids show significant advantages such as a high phase change enthalpy and no capsule for the paraffin particles, which makes them cheaper and easy to produce.

The paraffin/water emulsion is a system of two immiscible liquid phases in which small particles of paraffin are distributed in water and maintained in dispersion by a surfactant.

The results of Roy and Avanic (1997) showed that the heat transfer characteristics for PCMEs are similar to those of microencapsulated phase change slurries. A second conclusion was that the average heat transfer coefficient does not depend much on the paraffin concentration. Zhao *et al.* (2001) studied an oil-in-water (O/W) emulsion in a circular tube and showed that Nusselt numbers for an emulsion with 2 different paraffin concentrations had almost the same values. The convective heat transfer coefficients were increased by phase change but not affected by the concentration. Zhao *et al*. (2002) continued the work on emulsions but in coiled tubes and further showed that for the same concentration in paraffin, the Nusselt number of the emulsions is higher than that of water.

Up to now, a limited amount of work (Huang *et al.*, 2009; Huang *et al*., 2010; Youssef *et al.*, 2013; Shao *et al*., 2016; Delgado *et al.*, 2015; Kawanami et *al.*, 2016) has been conducted on the use of emulsions in air conditioning systems because of practical difficulties such as high viscosity and instability problems during the cooling process.

With continuous research on PCMEs (Huang and Petermann, 2015; Morimoto *et al.*, 2016; Zhang et al., 2016; Shao *et al.*, 2015), progress has been made but the majority of the studies in the literature are focused on the thermophysical properties and phase transition temperature while the studies on the heat transfer remain scarce.

The aim of the present thesis is to report on a study of a paraffin/water emulsion, especially its thermophysical properties, as well as its thermo-rheological behaviour. This PCME was developed for comfort cooling applications. The objectives of this thesis are set out in the following section.

The working methodology and the thesis structure are summarized in the figure below.

There are five main blocks:

1. State of the art on two-phase secondary refrigerants
2. Methods, instruments and experimental setup
3. Results and discussions
4. Design guidelines
5. Conclusions and perspectives.

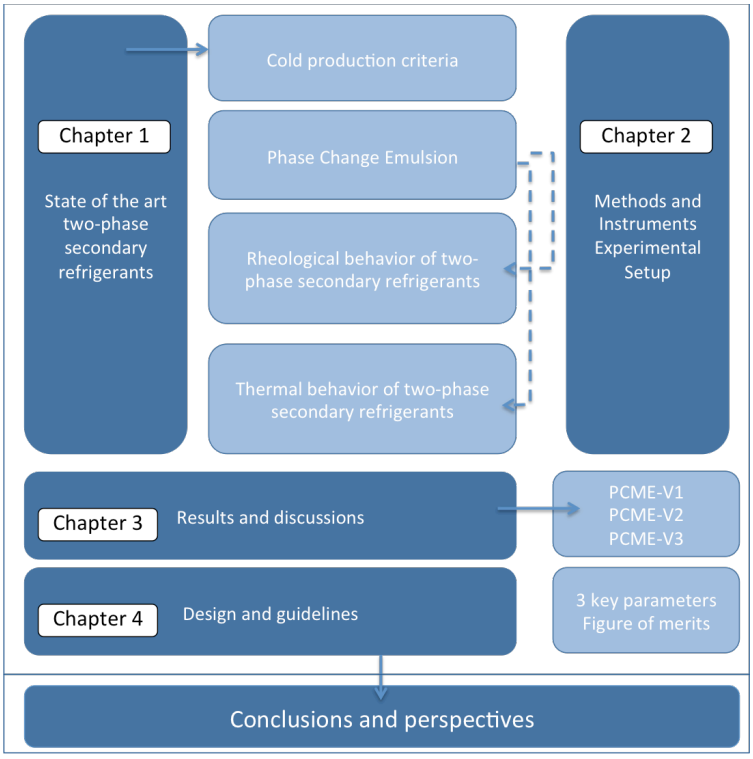

Methodology and thesis structure

The specific objectives of the present thesis are presented below:

1. Analysing of the literature about two-phase secondary refrigerants with focus on Phase Change Material Emulsions.

- cold production systems and two-phase secondary refrigerants;

- composition and manufacturing process of PCMEs;

- main characteristics of PCMEs;

- thermophysical properties;

- rheological behaviour;

- thermal behaviour.

2. Investigating the thermophysical properties of the PCMEs with different surfactant concentrations.

3. Investigating the subcooling degree during phase change for the PCMEs.

4. Studying the rheological behaviour and establish the impact of the concentration in surfactant over the rheological behaviour of the PCMEs.

5. Providing a thorough analysis on the heat transfer of the PCMEs during cooling in a rectangular channel during laminar flow.

6. Establishing correlations for the dimensionless Nusselt number and comparing with those already existing in the literature for Phase Change Slurries

Framework of the thesis

The development of this thesis is linked to a grant for Research awarded by the French Institute of Bucharest. This thesis comes within the research line into Phase Change Slurries carried out by CETHIL - National Institute of Applied Sciences of Lyon (INSA Lyon) and Energy Production and Use Department - Faculty of Power Engineering (University POLITEHNICA of Bucharest). This research line was initiated in 2002 with the doctoral thesis of Dr. Hélène Demasles, continued in 2008 with the doctoral thesis of Dr. Constantin Ionescu, who contributed to the subject of stabilized ice slurries in both institutions. Dr. Najib Boujaddaini investigated stabilized paraffin slurries, to push further the topic in 2013.

With the main focus on the development of the research topic, additional to the experimental work within UPB and INSA Lyon, the Ph.D. candidate collaborated with Lucerne University of Applied Sciences and Arts from Switzerland. The most relevant results

of this thesis have been made public in international scientific journals and in national and international scientific conferences.

CHAPTER I

Literature review: refrigeration and two phase-secondary refrigerants

The purpose of this chapter is to present a review on cold production systems and the different types of fluids used in these systems. The bibliography will then focus on paraffin emulsions, their composition, their manufacturing process, and their thermophysical properties. Although it is a new technology, the literature volume starts to be significant. This chapter will focus only on the necessary information, relevant to the results presented in this thesis.

I.1 Refrigeration production criteria

General information on refrigeration production will be succinctly presented using single phase secondary refrigerants and two-phase secondary refrigerants (Section I.1.1), then Phase Change Material Emulsions will be introduced (Section I.1.2) followed by the rheological characteristics of the two-phase secondary refrigerants (Section I.1.3) and the thermal characteristics of the two-phase secondary refrigerants (Section I.1.4).

I.1.1 Single phase secondary refrigerants and two-phase secondary refrigerants

Starting the year 2030, CFC, HCFC and HFC refrigerant gases will be completely banned from being produced. Fluids such as propane, butane, or ammonia, for which problems of intoxication, safety and nuisance to the environment still exist, will replace them.

Alternative solutions have been developed in order to reduce the use of these types of fluids, which are very promising, as they reconcile the reduction of the refrigerant load in the installations and obtaining attractive energy performances. Some of the alternative solution to the exclusive use of refrigerants for the production and distribution of cold is to decouple the production of cold from its distribution. Thus, the concept of secondary refrigeration system was developed.

The operation of a secondary refrigeration system is illustrated in Fig I-1. The difference between a primary refrigeration system and a secondary refrigeration system can be observed. The refrigerant charge is significantly reduced for the secondary refrigerant system.

Using secondary refrigeration systems, which presents a number of advantages, among which the most important are: the amount of refrigerant can be kept at a minimum and the risk of leakage of primary refrigerant is decreased. Beyond these advantages, other benefits of indirect refrigerant systems can be mentioned, such as:

- a reduced size of the system;
- a possibility of thermal energy storage;
- a flexibility of the system, which makes it extremely attractive for same production processes;
- fewer legally mandatory maintenance actions for the primary cooling circuits which are smaller in this case;

- no need to transport the refrigerant over a long distance is avoided, as the secondary fluid can be easily carried away from the system.

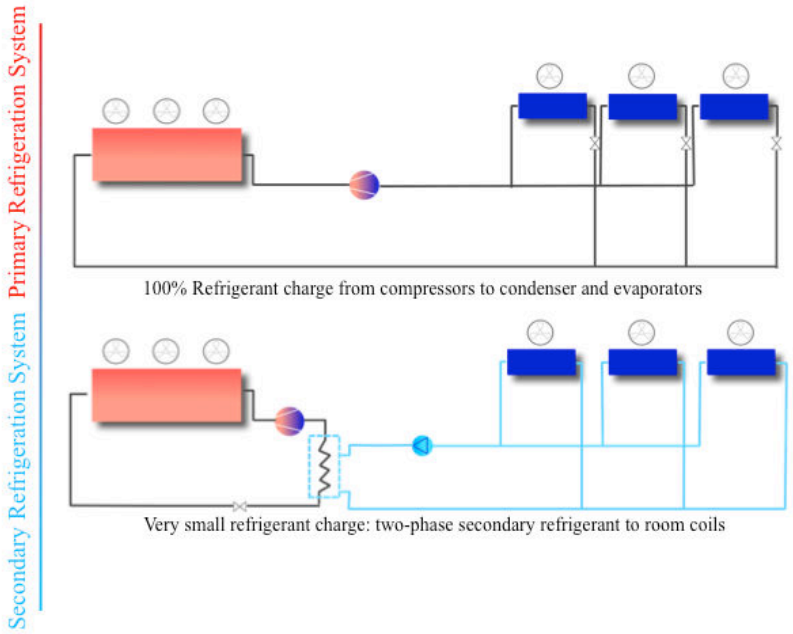

Figure I-1 Secondary refrigerant system

It is especially noteworthy that the addition of a cold storage exists and participates in the reduction of the refrigerant charge and therefore the installed power. Unfortunately, using this type of system for small-scale applications. It may become expensive due to the complexity of the system (Mellari, 2012). Apart from technical issues like aging of the secondary refrigerant and corrosion, the evaporators and additional circulation pumps generate additional investment and operation costs.

The selection of the secondary refrigerant is a critical issue, because depending on the choice, the additional costs caused by the evaporators and the circulation pumps can be reduced. Thus, the choice of the secondary refrigerants is based on several criteria including the following (Schroder and Gawron, 1981):

- a temperature ranges suitable for the desired application;
- good thermal physical properties that allow a high volume capacity of transport;
- good heat transfer coefficients (for a small temperature difference in heat exchangers);
- low pressure drop to limit the energy consumption of pumps;
- no environmental toxicity and flammability;
- good chemical stability and lack of ability to corrosion;

- a reasonable cost;
- safety.

The refrigerants used in secondary cooling systems are divided primarily into two large families: the single-phase refrigerants and the two-phase refrigerants.

I.1.1.1 Single-phase secondary refrigerants

The single-phase secondary refrigerants are the most commonly used in the industrial applications because they are better controlled, especially in terms of flows and heat balances, and they are very well developed. This type of fluid stores and transfers energy exclusively through sensible heat, which simplifies the design and operation of the systems in which it is present. The volumetric capacity of energy transferring of a single-phase secondary refrigerant depends on the specific heat and density. The higher these two values the higher the ability of the fluid to convey energy.

Nevertheless, the temperature variation of a single-phase secondary refrigerant is limited. Therefore, in order to transport a large amount of energy, the pipes are often of substantial size.

These fluids are generally mixtures with water with an adjuvant that lowers the crystallization of the mixture. Table 1 presents a number of different single-phase secondary refrigerants. It can be observed that water has a heat storage capacity far superior to other fluids presented, thus the interest in its most common use.

Aqueous solutions are often used because they can lower the freezing temperature depending on the solute concentration, and because they often do not present any character of toxicity or flammability. The most frequently used solutes are alcohols and salts.

Table 1 Single-phase secondary refrigerant characteristic, (Fournaison and Guilpart, 2000)

Fluid	Melting temp. [°C]	Boiling temp. [°C]	Thermal capacity $\rho \cdot Cp$ $[kJ \cdot m^{-3} \cdot K]$	Dynamic viscosity μ $[Pa \cdot s]$	Thermal conductivity λ $[W \cdot m^{-1} \cdot K^{-1}]$
Water	0	100	4168	$1x10^{-3}$	0,604
Acetone	-94.9	56.1	1762	$1.32x10^{-3}$	0.18 (at 20°C)
Ethanol	-114.5	78.3	1779	$1.19 \cdot x0^{-3}$	0.18 (at 20°C)
Methanol	-98	64.7	1884	$0.58x10^{-3}$	0.21 (at 20°C)
Propanol	-126.1	97.7	1779	$0.224\,x10^{-3}$	0.17 (at 20°C)
Trichloro Ethylene	-86.4	87.3	1369	$0.62x10^{-3}$	0.12 (at 0°C)
Dichloromethane	-96	40	1507	$0.44x10^{-3}$	0.155 (at 0°C)
n-pentane	-129.8	36.1	1428	$0.196x10^{-3}$ (at 36°C)	0.132 (at 20°C)
iso-pentane	-159.9	27.8	1403	$0.21x10^{-3}$ (at 28°C)	0.103 (at 20°C)
n-hexane	-95.3	68.7	1465	$0.202x10^{-3}$ (at 68°C)	0.139 (at 0°C)
n-heptane	-90.6	98.5	1578	$0.201x10^{-3}$ (at 98°C)	0.139 (at 0°C)
Glycol+water					(at 20°C)
12 wt.% EG	-5	>100°C	4081	$1.37x10^{-3}$	0.54
35 wt.% EG	-21		3809	$2.45x10^{-3}$	0.46
46 wt.% EG	-33		3600	$3.43x10^{-3}$	0.43
Solution water+ $CaCl_2$					(at °C)
10 wt.%	-6	>100°C	3893	$1.28x10^{-3}$	0.553
20 wt.%	-17.4		3650	$1.9x10^{-3}$	0.542
28,4 wt.%	-43.6		3529	$3.14x10^{-3}$	0.528

I.1.1.2 Two-phase secondary refrigerant

It has been 20 years since a new technique solution was proposed to use phase change materials in refrigeration systems, heat exchangers and thermal control systems. However, over the last 10 years a greater progress in its study has been achieved.

Two-phase secondary refrigerants are capable of providing higher energy density than single-phase secondary refrigerants, and hence a substantial reduction in the size of the facility, including the size of pipes. One of two-phase secondary refrigerants particularity is that they present two phases: solid-liquid or liquid-vapour.

The main advantages of *two-phase liquid-vapour secondary refrigerant* fluids can be listed, i.e. very high phase change enthalpy (for water at 0°C under 0.0612 bar, vaporization enthalpy is 2500 $kJ.kg^{-1}$ while the melting enthalpy is 335 $kJ.kg^{-1}$at 0°C), a constant temperature delivered to the user during the phase change and satisfactory heat transfer coefficients during the evaporation and condensation.

The first major disadvantage is related to the large volume occupied by the gaseous phase, which poses problems of storage and pipe sizes. For example, in the case of water the ratio of specific volumes between the gas phase and the liquid phase is of the order of 1600. The second major disadvantage is associated to the risk of cavitation when the secondary refrigerant in the gaseous state does not condense completely. Currently, CO_2 is the most common for cold transportation as two-phase secondary refrigerant. Even though the CO_2 provides a constant temperature, high heat exchange coefficients, a low viscosity and a low cost, various practical experiments show a number of technical disadvantages (cavitation phenomena in the pumps, sealing of the pressurized system) that limit the use of this fluid.

A *two-phase solid-liquid secondary refrigerant* is a binary system, which consists of a carrier fluid; mostly water, as the continuous phase and a Phase Change Material (PCM) as the dispersed phase. It is mostly known as Phase Change Slurry (PCS). Phase Change Slurries store and transfer energy by using the latent heat capacity of the PCM as well as the sensible heat capacity of the carrier fluid and that of the PCM.

Several types of PCSs have been studied over the years, as it follows:

- pure solutions, such as ice slurry, the most widely known and used;
- mixtures, as aqueous salt solutions (brines liquids) with ice or aqueous solutions of organic compounds (water-ethanol);

- slurries of reacting chemical compounds, for example the hydrates and chlorates of fluorinated compounds (hydration reaction of organic compounds);
- microcapsules of aqueous gel
- emulsions, mixture of water and paraffin, tetradecane, etc.

Phase Change Slurries will be detailed in the following paragraphs. We will approach the advantages of their use in the transport and storage of the cold, and we will mention the different types of PCSs while emphasizing the one that is at the heart of the present work.

I.1.1.3 Benefits of two-phase secondary refrigerants

The main advantages of two-phase secondary refrigerants in comparison to single-phase secondary refrigerants are:

- high heat transfer rates due to the large surface to volume ratio of the PCM;
- high energy density, which greatly reduces the conveyed flow and consequently the diameter of pipes and power of the pump;
- constant temperature at any point of the cooling distribution network, which guarantees the homogeneity of the temperature;
- high heat transfer coefficients, which reduce the heat exchange surface and optimize the production systems;
- the possibility of implementing thermal energy storage.

Throughout the last 10 years, researchers have proposed various such fluids. The literature is rich in information related to their use both as a medium for transporting and storing cold energy.

These two-phase fluids are also known as latent functional thermal fluids (LFTF) (Inaba, 2000). The most common of them, which are likely to be used in a secondary refrigerant system (Fournaison *et al.*, 2004) are the ice slurries, hydrate slurries, microencapsulated phase change slurries and phase change material emulsions.

Ice slurry was the subject of laborious research, the literature being very rich in information about its fundamental characteristics and practical deployment. Even though it represents the most straightforward choice as two-phase secondary refrigerant, because of the constraints related to the ice generator and ice concentration controller, the practical application of this fluid exists but remains still limited.

Microencapsulated phase change slurry (MPCS) and semi-clathrate hydrate slurry (SCH) are among the newest fluids. These LFTF present potential to be used in the secondary refrigeration and air conditioning systems. Their advantages over ice slurry are: a phase change temperature range suitable to air conditioning system, i.e. 5–12 °C, lower pressure losses for the same mass flow rate, a better adaptation to the pipes flow in term of risk of clogging and a better energy efficiency of the refrigerating system because of higher phase change temperature, (Zhang, 2010).

In practical comfort cooling applications where the temperature range is known to be 0-20°C, there are mainly two types of PCSs: ice slurries and hydrate slurries. In comparison to chilled water, the ice slurry has a cooling capacity 6 times higher (Ure, 2000), but the operation temperature must be lowered under 0°C in order to obtain crystallization. Regarding hydrate slurries, JFE Engineering Corporation managed to develop a mixture of an aqueous solution with particles of tetra-n-butyl ammonium bromide (TBAB) that yield phase transition within 5-12°C, which is over the usual temperature difference of chilled water in air conditioning. Anyway, since the comfort cooling applications demands on safety are higher, TBAB should be managed carefully, being a hazardous material and extremely flammable (Huang *et al.*, 2010).

Recently, researchers started paying more and more attention to the PCSs based on paraffin as PCM that can be easily applied in comfort cooling applications. There are three types of two-phase secondary refrigerant based on paraffin that can be found in the literature (Huang *et al.*, 2010):

- shape-stabilized paraffin in water suspensions (a cross-linked structure holds in paraffin suspended in water);
- microencapsulated paraffin in water suspensions (paraffin droplets are encapsulated in a film of polymethyl methacrylate and in suspension in water);
- paraffin in water emulsions (small droplets of paraffin are dispersed in water).

The main barrier affecting the use of the first two dispersions is related to the additional costs generated by the supporting or coating materials. Furthermore, this capsulation shell or film engenders an increase in the viscosity and the heat transfer resistance.

I.2 Phase Change Material Emulsions (PCMEs)

One of the newest two-phase secondary refrigerants studied more and more in the last 5 years are paraffin emulsions. This section will be introducing the reader the notion of PCME, their composition, thermophysical properties and all additional information found in the literature.

I.2.1 Classification of PCMEs

An emulsion can be defined as a colloid dispersion. Colloid dispersions are a two-phase systems consisting of a dispersed phase and a continuous phase (Mollet and Grubenmann, 2000). Therefore, an emulsion is a mixture of two immiscible liquids; more precisely, it consists in small droplets of one liquid representing the dispersed phase and a carrier fluid that is the continuous phase. Since the two main components are immiscible, a surfactant is added in order to stabilize the emulsion.

Emulsions can be classified depending on the size of the droplets (Table 2). The size of the droplets usually affects their stability.

Table 2 Classification of PCMEs depending on the droplet size, Allouche (2013)

Type	Droplet size	Characteristics
Micro-emulsion	10-100 nm	Thermodynamically stable behaviour
Mini-emulsion	100-1000 nm	Thermodynamically unstable behaviour
Macro-emulsion	Over 1µm	Thermodynamically unstable behaviour

A second classification can be done depending on the type of the dispersed phase and carrier fluid as it follows:

- oil-in-water (O/W) direct emulsion for oil droplets dispersed in water;
- water-in-oil (W/O) inversed emulsion for water droplets dispersed in oil;
- oil-in-oil (O/O) for oil droplets dispersed in oil;
- different combinations (W/O/W, O/W/O, W/O/O).

PCMEs are to be circulated in cold supply network systems, therefore O/W emulsions are preferable to W/O emulsions due to their lower viscosity, which is extremely important in terms of pump energy consumption. When oil and water emulsions are produced, it is difficult

to determine by physical appearance the type of the emulsion, if it is either O/W or W/O. For this particular reason, five basic tests are available in order to test the emulsion created, (Sharma, 2009; Tauer, 2006):

- **Dilution test**

O/W emulsion is diluted with water and W/O with oil in order to examine the solubility of the continuous phase. In the case of the O/W emulsion diluted with water, it should be stable otherwise the emulsion will break since oil and water are immiscible.

- **Filter paper**

This test consists in impregnating filter paper with Carbonyl Chloride ($CoCl_2$). As a result, O/W emulsion will then change the colour of the filter paper, from blue to pink.

- **Fluorescence**

The fluorescence test is based on UV light for testing emulsions. An O/W emulsion will have a spotty pattern while the W/O emulsion will be almost entirely fluorescent.

- **Dye-solubility**

For this type of test a water-soluble or oil-soluble dye is used with the emulsion and the colour pattern of the emulsion is visualized under microscope. For the O/W emulsion, the oil-soluble dye will dissolve the dispersed phase. While it will dissolve the continuous phase for the W/O emulsion.

- **Conductivity**

The main element needed to perform the conductivity test is a light bulb to be attached to two electrodes. When the electrode is immersed into an O/W emulsion, the bulb glows due to the very high conductance of water.

I.2.2 Formulation

As explained before, when forming a stable paraffin emulsion, due to the fact that paraffin and water are immiscible, a surfactant is added to the composition. In addition, for the paraffin emulsion as a secondary refrigerant, it is often desirable to add a nucleating agent that will act as a promoter for liquid-solid phase change.

I.2.3 Preparation Methods

Emulsifying methods for emulsion preparation can be classified in two groups: high-energy methods and low-energy methods (Shalbart *et al.*, 2010).

I.2.3.1 High energy methods

This type of preparation method requires a mechanical process, which consists in breaking large droplets into small ones. As the droplet size is smaller the energy input necessary is greater. In general, the most common device used to induce deformation on pre-emulsion droplets is the rotor-stator system (Allouche, 2013). The characteristics of the droplet depend a lot on the energy applied. For example, the dispersion speed has great influence on the quality of the final emulsion. If the dispersion speed is not high enough (i.e. the energy input not sufficient), the mixing of the paraffin and the surfactant will not be efficient. The result is an uneven distribution of the droplet size. Otherwise, if the dispersion speed is too high, energy is wasted, as it does not affect the droplet size and does not improve the quality of the distribution. A second disadvantage of the high speed is the risk of introducing air bubbles into the system, which might destabilize the emulsion (Chang, 2007).

Liu *et al.* (2004) showed that the dispersion speed should be between 800 and 1000 rpm in order to obtain a complete process of emulsification. Other authors, like Wang *et al.* (2004), affirm that in practical applications, a low pre-mixing speed of 200 rpm is used firstly for water and paraffin, to avoid slopping, and then the dispersion speed is raised up to 500 - 1000 rpm. Furthermore, their results showed that is recommendable to reduce the dispersing speed after a period of high mixing in order to allow the surfactant to be fully attached to the paraffin droplets.

High-energy methods are usually expensive, due to the use of different machines as for example ultrasonic generators, micro-fluidizers, pressure homogenizer, etc.

I.2.3.2 Low energy methods

Low energy methods are those for which the energy necessary to form the emulsion comes from transitions or phase changes during its production. Spontaneous emulsification is a low energy method of emulsion preparation. This type of method does not need external energy supply in order to complete the emulsification process. The most popular spontaneous

emulsifications method is Phase Inversion Method. Phase Inversion can be obtained either by changing the temperature (PIT-Phase Inversion Temperature) or by changing the volume fractions of water/oil (EIP-Emulsion Inversion Point) (Lu and Tassou, 2012).

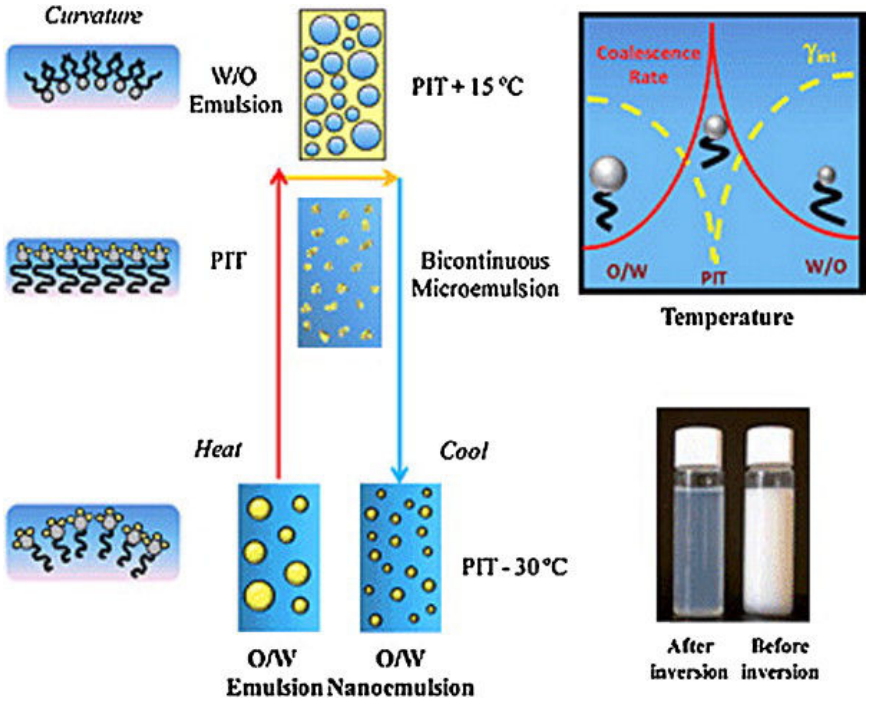

Figure I-2 Schematic diagram of the formation of emulsions by the PIT method (McClements, 2011)

PIT was first presented as an alternative solution to the shear emulsification methods by Shinoda and Saito (1969). Emulsions can change their original form from O/W into W/O and vice versa at a certain temperature, called Phase Inversion Temperature (PIT). Fig. I- 2 describes the main processes of PIT method when pre-mixing oil, water and non-ionic surfactants at room temperature. The surfactant becomes more soluble in oil (lipophilic) with the temperature increase and when reaching a particular Phase Inversion Temperature, it becomes equally soluble in oil and water in the same time. At this point the surfactant monolayer exhibits zero curvature. Phase inversion is based on the spontaneous change of the curvature, the molecular geometry of the non-ionic surfactant. When achieving a temperature higher than the PIT, the surfactant becomes more soluble in oil than in water and therefore in the end integrally dissolves in the oil phase, obtaining a W/O emulsion. In order to break the large droplets into smaller ones, mechanical energy is supplied at a temperature greater than the PIT temperature. When the procedure involves lowering the temperature below the PIT,

surfactant molecules move from the oil to the water phase very quickly, thus leading to the direct formation of small oil droplets.

The second spontaneous emulsification method is the EIP. It is based on a catastrophic phase inversion. Initially, a W/O emulsion with an increased oil content, is formed with different types of surfactants. The water is then added to the mixture gradually while stirring continuously. Fig. I-3 illustrates the procedure of the EIP method.

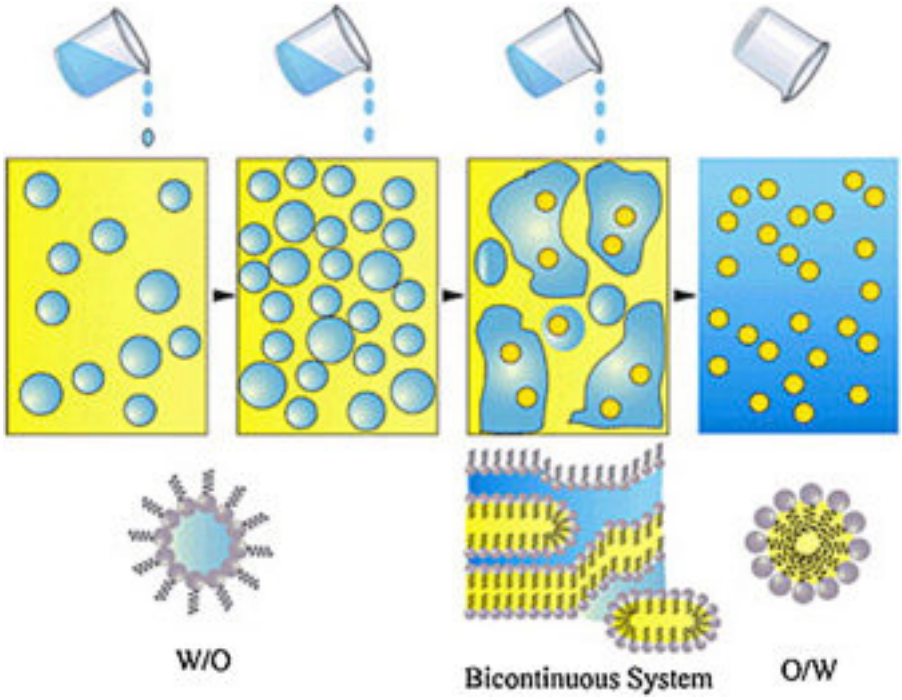

Figure I-3 Schematic diagram of the formation of emulsions by the EIP method (McClements, 2011)

The phase inversion takes place above critical water content and the mixture changes into O/W emulsion. Surfactants used can be both lipophilic and hydrophilic and the inversion can take place either in a catastrophic or transitional way as seen in Fig. I-4.

In 2010, Schalbart *et al.* (2010) tested three low-energy methods, the EIP, the mixing film and the PIT, in order to prepare tetradecane emulsions. The results showed that the PIT was the most appropriate and efficient.

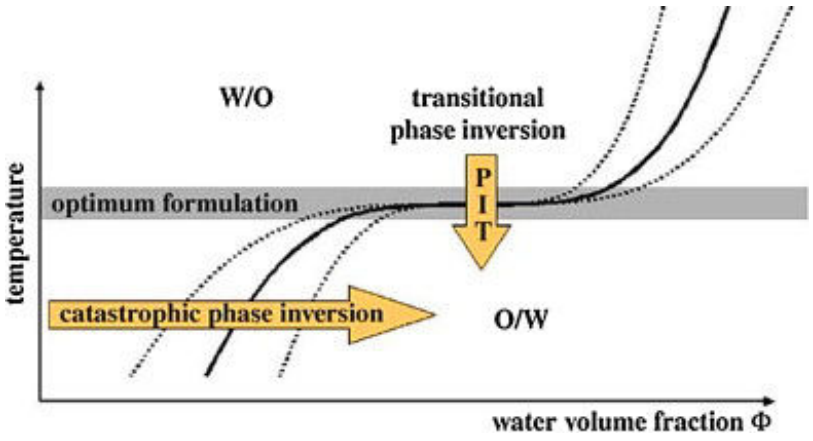

Figure I-4 Schematic illustration of phase inversion for preparation of O/W emulsions (Fernandez *et al.*, 2004)

I.2.4 Components

As already mentioned a paraffin emulsion is composed out of water, paraffin droplets, surfactant and nucleating agent. In this subchapter each component of the paraffin emulsion will be treated more thoroughly.

I.2.4.1 Paraffin

Paraffins are organic phase change materials that cover a wide phase change temperature from 0 to 130 °C (Mehling and Cabeza, 2008). Normal paraffins, as C_nH_{2n+2} are a set of saturated hydrocarbons with high similar properties (Sharma *et al.*, 2004). Both melting temperature and latent heat of fusion increase with the carbon chain length, (Sharma *et al.*, 2009).

When a PCM is selected for HVAC applications, it should have a melting temperature between 0-20 °C, (Huang *et al.*, 2009). Three paraffins fit this range of temperature: tetradecane $CH_3 - (CH_2)_{12} - CH_3$ with a melting temperature $T_m = 5{,}9$ °C and a latent heat of fusion $h_f = 227$ kJ.kg^{-1}, pentadecane $CH_3 - (CH_2)_{13} - CH_3$ with a melting temperature $T_m = 10$ °C and a latent heat of fusion $h_f = 206$ kJ.kg^{-1} and hexadecane $CH_3 - (CH_2)_{14} - CH_3$ with a melting temperature $T_m = 18$ °C and a latent heat of fusion $h_f = 236$ kJ.kg^{-1} (Bo *et al.*, 1999).

I.2.4.2 Surfactants

Surfactants are used for the emulsification process of two or more immiscible fluids. As a matter of fact, water and paraffin coexist, surface tension forces are generated at the

interface. Surfactants are then used to reduce the interfacial tension between water and paraffin molecules. Surfactants have two parts: a water attracting head (hydrophilic part) and a water resistant tale (lipophilic part). Therefore, surfactants mediate between the two fluids as they can form strong relations to both of them. Increasing the amount of surfactant adsorbed at the interface decreases the interfacial tension until saturation is reached. When saturation is reached, the addition of surfactant does not result in any further decrease of the interfacial tension but in a self-organisation of the surfactant molecules. It organises into aggregates called micelles. For the paraffin-in-water emulsion, the micelles are usually spherical as seen in Fig. I-5 with their hydrophilic part attached to the aqueous solution as water and the lipophilic one attached to the paraffin.

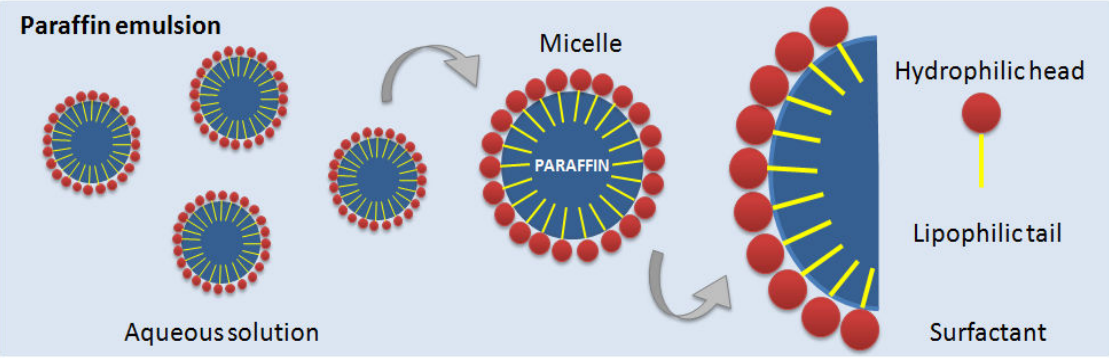

Figure I-5 Illustration of paraffin in water emulsion

Micelles only form when the concentration of surfactant is greater than the critical micelle concentration CMC. The critical micelle concentration is the concentration at which the interface becomes completely loaded with surfactant and any further addition starts the spontaneous formation of micelles. This concentration can be determined by measuring the surface tension for different surfactant concentrations. Using a logarithmic representation of the surface tension vs. the surfactant concentration gives two linear regimes below and above the CMC as seen in Fig. I-6.

Below the CMC, the surface tension decreases with the increase of the surfactant concentration and the number of surfactants at the interface increases. When CMC is exceeded, the surface tension is constant as there are no changes in the interfacial surfactant concentration and micelles form.

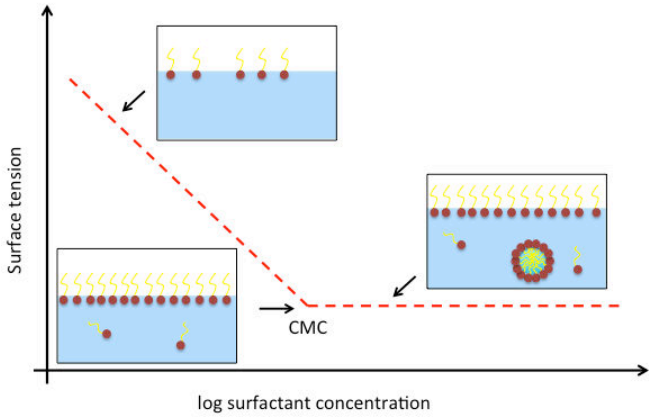

Figure I-6 Surface tension as a function of the surfactant concentration

Surfactants may be classified in four major groups: ionic, non-ionic, polymer surfactant and amphoteric surfactant, as seen in Fig. I-7, (Yu and Xie, 2012; Salager, 2002; Cullum, 1994a, 1994b).

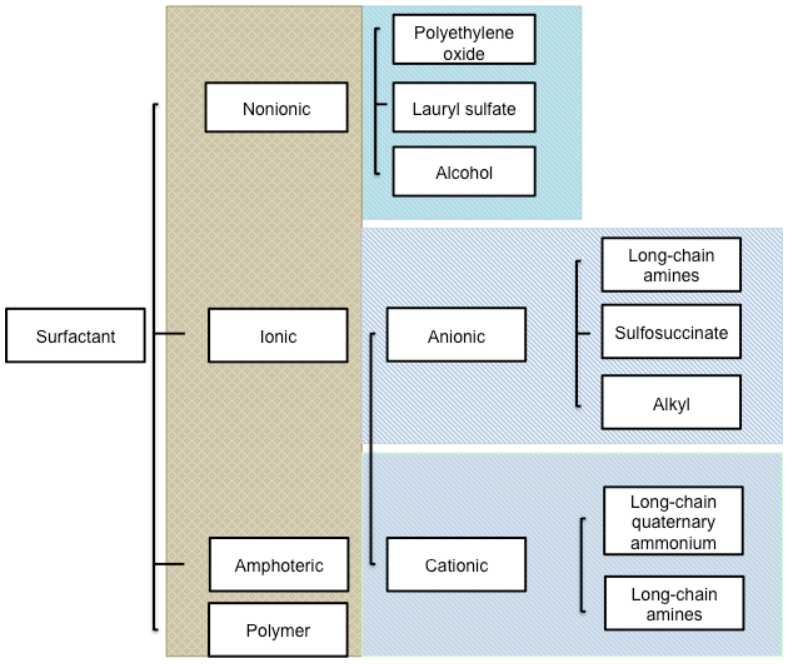

Figure I-7 Surfactant classification

Ionic surfactants are divided into two major groups: anionic surfactants and cationic surfactants. Anionic surfactants have a negative charge on their hydrophilic end. They are very soluble in water at room temperature. Among anionic surfactants, the following can be mentioned: salts of higher fatty acids, sodium dodecyl sulphate (SDS), sodium lauryl sulphate (SLS), sodium glycolate, etc. On the other hand, cationic surfactants have a positive charge on

their hydrophilic end. They are usually more expensive than anionic surfactants, mostly because during their synthesis, a high pressure of hydrogenation reaction must be carried out, (Salager, 2002). Major disadvantage of the ionic surfactants is related to the ability to cause precipitation or foaming in solutions.

Non-ionic surfactants differ from the ionic surfactants by not possessing any kind of charge on the hydrophilic end, nor positive or negative. For this particularly reason, they are resistant to water hardness deactivation. The hydrophilic end usually contains a polyethylene chain formed from a polycondensed ethylene oxide or polyol derivatives. The lipophilic part is made up of fatty acids or fatty alcohols. They are the most efficient surfactants used for stabilizing O/W or W/O emulsions (Salager, 2002; Cullum, 1994a, b; Tadros, 2013).

Some of the non-ionic surfactants show very low toxicity levels. There are four main types of these kinds of surfactants: fatty acid esters, amine and amide derivatives, ethoxylated linear alcohols and ethoxylated alkyl phenols. The most common non-ionic surfactants are: polyhydric alcohol like Tween and Spans, or alkylpolyoxyethylenes. Spans are generally non soluble in water with a low hydrophile-lipophile balance value. This is why they are particularly used in water-in-oil emulsions. Tweens are more soluble in water with a larger hydrophile-lipophile balance value, and commonly are used in oil-in-water emulsions.

Amphoteric surfactants can be anionic, cationic or non-ionic depending on the pH or acidity of water. They have excellent dermatological properties and are generally very expensive, thus being used mostly in the cosmetics industry. Polymer surfactants are the newest surface-active substances. They are composed of two or more macromolecular structures with hydrophilic and lipophilic characters.

Other than the thermodynamically stabilization of the emulsion, surfactants also form a protective layer around paraffin droplet to prevent coalescence. This layer also acts against the deposition of paraffin droplets in cooling systems, therefore reducing the risk of obstruction.

The selection of surfactants for a PCME is critical. The type of surfactant used affects both mechanical and kinetic stability of the emulsion. On the other hand the selection process should also take into consideration different factors that can make a potential surfactant a good choice for the needed application. These factors can include the chemical structure of the surfactant, the regulations regarding the use of the surfactant, the ecological impact, the financial costs etc.

Some key factors that need to be taken into consideration when choosing a surfactant are listed below (Myers, 2006):

- biological or chemical compatibility requirements;
- surface and interfacial properties;
- relationship between structural properties of the surfactant and their effects on the interfacial surface;
- chemical and physical properties of the possible surfactants;
- regulations on the use of surfactants concerning toxicity, ecological impact or allergenic reactions.

There are different methods for choosing the most appropiate surfactant but the most common method used for the selection is based on the Hydrophile-Lipophile Balance (HLB) system, devised in 1949 by Griffin, (Krugliakov, 2000). This method uses arbitrary numbers to describe the ratio between the hydrophilic and lipophilic part of various surfactants. Each surfactant is designated a HLB number, that can be calculated according to an empirical formula, (Davies and Rideal 1961) or determined experimentally (Americas, 1987). According to Griffin's scale, HLB values can be calculated using Eq. I.1:

$$HLB_{value} = \frac{\text{molar mass of the hydrophilic part}}{\text{molar mass of the surfactant}} \times 20 \qquad \text{(I.1)}$$

Applications for surfactants have an HLB requirement; therefore, matching the HLB number of a surfactant with the HLB of the required application is very important. This method was particularly intended for use with non-ionic surfactants, which have numbers ranging from 0 to 20. For the higher end of the scale, which can be seen in Fig. 8, the surfactants are hydrophilic and act as solubilising agents, detergent and oil-in-water surfactants. Authors such as Shinoda and Saito (1969) point out that HLB value has a major influence on the stability of an emulsion and so finding the correct HLB value for oil is very important

When investigating the optimum HLB value for a paraffin-in-water emulsion, a mixture of two surfactants is required. One of them is to be hydrophilic with a low HLB value and the other one is to be lipophilic with a large HLB value. After mixing the two surfactants, the new HLB value of an oil (paraffin) can be determined using Eq. I.2:

$$HLB_{oil}=\frac{m_A \times HLB_A + m_B \times HLB_B}{m_A + m_B} \quad (I.2)$$

where m_A is the molar mass of the surfactant A, m_B is the molar mass of the surfactant B, HLB_A is the HLB of the surfactant A and the HLB_B is the HLB of the surfactant B.

Stability of the final solution can be tested in order to validate the different HLB values calculated. The optimum HLB value can be reached with stable emulsions. The more stable emulsion means the most accurate HLB value. Different approaches for determining the optimal value for HLB are available. The first one involves testing the droplet size since there is a connection between the kinetic stability of the emulsions and the droplet size. Another approach is related to visual investigation of the emulsion after preparing it.

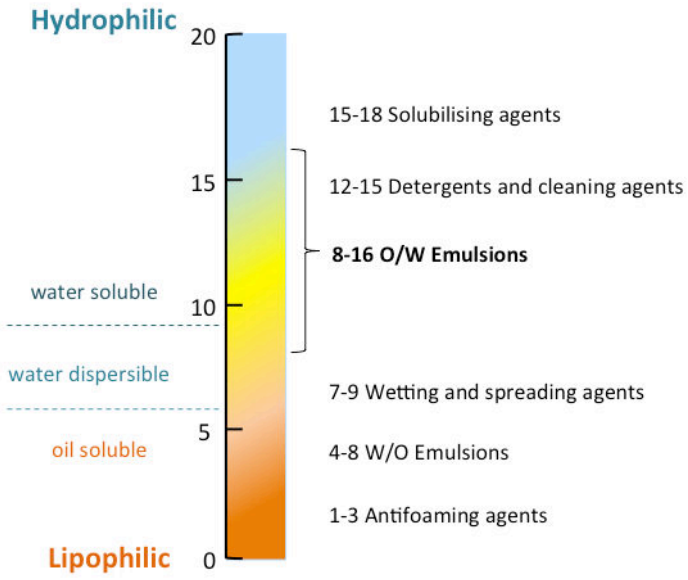

Figure I-8 The HLB scale and the approximate ranges for solubilising agents, detergents, surfactants and antifoaming agents, based on the method devised by Griffin

As previously mentioned, the selection of a correct HLB value for an oil-in-water emulsion, therefore for a paraffin-in-water emulsion is very important. Previous studies show that for the preparation of an oil-in-water emulsion, the surfactant is required to have a HLB value between 8 and 16, (Tadros, 2006). Test were conducted on Tween and Span 60 surfactants by Xu *et al.* (2005) and the results showed that emulsions with a shelf life of at least one week could be produced. The binary mixture of Tween and Span with a HLB value of 12 was noted effective for the use with an alkane, (Boyd *et al.*, 1972).

The most recent method for finding the optimal HLB value is based on the Phase Inversion Temperature (PIT) method. When using non-ionic emulsifiers, as the temperature is raised, their hydrophilic part tends to become less hydrophilic. Thus the surfactant is prevented from reducing the interfacial tension between water and oil. Therefore, at some point the inversion of the solution takes place.

Table 3 Different surfactants used in the study of PCMEs

Paraffin	Interface Component	Interface Component Concentration	Reference
Paraffin	Surfactant: mixture of Span 80 and Tween 80	Span 41,2 wt.% Tween 58,8 wt.% or Span 34 wt.% Tween 36 wt.%	(Li *et al.*, 1992)
Tetradecane $C_{14}H_{30}$	Surfactant: polyethylene glycostearylether and alkylbenzene- sulfanate (10:1)	Tetradecane 5-40 wt. %	(Inaba *et al.*, 1994)
Hexadecane $C_{16}H_{34}$	Surfactant: Titron X- 100	Hexadecane 10 -70 wt. %	(Clarksean, 2003)
Tetradecane $C_{14}H_{30}$	Surfactant: mixture of Span and Tween 60	Span 32,4 wt.% Tween 67,6 wt.%	(Xu *et al.*, 2005)
Tetradecane $C_{14}H_{30}$	Surfactant: mixture of Span and Tween 60	Surfactant 6 wt.%	(Scalbart *et al.*, 2010)
Paraffin with melting temperatures between 0 – 20 °C	Surfactant: Alcohol ethoxylates	Surfactant 1,5wt. % Nucleating Agent 2,5wt. % Paraffin 30 wt.%	(Huang *et al.*, 2010a & Huang *et al.*,2010c)
Paraffin with melting temperatures between 0 – 20 °C	Surfactant: sodium dodecyl sulfate (SDS) Tween40 polyethylene glycostearylether and alkylbenzene- sulfanate (10:1) Nucleating Agent: paraffin with freezing peak of 50 °C		(Huang *et al.*, 2010b)
Hexadecane $C_{16}H_{34}$	SDS or Tween 40	Surfactant 1 wt. %	(Günther, 2011)
n-Octacosane $C_{28}H_{58}$	Tween 20, 60, 80 Span 20, 60, 80 Mixture of Tween and Span	Surfactant mixture: 5 wt. % Non-ionic surfactant 1-9	(Zhang *et al.*, 2016)

		wt. %	
n-Octadecane	Non-Ionic Surfactant with HLB=12	7 wt.%	(Niedermaie *et al.*, 2016)
Tetradecane Hexadecane Octadecane	Polyoxyethylene sorbitan mobooleate	-	(Kawanami *et al.*, 2016)

For an oil-in-water emulsion this means converting to water-in-oil-emulsion. The temperature, at which these phenomena occur, is known as the phase inversion temperature. PIT has an almost linear correlation with the HLB value. The emulsion with the lowest PIT should have the optimal HLB value, (Mollet and Grubenmann, 2001). In the literature, many authors are focused on the influence of the surfactant on the emulsions. For instance, Lu and Tassou (2012) showed that a mixture of two surfactants, one of them being Tween 60 can reduce the supercooling effect, usually present in PCMEs. Other types of surfactants used in the literature, over time, can be seen in Table 3.

I.2.4.3 Nucleating agent

Nucleating agents are substances with a very small phase tension. They are usually used in order to enhance the process of nucleation. Nucleating agents are considered impurities in contact with the liquid. They act as active seeds inside the PCM droplet, initializing the nucleation. The type and fraction of the nucleating play an important role on the melting and nucleation temperature. Huang *et al.* (2010b) used a paraffin wax with a higher freezing point than the PCM selected for the studied emulsion. The authors reported a reduction of the supercooling degree of 6,9 °C. Fischer *et al.* (2017) studied the supercooling on PCMEs with the same PCM concentration, of approximately 40 wt. % but different concentration of nucleating agent. They used myristic acid as nucleating agent with the following concentrations: 0 wt. %, 1 wt. % and 2 wt. %. Their interpretations on the results suggested that the supercooling degree could be reduced for the same droplet size by adjusting the concentration of the nucleating agent. The supercooling decreases with increasing the amount of myristic acid.

I.2.5 Stability

Stability of an emulsion can be defined as the ability to resist changes in both of its physical and chemical properties over time.

"Dispersion stability refers to the ability of a dispersion to resist change in its properties over time." D.J. McClements.

I.2.5.1 Kinetic stability

From a thermodynamic point of view, PCMEs are unstable systems because there is a natural tendency of separation between the two major components of PCMEs, water and oil. However, most of them demonstrate kinetic stability over a long period of time, which determines their shelf life.

Stability has always been a priority in the studies of PCMEs. If industrial applications are considered for thermal storage and transfer media, emulsions should be stable under thermo-mechanical cycles and also for a long-term storage. Stability can be evaluated by determination of changes in the thermophysical properties, including droplet size and viscosity, (Youssef *et al.*, 2013). Fig. I-9 is a pictorial representation of the six different types of instability that may occur to a PCME. These breakdown processes may take place simultaneously rather than consecutively, thus making it very difficult to observe and analyse the consequences on the properties of the fluid.

In the following section a description of every instability process will be given together with solutions and methods of prevention.

Creaming and sedimentation refers to the process of forming a concentrated layer at the superior part of the fluid as a result of gravitational forces. This phenomenon is present in emulsions when the dispersed and continuous phases have different densities. A concentration gradient can be observed from the top of the fluid to the bottom of the container.

Flocculation occurs as a result of a weak van der Waals attraction and refers to the aggregation of droplets into forming clumps. This happens without altering the protective layer of surfactant existing around droplets. The process may be described in some cases strong or in other weak, depending on the attractive energy involved.

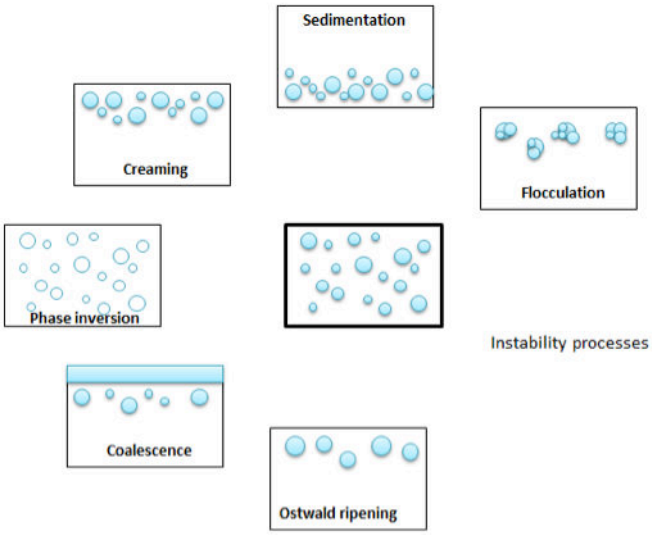

Figure I-9 Various breakdown processes in emulsions

Coalescence appears when the liquid film between droplets breaks. The result of this phenomenon is the fusion of droplets into larger ones. In the worst case, the result is a complete separation of the PCME into two distinct liquid phases.

Ostwald ripening is the process of forming larger droplets due to solubility differences between the oil droplets of different sizes. Smaller droplets have usually a larger solubility in comparison with larger droplets. In time the droplet size distribution increases due to the smaller droplets, which tend to disappear. Their molecules diffuse to the bulk and attach to the larger droplets.

Phase inversion is the process through which there is an exchange between the disperse phase and the continuous phase. It means that the original continuous phase inverts and becomes the dispersed phase and the dispersed phase becomes the continuous one, (Huang *et al.*, 2009).

Creaming, sedimentation and flocculation are reversible and do not lead to any changes into the droplet size distribution. On the other hand, Ostwald ripening and coalescence have a major contribution to the increase of droplet size, to the increase of droplet distribution and to the decrease of the interfacial area. The most common process of instability is coalescence. The first signals of coalescence in PCMEs would be creaming and flocculation, even though they have no impact on the droplet size, (Shao *et al.*, 2015). Clarksean (2003), studied hexadecane in water emulsions with different types of surfactants. The author measured the droplet size as a function of time. The results showed that all samples prepared with Trinton X-100 surfactant and a paraffin fraction inferior to 50 wt.%,

remained in a dispersed state during 6 months of storage at room temperature. Schalbart *et al.* (2010), studied stability of a tetradecane-in-water emulsion during storage over a period of 6 months at room temperature. The results showed good stability signs over time but an Ostwald ripening destabilization, as a result of slight increase in the droplet size. Fumoto *et al.* (2009) analysed the stability of a tetradecane in water emulsion after three weeks of storage. There were no changes in the droplet size, an average droplet size of 200 nm or less was maintained. Huang *et al.* (2010a) investigated different paraffin-in-water emulsions under different conditions. They reported minor changes in the droplet size distribution after 28 months of storage at room temperature. The PCMEs were also subject of 100 thermal-mechanical cycles and the results showed a slight coalescence phenomenon. Latest research on stability of paraffin-in-water emulsions was done for cooling storage, during multiple freeze-thaw cycles, Zhang *et al.* (2015). They suggested that the interfacial film between aggregated droplets could be broken by the crystallisation growth of the droplets. As a result, the fused droplets would form an oil layer at the top of the product.

In addition, in 2016, Zhang *et al.* tested multiple samples of paraffin-in-water emulsion with different types of surfactant for stability. They were subjected to multiple freeze-thaw cycles and the results showed the existence of a separated oil layer caused by coalescence phenomenon. Authors also tested stability during 6 months, at room temperature, for three different surfactants systems. Regardless the appearance of a cream layer, there was no significant change in the droplet size. The uniformity of the PCME could be regained after stirring. Despite the stability problems encountered by most of the researchers, Kawanami *et al.* (2016) managed to create perhaps one of the most stable emulsions up to present. Their PCME was highly stable, with almost no distinct changes in the droplet size even after 65 days.

I.2.5.2 Solutions to instability

The desirable PCME should be perfectly stable with no signs of instability. In reality, during storage and under thermal-mechanical cycles, most of the PCMEs show some instability manifestations. They can though, when applied in practical applications, present some changes in the properties but within an adequate range Huang *et al.* (2009). According to Huang *et al.* (2010a), a PCME can be considered stable when during storage time, no evident increase in the droplet size or any phase separation occurs. Concerning practical

applications, the authors indicate the PCME is stable if the emulsion remains in dispersion and the heat capacity maintains a value within the designed operational conditions.

Stability may be tested using the standard procedure, which means subject the emulsion to different shear rates. Vilasau *et al.* (2011) tested the stability of an emulsion under shear stress using a test rig designed especially for this. The results showed that after a number of freeze-thaw cycles if the PCME was unstable, a visible separation could be observed. The authors also suggested that no precise quantification of the PCME stability could be possible. With attention to actual air-conditioning systems, where the working parameters are strong mechanical stresses, coalescence is the most common instability phenomenon that may occur, even though the PCME is stable under static conditions, (Taylor, 1998).

Different authors, Zou *et al.* (2010), Delagdo *et al.* (2012) propose two major solutions to overcome instability, which are listed below:

- optimal PCM concentration

While higher concentration of PCM cause droplets agglomeration, smaller amounts of PCM is translated into smaller latent heat capacity values. Therefore, an optimal PCM concentration should be found, appropriate to the type of application for which the PCME is intended.

- a reduction in the diameter of the droplet.

The stability of a PCME is related to the separation speed. The separation speed can be described using Eq. I.3, (Wang *et al.*, 2004):

$$V = \frac{\Delta\rho d^2 g}{18\mu} \tag{I.3}$$

where V is the separation speed, $\Delta\rho$ the density difference, g the gravity acceleration, d the diameter of the droplet and μ the viscosity of the continuous phase.

Therefore, a stable emulsion will have a high viscosity, a low separation speed, a small density difference between the two phases and a small droplet diameter. Since it is very difficult to reduce density difference, the solution is to reduce the droplet size in order to reduce the influence of gravity. There are many parameters influencing the droplet size, as the formulation and composition of the surfactant or the stirring conditions, as the agitation speed, duration of emulsification etc (Shao *et al.*, 2015).

I.2.5.3 Factors affecting stability

The surfactant is the most important factor, which affects stability of a PCME. Stability of a PCME and the surfactant are strongly related. The amount of surfactant must be above a critical value in order to produce small, uniform and stable paraffin droplets, (Choi and Cho, 2001). Small droplets of paraffin as we previously mentioned, result in a higher PCME stability. In 2006, Golemanov *et al.* studied the effect of surfactant on the stability of PCME. According to the authors, the stability of the PCME reduced as a result of the solid-liquid phase transition of the droplets. Furthermore, stability could be strongly affected by the irregular shaped crystals during the freezing-thaw cycles. Results also showed that compared to all other types of available surfactants, the non-ionic polyethoxylated ones (Tween series) are the most effective at stabilizing the PCMEs. Furthermore, the mixtures of hydrophilic and hydrophobic surfactants were found good in preventing instability, due to their capacity to form denser protective layers around droplets. In addition, observations on the HLB number were made. For emulsions designed to undergo freeze-thaw cycles, the existing HLB number might not be adequate. Vilasau *et al.* (2011) concentrated on emulsions stabilized with a mixture of ionic and non-ionic surfactants. Three different parameters were taken into consideration when preparing the emulsion: the ionic surfactant fraction (the ionic fraction was varied while keeping the total concentration of surfactant constant), the total concentration of surfactant (was varied while the ionic surfactant fraction was kept constant) and the homogenization pressure. One of the results was that emulsions with high ionic surfactant concentration were more stable. Furthermore, authors reported that stability increased with both the increase of surfactant concentration and pressure, which generated emulsions with small droplet sizes.

Tadros (2004) studied the relation between viscosity and long-term stability of emulsions. He stated that a high viscosity could prevent the instability of PCME by supressing the movement of droplets. Moreover, the author pointed out that the viscosity of a PCME is highly dependent on the type of surfactant and especially on the concentration of surfactant.

Among factors that may influence stability, there are also environmental factors such as the storage temperature and external forces, (Degner *et al.*, 2014; Rosen, 2004). A basic formulation of PCME emulsified using 7 wt. % non-ionic surfactants, with a HLB value of 12

was tested by Niedermaier *et al.* (2016). Samples were subject to over 10000 freezing-heating cycles into a cycling-test facility and they remained both thermal and mechanical stable

In 2016, Zhang *et al.* tested the effects of emulsifier concentration on the PCME. They reported that by increasing the concentration of surfactant to 7 wt. %, the excess tended to migrate into the continuous phase. This phenomenon resulted in a brutal increase in the apparent viscosity of the PCME. Results showed that the concentration of surfactant should be maintained within specific range. An optimum concentration of surfactant should be within 3-5 wt. %.

The above-mentioned studies and work show how important is the selection of the most appropriate processing conditions and how the formulation of the product is more than essential for the formation of PCMEs.

I.2.6 Main characteristics of PCME

Phase Change Material Emulsions have several characteristics such as thermophysical properties, supercooling and nucleation that need to be studied in order to better understand how they work.

I.2.6.1 Thermophysical properties

The *total heat capacity* of a PCME, Δh_e, in a temperature range from T_1 to T_2 consists of the latent heat of the emulsion, $\Delta h_{f,e}$ but also the sensible heat capacity of the water, Δh_w and the sensible heat capacity of the paraffin, Δh_{PCM}, (Huang *et al.*, 2010c):

$$\begin{aligned}\Delta h_e &= \Delta h_{f,e} + \Delta h_w + \Delta h_{PCM} \\ &= X_{PCM}\Delta h_{f,PCM} + X_w C_{p,w}(T_2 - T_1) + X_{PCM}\overline{C_{p,PCM}}(T_2 - T_1)\end{aligned} \quad \text{(I.4)}$$

Where X_{PCM} and X_w are the mass fractions of paraffin and water, $\Delta h_{f,PCM}$ is the heat of fusion of the paraffin in the temperature range T_1-T_2, $C_{p,w}$ is the specific heat capacity of water and $\overline{C_{p,PCM}}$ the average specific heat capacity of the paraffin. The heat of fusion of the paraffin, i.e the enthalpy change during phase transition, can be obtained by estimating the peak area of a DSC melting curve (He *et al.*, 2004). Huang *et al.,* (2010c) managed to experimentally estimate the total heat capacity. Tests were carried out by the authors, in a specific test rig that followed operational conditions of practical applications. The results

agreed well with those obtained according to Eq. I.4. In order to fit as a PCS, the PCME should have a heat capacity that is minimum 2 times as high of that of water. Hence, the PCME should have a minimum paraffin fraction of 30 wt. % (Huang *et al.*, 2010c).

Thermal conductivity of PCMEs is considerably higher than that of PCMs (Murshed *et al.*, 2008; Sohn and Chen, 1981). There are three major factors that have a great impact on the thermal conductivity of a PCME: the size and shape of the droplets, and the components of the dispersed phase. A dispersed phase with small droplets will have a higher thermal conductivity than one with larger droplets. Regarding the shape of droplets, the spherical ones usually exhibit a small increase in the thermal conductivity than the ones with irregular shapes. Although the thermal conductivity emulsions is generally larger that that of PCMs, it is often low compared to that of water. Different researchers have worked on increasing the conductivity of PCMEs, and tried various solutions with different materials. Zou *et al.* (2012) tried to increase the thermal conductivity of paraffin emulsions by using 1 wt. % Aluminium nanoparticles. They showed that conductivity increased by about 29.4 % being almost equal to that of water. A n-octadecane emulsion was prepared with two different percentages of Alumina (Al_2O_3) particles, 5 wt. % and 10 wt. %, by Ho and Gao (2009). Samples were examined at a temperature of 30 °C and the results showed enhancements for the thermal conductivity by 2 % and 6 % respectively. A first major disadvantage of using alumina as a solution for the increase of the conductivity is that it also leading to an increase of the dynamic viscosity of the emulsion, which is undesirable for application in air-conditioning. The second major disadvantage is related to the fact that metals materials displace a great amount of PCM, therefore increasing the amount of the dispersed phase, which causes sedimentation (Youssef *et al.*, 2013; Ho and Gao, 2009). Thus, alternative materials to increase the thermal conductivity were taken into consideration. Investigations were further carried out on lightweight materials, such as carbon fibres and graphite nanofibres (Elgafy and Lafdi, 2005; Kumaresan *et al.*, 2012; Fleischer *et al.*, 2008). Elgafi and Lafdi (2005) used carbon nanofibres and showed that the thermal conductivity at room temperature increased with the increase in the mass fraction of carbon nanofibres. As a result, the cooling rate during solidification process increased. Even though this seemed to be a very promising solution, Fleischer *et al.* (2008) observed that after several freeze-thaw cycles, settlement of nanoparticles intervened. This was attributed by these authors to the change of density caused by the liquid to solid phase transition.

If not determined experimentally, the thermal conductivity or calculated with empirical relations, such as Eurken's model (Youssef *et al.*, 2013) or by using laws of mixtures, (Lu and Tassou, 2012). These calculating methods are still not very reliable since they are not robust or complex enough to obtain accurate results.

I.2.6.2 Supercooling

The supercooling phenomenon is a very serious issue in PCMEs investigation and application fields. Supercooling is the cooling of a fluid below its melting point without it showing crystallization. When supercooling occurs, the crystallization temperature is lowered and the latent heat is released at a lower temperature or in a wider temperature range, (Zhang *et al.*, 2005). As a consequence, supercooling deteriorates the system performance and reduces its energy efficiency. Even though many PCMs are not likely to be supercooled (or to a negligible extent), the PCMEs still crystalize below the freezing point of their constitutive PCM (Huang *et al.*, 2009; Delgado *et al.*, 2012; Golemanov *et al.*, 2006). The explanation is found in the fact that many PCMs present differently from microscopic geometries to macroscopic ones. For example, the emulsions prepared by Huang et al. (2009) showed a supercooling degree between (i.e. temperature difference between the theoretical crystallization temperature and the practical crystallization temperature) 4.3 K and 14.7 K, despite the fact that the paraffin used (tetradecane and hexadecane) has a supercooling degree of only 0.5 K and 1.9 K. In addition to the type of PCM used in the PCME, the degree of supercooling also depends on other factors such as the particle size or type of surfactant. These two factors will be further detailed in the following sections.

Influence of the droplet size

Previous studies indicate that droplet size has an effect on the supercooling degree of a PCME. A higher supercooling degree is more likely to be present for emulsions with smaller droplets, (Golemanov *et al.*, 2006; Schramm, 2005; McClements *et al.*, 1993). Huang *et al.* (2009), (2010a, b,c) studied different PCME with different droplet sizes. According to the results, droplet sizes and their distribution highly affected the melting and crystallization temperature. Reduction of the droplet size resulted in a decrease of the melting and crystallisation temperature of the emulsion in comparison with the pure PCM. The most affected by the reduction of the droplet size was the process of solidification, with almost 15 °C for the PCME with the smallest droplets. A PCME with smaller droplets will be much more stable, therefore droplets would not be in direct contact the ones with the others, thus

affecting the ability of crystallisation. A much more detailed description of the phenomenon of crystallisation will be presented in the next section (I.2.6.3 Nucleation theory).

Influence of the surfactant

The supercooling degree depends both on the droplet size and the type of surfactant, (Shao *et al.*, 2013). According to Huang *et al.* (2010b), nucleation and supercooling temperature change with different types of surfactants. These authors tested several hexadecane emulsions with different surfactants (SDS, Tween40 and a surfactant mixture). The PCME with SDS surfactant had the lowest nucleation temperature with a supercooling degree of 15 K. The PCME with Tween40 presented a smaller supercooling degree of 11 K. The most promising sample was the one using a surfactant mixture which obtained two levels of nucleation corresponding to the following supercooling degrees: 5.7 K and 11.3 K. Some studies that highlight the fact that surfactant molecules at the interface act as a template and therefore increasing the ordering of oil molecules (McClements *et al.*, 1993; Awad *et al.*, 2001). As a result, nuclei of a critical size are formed and nucleation is thus initiated. Golemanov *et al.* (2006) showed that surfactants with longer alkyl tails presented a lower degree of supercooling. They suggested out that an oil-soluble co-surfactant could be added to beat the supercooling effect.

I.2.6.3 Nucleation theory

In general, the crystallization process can be considered as two-step process, (El Rhafiki *et al.*, 2011). The first one corresponds to the development of a cluster larger than the critical radius and the second one to the crystalline growth, which leads to the crystallization of the entire system. The theory of nucleation describes the formation of small particles of a new phase within the mother phase at the beginning of a phase transition.

Günther et al. (2011) used this theory in order to try to interpret the supercooling cause. When cooling the bulk fluid below its melting point, the phenomenon of solidification should be spontaneous. During phase transition, two phases are present at the same time. The two phases meet at an interface. This is related with interface energy, which is related to a surface tension force. This surface tension prevents the reducing of the liquid surface. Hence, the creation of the interface between the two phases needs an energy input to fight against this tension surface. In the case of very smalls PCM droplets, the energy released during the liquid-solid phase change is not enough. Therefore, the effect of the surface tension cannot be overcome and the spontaneous solidification of droplets is blocked. The description of this

effect is based on the Gibb's free energy, G. The maximum difference in Gibb's free energy, between the two phases, corresponds to a critical radius r_{crit} of the solid particle, as illustrated in Fig. I-10, (Günther *et al.*, 2010).

The critical radius corresponds to the minimum size at which a particle can resist in a solution without being re-dissolved. The difference in Gibb's free energy, ΔG is also called the nucleation barrier. For the macroscopic nucleation to start, this barrier should be exceeded. In other words, it means that for clusters larger than the critical radius, solidification can start. The nucleation barrier can be overcome by thermal fluctuations, which are considered statistic events, making the nucleation a probabilistic phenomenon. For small volumes of PCM, usually nucleation starts in every single small volume. Especially for PCMEs, in which case, the volume corresponding to a droplet is very small. As already mentioned, if droplets are smaller than critical radius, nucleation is blocked.

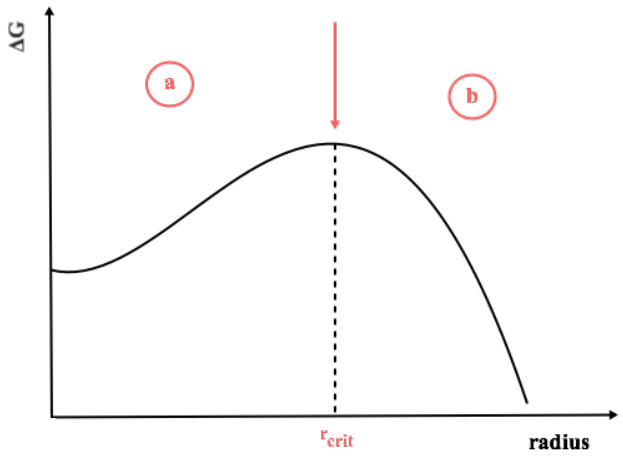

Figure I-10 The maximum difference in Gibb's free energy as a function of the radius

Authors also suggested that the surfactant used for the PCME could interfere in the process of nucleation. For instance, in the case of large droplets, the alignment of the surfactants tails is almost parallel, which represents a pattern for crystallization. In the event of small droplets, this alignment is much more complicated.

Nucleation can be homogeneous, in the absence of foreign particles, impurities, or heterogeneous, in the presence of foreign particles in the fluid. The presence of heterogeneities, impurities, foreign particles, etc. can foster phase transition (by reducing formation energies), especially crystallization. If adequate geometric irregularities exist, if chemical impurities are added to the fluid, nucleation may occur on the surface of these

impurities. The impurities or the irregularities can act as nucleation sites and with a low concentration of PCM, they are only found in some droplets. Nucleation sites are like this isolated from the other droplets and thus the main PCM mass.

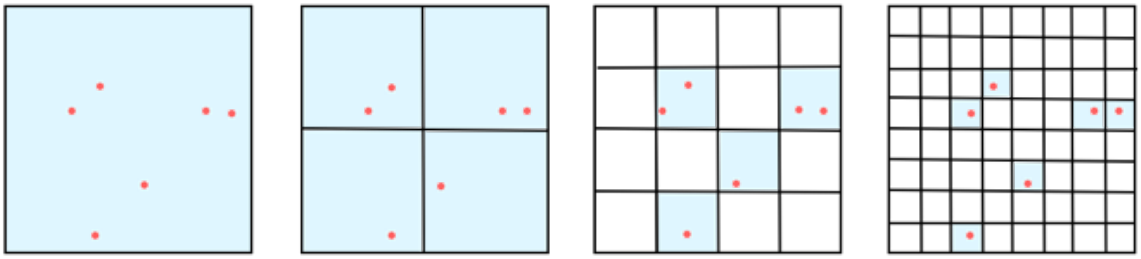

Figure I-11 Heterogeneous nucleation with a given seed concentration (the total activated volume depends on the size of the volume elements)

Therefore, heterogeneous nucleation is limited to these few droplets. The rest of the PCM mass being able to solidify after homogenous nucleation. This theory is briefly illustrated in Fig. I-11.

To resume, the solidifying process in emulsions is predominately a homogeneous nucleation, which is associated with a lower crystallization temperature of the fluid. Taking into account the above-mentioned theory, one of the solutions proposed to fight this effect is adding nucleating agent.

I.3 Rheological behavior of two-phase secondary refrigerants

The viscosity measurement and rheological characterization of the PCMEs must be taken into account. Although PCMEs seem homogeneous from a macroscopic point of view, the presence of other phases at a microscopic level modifies their rheological behaviour significantly.

I.3.1 Theoretical background

Understanding the rheological behaviour of a PCME is of major importance since it is proposed for cold distribution applications. Disperse systems exhibit a behaviour that is different from the behaviour observed in homogeneous fluids, due to the presence of the two phases. As a result, the rheological behaviour of the PCME can range from Newtonian in diluted particle system to highly non-Newtonian behaviour in concentrated particle system.

Such a rheological behaviour may have serious consequences for the use of the PCME in industrial applications.

I.3.1.1 Constitutive laws

Rheology aims at characterizing of fluids through the expression of the stress-strain relationship related to their mechanical properties. From a rheological point of view, fluids can be defined by the following relationship, as seen in Eq. I.5:

$$\tau = f(\mu\dot{\gamma}) \tag{I.5}$$

where τ is the shear stress, μ the dynamic viscosity and $\dot{\gamma}$ the shear rate. This relationship characterizes the response of a fluid to a mechanical stress, which is imposed on the system, stress or shear rate.

Fluids are classified into three major categories as following:

- **Non-viscous fluids or Pascal fluids** for which the shear stress is always zero;
- **Newtonian fluids** for which shear stress and shear rate are proportional according to a constant, the dynamic viscosity of the fluid, as seen in Eq. I.6:

$$\tau = \mu\dot{\gamma} \tag{I.6}$$

The dynamic viscosity, μ is a coefficient, function of the fluid and temperature. Under the action of friction, the fluid layer in contact with the walls have the same speed as the walls and the intermediate layers' slide over each other with speeds proportional to their distance from the wall.

Non-Newtonian fluids for which shear stress and shear rate do not follow that expression of proportionality. For this type of fluid, viscosity changes with the applied shear rate. Accordingly, the non-Newtonian fluids may not have a well-defined viscosity. They are divided into three groups as illustrated in Table 4.

Table 4 Different types of non-Newtonian fluids

Purely viscous fluids independent behaviour of the time	Viscous fluids time-dependent behaviour	Viscoelastic fluids behaviour is dependent on both time and the shear angle, γ
$\tau = \tau(\dot{\gamma})$	$\tau = \tau(\dot{\gamma}, t)$	$\tau = \tau(\gamma, \dot{\gamma}, t)$

For purely viscous fluids it is possible to make an analogy with Newtonian fluids, therefore an apparent dynamic viscosity can be considered, as illustrated in Eq. I.7:

$$\tau = \mu_{app}\dot{\gamma} \tag{I.7}$$

There are four types of non-Newtonian fluids independents of time presented in Table 5.

There are multiple types of models (Bingham, Ostwald - de Waele, Sisko, ...) able to represent the behaviour of Phase Change Slurries.

Table 5 Non-Newtonian fluids independent of time

non-Newtonian fluids (independent of time)			
Fluids that need a minimal shear stress in order to permit flow		Fluids that do not need a minimal shear stress to permit flow (Ostwald – de Waele)	
plastic fluids called Bingham fluids	plastic fluids called Herschel-Bulkley fluids	pseudo-plastic or shear-thinning fluids	dilatants or shear-thickening fluids

The Herchel-Bulkley model presented below (Eq. I.8), also called generalized Bingham model, and is generally used to describe the behaviour of PCME:

$$\tau = \tau_0 + K\dot{\gamma}^n \tag{I.8}$$

where τ_0 is the minimal shear stress, K is a coefficient, n an exponent characteristic of the fluid that represents the degree of non-Newtonian behaviour, τ the shear stress and $\dot{\gamma}$ the shear rate. For a Newtonian fluid, e.g. water, n is equal to 1. If the fluid is pseudo-plastic, then n<1. The coefficient K represents the consistency of the fluid. If τ_0 is negligible then Eq. I.8 can be rewritten under the form of the so-called Ostwald-de Waele model:

$$\tau = K\dot{\gamma}^n \tag{I.9}$$

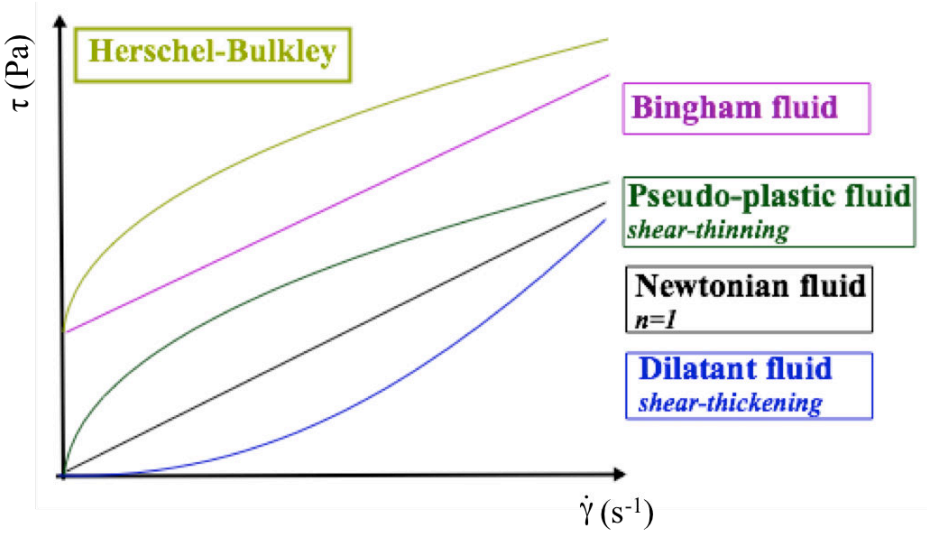

Figure I- 12 Characteristic τ -$\dot{\gamma}$ relationship for purely viscous fluids (with independent behaviour of the time) and for a Newtonian fluid

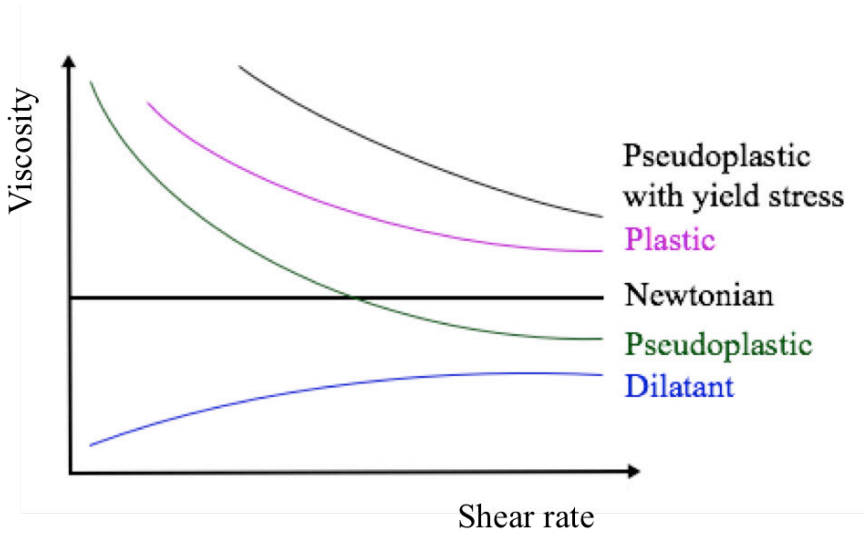

Figure I-13 Typical curves of viscosity versus shear rate

I.3.1.2 Measuring rheological properties

Determination of the rheological behaviour of a viscous fluid can be mainly done by using two types of viscometers:

- rotational viscometers (cylinders, cones, plates systems) - the fluid is subjected to a uniform shear rate and the shear stress is directly measured;
- capillary viscometers (Ostwald viscometer) - the fluid circulates in a straight pipe and both pressure drop and flow rate measurements are necessary in order to determine the rheological behaviour of the working fluid.

One advantage of the Ostwald viscometer is that it can be integrated within the experimental installation that was developed at CETHIL over the last two decades, from the pioneering work of Bel (1996) and other researchers. This kind of viscometer is relatively representative of real application. Besides a rotational viscometer are self-standing devices available in several laboratories. When using them, case must be taken regarding the sampling-related problems and the constraint related to acquiring a representative and homogeneous sample.

I.3.1.3 Operating principle of capillary viscometer

The operating principle of capillary viscometers is based on measuring the pressure drop of the viscous fluid as it flows into a calibrated tube with a given flow rate. For the analysis of the relationship between the volumetric flow rate and the shear stress at the wall, when a laminar flow is considered the Rabinowitsch relationship can be used, as seen in Eq. I.10:

$$\frac{Q}{\pi r^3} = \frac{1}{\tau_w}\int_0^{\tau_p} \tau^2 f(\tau) d\tau \tag{I.10}$$

where τ_w is the shear stress at the wall and can be calculated as:

$$\tau_w = \frac{D}{4}\frac{\Delta P}{L} \tag{I.11}$$

where $f(\tau) = \dot{\gamma}$ is the shear rate.

The differentiation of the Rabinowitsch expression Eq. I.10, with respect to τ_w, enables to obtain an expression of the shear rate at the wall, $\dot{\gamma_w}$:

$$\dot{\gamma}_w = \frac{3}{4}\left(\frac{8u_d}{D}\right) + \frac{1}{4}\left(\frac{8u_d}{D}\right)\frac{d\ln\frac{8u_d}{D}}{d\ln\tau_w} \tag{I.12}$$

with

$$n = \frac{d\ln\frac{8u_d}{D}}{d\ln\tau_p} \tag{I.13}$$

Therefore, the shear rate at the wall can be expressed as:

$$\dot{\gamma}_p = \frac{3n+1}{4n}\frac{8u_d}{D} \tag{I.14}$$

Thus, measurements of both pressure drop and flow rate are used to establish the rheological behaviour of the fluid, based on equations (I.11) and (I.14), i.e. the relationship between the shear stress at the wall τ_w and the shear rate $\dot{\gamma}_w$:

$$\tau_w = \tau(\dot{\gamma}_w) \tag{I.15}$$

I.3.2 Rheology of paraffin in water emulsion

"When using a PCME in the air conditioning field, it should be pumped continuously while going through multiple cycles of heating and cooling. Consequently, it is very important to characterize the rheological behaviour of the fluid in order to attain a stable emulsion, and to maintain a lower pump energy consumption. Different authors like Huang et al. (2009) and Huang et al. (2010a) or Inaba and Morita (1995), studied the paraffin in water emulsion and concluded that in order to be suitable as LFTF, a good knowledge of the rheological behaviour is needed."

Most of the results showed a non-Newtonian behaviour. The works of the literature also insist on the importance of understanding and controlling the dependence between the droplet size distribution and the viscosity of the emulsion, since the viscosity tends to increase as the droplet sizes decrease, (Schramm, 2005). Although PCMEs with fine droplets are much more stable than those with large droplets, they lead to a larger supercooling degree, (Wang *et al.*, 2004). Therefore, is imperative to find o trade-off when formulating the emulsion in order to obtain a PCME with low viscosity, small supercooling degree and good stability. In terms of stability of the emulsion, viscosity plays a very important role. An emulsion requires many

mechanical heating and cooling cycles, depending on its application, and therefore if it remains stable after pumping, the emulsion is considered kinetically stable. If we relate to applications in the air conditioning field, then a well-defined and as low as possible viscosity is required for a low pump energy consumption. Li-Xin (2001) investigated the rheological behaviour of two different concentrations of tetradecane emulsion, 49.8 wt. % and 16,3 wt. %. Authors used rotational viscometer for the study. Results showed a non-Newtonian behaviour and a very high viscosity for the concentrated emulsion. For the 49,8 wt. % PCME, the viscosity was 5 to 10 times higher than the one of 16.3 wt. % PCME after solidification of paraffin droplets. Moreover, the authors plotted the evolution of the viscosity as a function of the temperature. They determined that the viscosity of the 16.3 wt. % emulsion has a linear evolution with the temperature after the solidification point, while for the 49.8 wt. % the variation is much more visible.

Huang *et al.* (2009) studied different samples of paraffin emulsion. They concluded that for a 15-75 wt. % paraffin, all samples showed a pseudo plastic behaviour and the viscosity decreased with the increasing of the shear rate. According to authors the samples with 55-75 wt. % paraffin presented a viscosity larger than the ones with 15-50 wt. %. More results were presented by Huang *et al.* (2010a), who focused on the relationship between viscosity and temperature. Three types of PCMEs were tested and the results showed a shear-thinning behaviour for the fluids. These authors also tried to test the viscosity during phase change transition. They concluded that the temperature is very a important parameter when studying the rheology of emulsions. High jumps in the viscosity of the PCME were observed during tests, corresponding to the freezing point. In 2015, Huang and Petermann (2015) further studied different samples of 15-75 wt. % paraffin emulsion with 1.5 wt. % surfactant, using both rotation rheometer and pipe measurements. All samples showed a pseudo plastic behaviour. When the paraffin fraction exceeds 50 wt. %, the non-Newtonian behaviour and the viscosity presented a distinct increase. These authors suggested that a paraffin fraction between 20-50 wt. % is the most appropriate for applications in terms of rheology and thermal capacity. Therefore, a fraction of 30 wt. % was further investigated at different temperatures and pumped in a specific experimental rig, according to refrigeration applications requirements. These authors also reported pressure drops 1.5-3 times higher than the pressure drops of water, for a laminar flow.

Different values of viscosity are presented in Table 6. These first values of the viscosity are the first reported by literature for a PCME and show how large the viscosity of an emulsion depends on the concentration of the paraffin.

Table 6 Different values of viscosity reported in the literature

Author	Apparent viscosity [mPa·s]	Paraffin concentration	Information
Inaba and Morita (1995)	31,1 $2{,}5 \cdot 10^3$	c_m=5,0% c_m=40%	278,15 K
Ping-Yuan (2002)	24,5 150	c_m=16,3% c_m=49,8%	278,15 K
Chen *et al.* (2006)	8,46	c_m=30%	278,15 K

Among the work of Dai *et al.* (1997) the authors studied the dependence between the surfactant concentration and the viscosity. The experiment they performed showed that the viscosity of the PCME had a large increase from 0.55 to 2.94 $mm^2.s^{-1}$ when the concentration of surfactant increased from 2.6 wt. % to 4.7 wt. %.

Kappels *et al.* (2016) studied a PCME with three different paraffin concentrations, 25, 30 and 35 wt. % using a pipe viscometer. Tests were conducted for temperatures between 5 and 55 °C and shear rates from 0 to 1700 s^{-1}. Measured viscosities fell in the range 2.8 - 27.7 mPa.s. The dependency between the viscosity and paraffin concentration, temperature and state of the dispersed phase was demonstrated. According to the results, viscosity increases with the paraffin concentration and decreases linearly with the increase in temperature. Furthermore, during phase change a discontinuity in the rheological behaviour was observed.

I.4 Thermal behavior of two-phase secondary refrigerants

The main objective for the use of two-secondary refrigerants resides from the benefits such as the improvement in heat transfer and increase heat transport capacity.

Improvement in heat transfer occurs in two-phase secondary refrigerants, with or without phase change. This improvement is the main topic of this section (Section I.4). Several general characteristics, mechanisms responsible for this improvement and several drawbacks were examined, including thermal behaviour during cooling (Section I.4.1), heat transfer by

convection (Section I.4.2). Specific characteristics on the thermal behaviour of the PCMEs are then presented (Section I.4.3).

I.4.1 Thermal behaviour during cooling

This section will address topics as cooling in the absence of supercooling and the influence of the supercooling.

I.4.1.1 Cooling in the absence of supercooling

The ideal conditions for the cooling of a two-phase secondary refrigerant are satisfied when the PCM droplets change phase from liquid to solid, i.e. solidify, at the freezing temperature of the PCM, i.e. when the supercooling phenomenon is not present. Under these conditions, the thermogram for the cooling of a two-phase secondary refrigerant is divided into three parts, as shown in Fig. I-14.

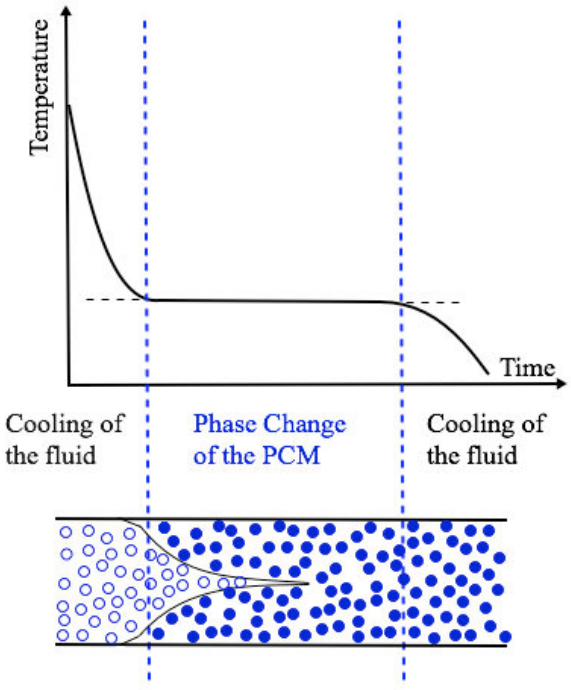

Figure I-14 Thermogram for cooling of a two-phase secondary refrigerant in ideal conditions

Let us imagine, by observing Fig. I-14 that a two-phase secondary refrigerant enters into a duct, from which heat is extracted. It enters at a temperature higher than the phase change temperature. It cools down until it reaches the phase change temperature. Beyond this point, the PCM droplets progressively change phase from liquid to solid state. The temperature remains constant during the process of solidification. Then, the temperature of

the suspension begins to decrease. This phenomenon involves a thermal equilibrium between the solid droplets and the carrier phase.

I.4.1.2 Influence of the supercooling over the heat transfer

When the two-phase secondary refrigerant reaches its freezing temperature, temperature is expected to remain constant and phase transition is expected to occur. However, there are circumstances in which two-phase secondary refrigerants temperature drops below this freezing point, and no transition happens. This condition is called supercooling and it was previously defined and presented in subchapters I.2.6.2 and I.2.6.3.

Unlike cooling, during heating of a two-phase secondary refrigerant, a liquid-solid equilibrium can be observed. We can define the degree of supercooling, as the difference between the melting temperature and the average temperature of crystallization. It represents the delay to the phase change. This degree of supercooling depends on many parameters (Dumas, 2002):

- volume of the sample: the smaller the volume is the higher degree of supercooling;
- the cooling rate: this setting has little effect;
- the number of cooling and heating cycles: from one cycle to another, there may be change in the results;
- concentration in the case of solutions;
- pressure: very high pressures are needed to have a significant influence on the degree of supercooling which then increases with pressure.

I.4.2 Convection heat transfer

In order to discuss the heat transfer for two-phase secondary refrigerants, we must refer to the heat transfer for single-phase secondary refrigerants. Since these fluids are still considered novel fluids, researcher in terms of heat transfer is based upon the fundamentals in the heat transfer of single-phase refrigerants. Therefore, a synthesis of the heat transfer by convection for single-phase fluids is presented before we develop what is truly specific to two-phase secondary refrigerants.

I.4.2.1 Theoretical background

Heat transfer is an exchange of thermal energy between a system and its environment or between two parts of a system when there is a temperature gradient between them. The transmission of heat by convection primarily occurs between a solid wall and a fluid that moves in contact therewith. Hence, when a fluid with the temperature T flowing in a channel with the wall temperature T_w, the temperature gradient between the wall and the fluid creates a heat transfer by convection, which tends to homogenize the temperature. Convection is governed by Newton's law, which states that the heat flux transferred is proportional to the difference between the wall temperature and the fluid temperature:

$$\dot{Q} = hS(T - T_w) \tag{I.16}$$

where h is the heat transfer coefficient and S the heat transfer area.

More commonly used is the dimensionless magnitude associated therewith: the Nusselt number Nu, which characterizes the intensity of the heat transfer. It represents the ratio between the convection heat flux and the conduction flux associated with the heat transfer fluid through a layer of equivalent thickness to the hydraulic diameter D_h. The Nusselt number depends mainly on the fluid properties and its flow regime:

$$Nu = \frac{h(T - T_w)}{-\lambda[(T_w - T)/D_h]} = \frac{hD_h}{\lambda} \tag{I.17}$$

Shah and London (1978) studied the forced convection heat transfer for a Newtonian single-phase fluid in laminar flow, incompressible, with constant physical properties. The heat equation they used, takes into account the sources of thermal energy, viscous dissipation, axial conduction and pressure forces. The study was done for a flow between two plates, with the following boundary conditions: heat flux density on the wall, $\dot{q} = cst$ and wall temperature $T_w = cst$.

Figure I-15 represents the flow of a fluid entering a channel with a constant velocity u_e. When a fluid flows along a wall, the fluid right next to the wall sticks to the wall. That fluid shears the fluid next to it and slows it down. Therefore, because of contact with the inner surface of the channel, a *hydrodynamic boundary layer* appears. The increase of the boundary

layer thickness with the distance determines the shrinkage of the inviscid region (without viscosity) and leads to its disappearance.

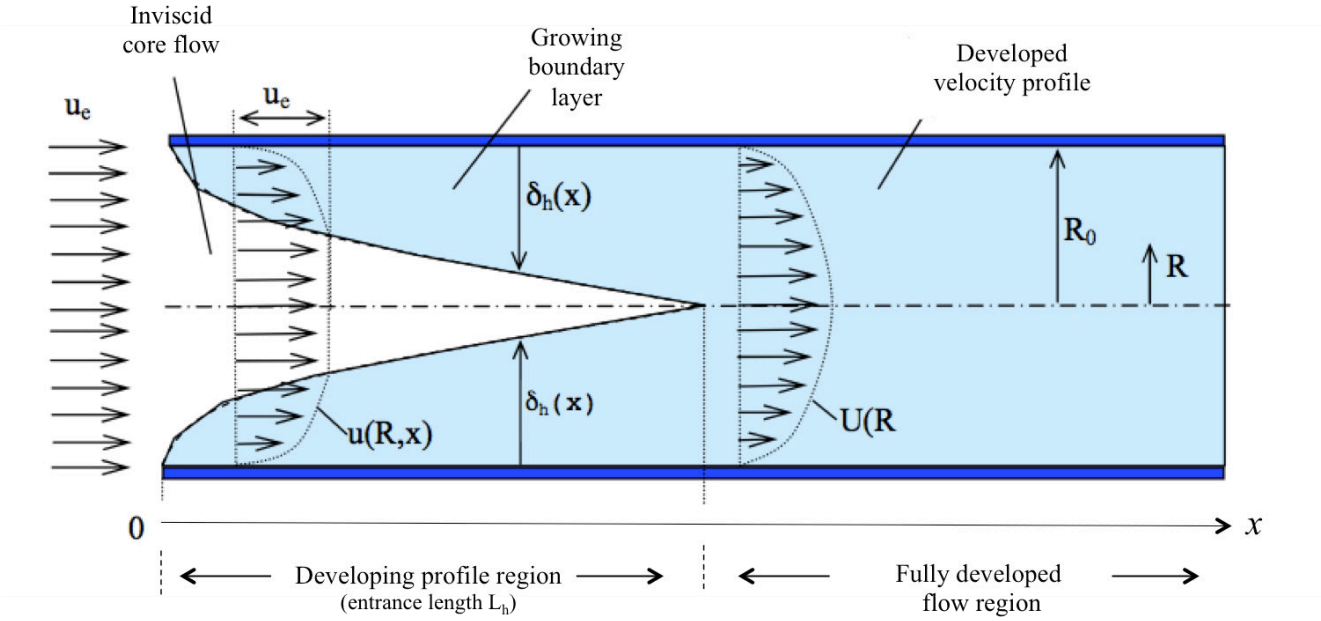

Figure I-15 Development of the hydrodynamic boundary layer

The distance from the entrance of the channel where the thickness of the boundary layer reaches the symmetry axis of the channel ($\delta_h = R_0$) is called the hydrodynamic entry length. The thickness of the hydrodynamic boundary layer is a function of the rate of increase of the boundary layer with the distance, which in turn is a function of the flow regime (laminar or turbulent). For laminar flow between two parallel plates, Atkinson *et al.* (1969) cited by Huetz and Petit (1990) proposed the following correlation to evaluate the entry length:

$$\frac{L_h}{D_h} = 0{,}3125 + 0{,}011 Re_{D_h} \tag{I.18}$$

For the same type of flow, Barber and Emerson (2000) propose the use of a more sophisticated correlation suggested by Chen (1973):

$$\frac{L_h}{D_h} = \frac{0{,}315}{0{,}175 Re_{D_h} + 1} + 0{,}011 Re_{D_h} \tag{I.19}$$

When a fluid enters a channel or a conduit with a uniform temperature different from that of the of the surface temperature, a heat transfer process occurs and a *thermal boundary layer* starts to grow, as illustrated in Fig. I-16.

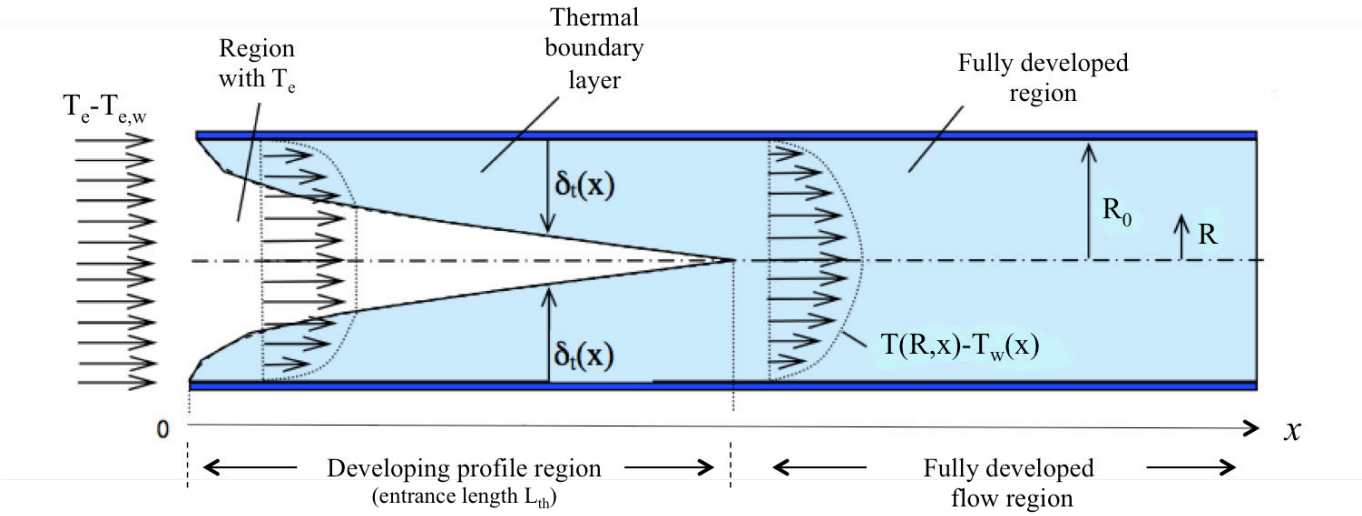

Figure I-16 Development of the thermal boundary layer

As in the case of the hydrodynamic boundary layer, there is an axial coordinate for which the thermal boundary layer fills the whole cross-section. The distance between the inlet of the channel and this coordinate is called thermal entrance length, L_{th}. This length is important in laminar flow, as it becomes very important for a high value of the Prandtl number.

The length required to establish the temperature profile for a flow between two plates and for a uniform temperature on the surface can be calculated by the relationship Shah (1975), cited by Huetz and Petit (1990):

$$\frac{L_{th}}{D_h} = 8 \cdot 10^{-3} Pe_{D_h} \tag{I.20}$$

where Pe_{Dh} represents the number Peclet of the fluid ($Pe_{Dh} = Re_{Dh} \cdot Pr$).

For a heat flux density, $\dot{q} = cst$, Shah suggested the following correlation:

$$\frac{L_{th}}{D_h} = 0{,}0115 Pe_{D_h} \tag{I.21}$$

Table 7 illustrates different correlations for the Nusselt number, that were proposed by Shah. They are based on the dimensionless length, x^* or L^*, following the local nature (x^*) or

overall (L^*) of the Nusselt number.

$$x^* = \frac{x}{D_h Pe_{D_h}} \text{ and } L^* = \frac{L}{D_L Pe_{D_L}} \quad \text{(I.22)}$$

The correlations of Table 7 are valid for a fully developed velocity profile and a developing temperature profile. In the literature, the formulation of the Nusselt number based on Graetz theory is used. The Graetz number (Gz) represents the inverse of x^* or L^*, depending on the nature of the phenomenon: local or global.

Table 7 Expression of the Nusselt number for a developed velocity profile and a developing thermal profile (Huetz and Petit, 1991)

Expression of the Nusselt number		Validity
Isothermal parallel plates (T_w=cst)		
Local Nu	$Nu_{D_h}(x) = 1.233(x^*)^{-1/3} + 0.4$	$x^* \leq 10^{-3}$
	$Nu_{D_h}(x) = 7.541 + 6.874(10^3 x^*)^{-0,488} e^{-245x^*}$	$x^* > 10^{-3}$
Average Nu	$Nu_a = 1.849(L^*)^{-1/3}$	$L^* \leq 5 \cdot 10^{-4}$
	$Nu_a = 1.849(L^*)^{-1/3} + 0,6$	$5 \cdot 10^{-4} < L^* \leq 6 \cdot 10^{-3}$
	$Nu_a = 7.541 + \frac{0.0235}{L^*}$	$L^* > 6 \cdot 10^{-3}$
Parallel plates at constant surface heat flux		
Local Nu	$Nu_{D_h}(x) = 1.490(x^*)^{-1/3}$	$x^* \leq 2 \cdot 10^{-4}$
	$Nu_{D_h}(x) = 1.490(x^*)^{-1/3} - 0.4$	$2 \cdot 10^{-4} < x^* \leq 10^{-3}$
	$Nu_{D_h}(x) = 8.235 + 8.68(10^3 x^*)^{-0,506} e^{-164x^*}$	$x^* > 10^{-3}$
Average Nu	$Nu_a = 2.236(L^*)^{-1/3}$	$L^* \leq 10^{-3}$
	$Nu_a = 2.236(L^*)^{-1/3} + 0.9$	$10^{-3} < L^* < 10^{-2}$
	$Nu_a = 8.235 + \frac{0.0364}{L^*}$	$L^* \geq 6 \cdot 10^{-2}$

When the hydrodynamic profile and temperature profile are established, the flow is called fully developed. At the inlet of the channel (x=0) the Nusselt number has an infinite value, and after, it decreases asymptotically towards the fully developed region where it becomes constant, independent of the values of both Reynolds and Prandtl numbers. In this case, for a rectangular channel (with a width *a* and a height *b)* with an a/b ratio (width / height) larger than 10 (in our case a/b = 13.33), the values proposed by Shah and London (1978) are:

- for a constant wall temperature: Nu=7.541;
- for a constant heat flux: Nu=8.23

I.4.2.2 Heat transfer studies for two-phase secondary refrigerants

For suspensions with PCM droplets, the convection heat transfer can be greatly increased by the phase change of the droplets. Phase change may modify the temperature distribution and velocities in the flow, viscosity, average specific heat capacity and other thermodynamic parameters of the suspension. Because of the large number of parameters involved, theoretical and experimental approaches to phase change slurries are difficult. Hu and Zhang (2002) found that conventional correlations for the Nusselt number could not describe with accuracy the behaviour of a suspension with phase change for which the apparent specific heat is strongly dependent on temperature.

For calculating the Nusselt number in the laminar flow of ice slurry in a conduit circular with constant surface heat flux, Ben Lakhdar *et al.* (1999) suggested a correlation based on the number of Graetz (Gz):

$$Nu_D = 38.3 Gz^{0,15} c_m^{0,52} \quad \text{(I.23)}$$

where $Gz = \pi RePrD/4x$ and x is the axial postion; Re and Pr in the expression of Graetz are calculated for the average properties of the ice slurry. Equation I.23 is valid for $3 < Re < 2000$ and $5 \cdot 10^3 < Gz < 10^6$ and $0 < c_m < 35\%$. The uncertainty of the correlation is about 13% and was deducted from 245 experimental points.

Stamatiou and Kawaji (2005) conducted an experimental study in order to characterize the thermal behaviour of the ice slurry flowing vertically, upward in a rectangular channel

having a height/width ratio equal to 1/12. The authors modified the correlation Ben Lakdar *et al.* (1999) by adding a correction on viscosity using 180 experimental points:

$$Nu_D = 4Gz^{0,486} c_m^{0,30} \left(\frac{\mu_f}{\mu_w}\right)^{0,24} \quad \text{(I.24)}$$

The uncertainty of the correlation is about 15% and is valid for $2100 < Re < 4000$ and $1 < c_m < 25\%$.

El Boujaddaini (2013) conducted an experimental study in order to characterize the thermal behaviour of a paraffin slurry flowing vertically, upward in a rectangular channel designed at The Centre for Energy and Thermal Sciences of Lyon (CETHIL). The author proposed a correlation between the local Nusselt number ($\frac{hD_h}{\lambda}$), the Reynolds number, the Prandtl number ($\frac{c_p \mu}{\lambda}$), the dimensionless axial position ($\frac{x}{D_h}$) and the paraffin mass fraction C_m :

$$Nu(x) = 0.223\mathrm{Re}^{0,78}\mathrm{Pr}^{0,34} \left(\frac{x}{D_h}\right)^{-0,082} (1 + C_m)^{2,5} \quad \text{(I.25)}$$

For the average Nusselt number, the author proposed two different correlations, one for 6 wt. % paraffin and a second one for 12 wt. % paraffin.

$$Nu_{6\%} = 0.726\mathrm{Re}^{0,76}\mathrm{Pr}^{0,34} \quad \text{(I.26)}$$

$$Nu_{12\%} = 0.893\mathrm{Re}^{0,68}\mathrm{Pr}^{0,34} \quad \text{(I.27)}$$

These correlation are valid for $400 \leq \mathrm{Re} \leq 2500$, $30 \leq \mathrm{PR} \leq 110$ and $\frac{L}{D_h} \geq 20$.

I.4.3 Thermal behaviour of a paraffin in water emulsion

As other PCSs, phase change emulsions, in comparison to conventional single-phase heat transfer fluids present considerable heat transfer enhancements. Huang *et al.* (2010a)

showed that the micro-sized PCM droplets can enlarge the surface-to-volume rate, respectively increase the heat transfer rate. Furthermore, as the PCME remains pumpable and fluid after phase change, the domination heat transfer process during solidification is the convection heat transfer instead of conduction heat transfer.

The results of Roy and Avanic (1997) showed that the heat transfer characteristics for PCMEs are similar to those of microencapsulated phase change slurries. A second conclusion was that the global heat transfer coefficient did not change too much for different paraffin concentrations. The authors also confirmed, that the supercooling degree and its melting temperature need to be further investigated as they are very important topics for PCMEs.

Zhao *et al.* (2001) studied an oil-in-water (O/W) emulsion in a circular tube and showed that Nusselt numbers for an emulsion with 2 (13 and 40 wt. %) different paraffin concentrations had almost the same values. The convection heat transfer coefficients were increased by phase change but not affected by the concentration. Zhao *et al.* (2002) continued the work on emulsions but in coiled tubes and further showed that for the same concentration in paraffin, the Nusselt number of the emulsions is higher than that of water.

Eunusoo *et al.* (1994) studied the turbulent flow of a hexadecane emulsion, circulating through a circular tube. They proposed a three-region melting model, which was used to determine the bulk mean temperature of the emulsion along the heating section. Results showed that local convection heat transfer coefficient was increasing in Region I, decreasing in Region II (during phase change) and increasing again in Region III. The authors suggested that due to the increase of the temperature along the channel, viscosity dropped and therefore heat transfer coefficients increased. On the other hand, because the melted PCM formed a thicker layer close to the wall when the heat flux was very high, the heat transfer coefficients presented lower values.

In 2001, Choi and Cho did further studies on PCMEs. They particularly investigated the influence of the aspect ratio (AR, height/width ratio) of a rectangular channel during cooling of a PCME. They demonstrated that local heat transfer coefficients for 5 wt. % PCME were larger than for water. Other results showed that differences of the local heat transfer coefficients between the emulsion and water increased with the reduction of the aspect ratio.

Up to now, a limited amount of work (Huang *et al.*, 2009; Huang *et al.*, 2010a,b,c; Youssef *et al.*, 2013; Shao *et al.*, 2016; Delgado *et al.*, 2015; Kawanami *et al.*, 2016) has been conducted on the use of emulsions in air conditioning systems because of practical difficulties such as high viscosity and instability problems during the cooling process.

With continuous research on PCMEs (Huang and Petermann, 2015; Morimoto *et al.*, 2016; Zhang *et al.*, 2016; Shao *et al.*, 2015), progress has been made but the majority of the studies in the literature are focused on the thermophysical properties and phase transition temperature while the studies on the heat transfer remain scarce.

In this chapter, a literature review regarding refrigeration production was introduced as a necessary background for the experimental results presented in this thesis. Single-phase refrigerants and two-phase secondary refrigerants were presented. Their thermal and rheological behaviour was exposed. Main criteria on the Phase Change Material Emulsions that are already reported in the literature were then presented:

- *Composition and production technology*
- *Description of the components*
- *Thermophysicial properties*
- *Stability problems*
- *Practical applications*

This review has focused, on one hand, on the elaboration and fabrication of the PCMEs. On the other hand, this review focused on the analysis of thermophysical properties, which is a key factor in the development of paraffin emulsions. The main problems concerning PCMEs are the subcooling and instability problems. Regarding heat transfer applications, high heat transfer coefficients are desirable in comparison to a single-phase refrigerant.

At the present time, there is a lack of experimental studies, which are necessary to fully characterize the PCMEs and their potential use in industrial applications.

CHAPTER II

The purpose of this chapter is to provide information about the test facility and the methods used to study experimentally a two-phase secondary refrigerant. Section II.1 Experimental setup and instrumentation) consists in three parts: experimental setup for heat transfer detailed in Section II.1.1, experimental setup for rheology detailed in Section II.1.2 and other measuring instruments presented in Section II.1.3. Measurement and

II. Materials and methods

The instrumentation used for the experiments was selected and applied for the measurement of all the physical quantities necessary for determining the thermal and rheological performance of the PCME. The measured quantities, in both heat transfer setup and rheology setup tests, included temperatures and flow rates. All instruments have analogue outputs, which are sent to a PC via the data acquisition system. A description of the supplementary measuring instruments used for the thermophysical properties of the fluid is presented in this section, organized separately from the heat transfer setup and rheology setup.

II.1 Experimental set up and instrumentation

The test bench designed by Ionescu (2008) during his thesis represents the starting point of the present work.

II.1.1 Heat transfer setup

The design and assembly of the experimental heat transfer setup was made within the laboratory CETHIL from the early work of Bel (1996) through successive PhD thesis. The two-phase secondary refrigerant studied is a phase change material emulsion (paraffin droplets) with water as carrier fluid.

Figure II-1 Illustration of the experimental heat transfer setup

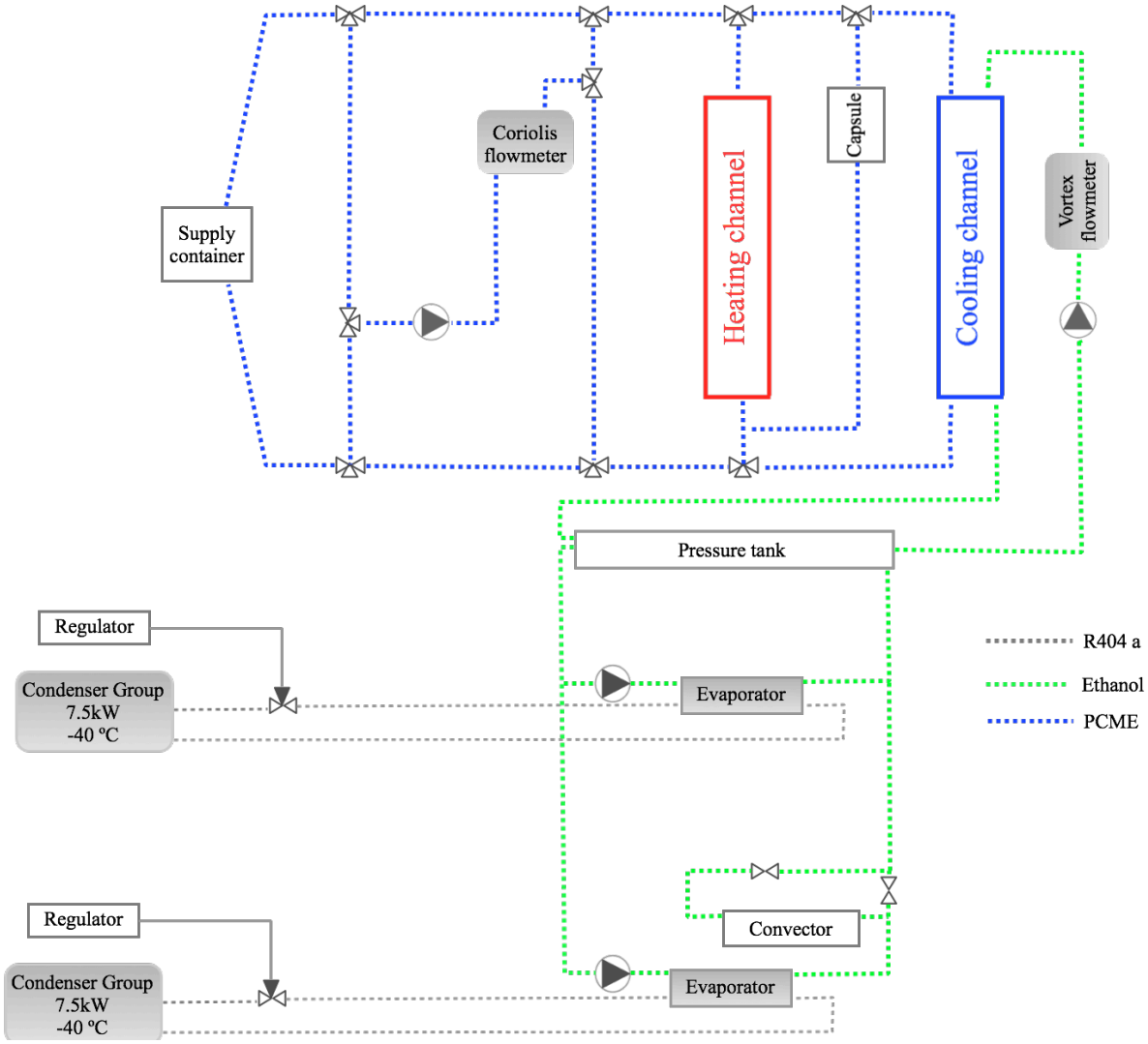

Figure II-2 Schematic of the experimental heat transfer setup

The diagram of the experimental set up is represented photographally in Fig. II-1 and schematically in Fig. II-2. The experimental heat transfer setup is composed of three circuits; a circuit of ethanol which is used as the cold source that achieves temperatures as low as - 40 °C, a refrigerant used to prepare the ethanol at - 40 °C circuit and a PCME circuit which is used for the characterization of the thermal and rheological behaviour of the emulsion. The three circuits are connected by plate heat exchangers, which will be presented later.

II.1.1.1 Refrigerant circuit

The refrigerant used is R404a. R404A is a HFC blend consisting of 44 wt. % of R125, 52 wt. % of R143a and 4 wt. % of R134a. It is widely used in low and medium temperature refrigeration applications, such as those used in commercial refrigeration. The refrigerant

circuit (Fig. II-3) is composed of two identical condensing units (COPELAND). The refrigeration capacity of each unit is between 6.18 and 34.36 kilowatts, depending on temperature. Throughout the tests, it was used at an evaporation temperature of -40 ° C which corresponds to a cooling capacity of 7.5 kW.

Each refrigerant group consists of the following elements:

- a condenser wherein the refrigerant is cooled by the atmospheric air;
- a hermetic compressor (COPELAND, ZF48KE-model TWD);
- a storage tank for the refrigerant;
- an electronic expansion valve (type EX2), which regulates the supply of the evaporator with refrigerant (depending on the temperature of the ethanol at the outlet of evaporators). An electronic controller, ALCO CONTROLS EC2, controls the regulator.

These condensing units are equipped with an electronic controller ALCO CONTROLS EC2, which has the function of controlling the electronic expansion valve ALCO CONTROLS EX2 that adjusts the refrigerant superheat at the outlet of the evaporator. The refrigerant circuit includes two identical evaporators, which are typical plate heat exchangers (SWEP SSP 2000 model V80x40H / 1P) with 40 stainless steel plates (AINSI 316L). In the primary circuit of the heat exchanger circulates the refrigerant R404a and in the secondary circuit circulates in counter current, the ethanol. For an exchanged heat power of 8 kW, these exchangers are capable of cooling 4 $m^3.h^{-1}$ ethanol from– 40 °C down to – 45 °C.

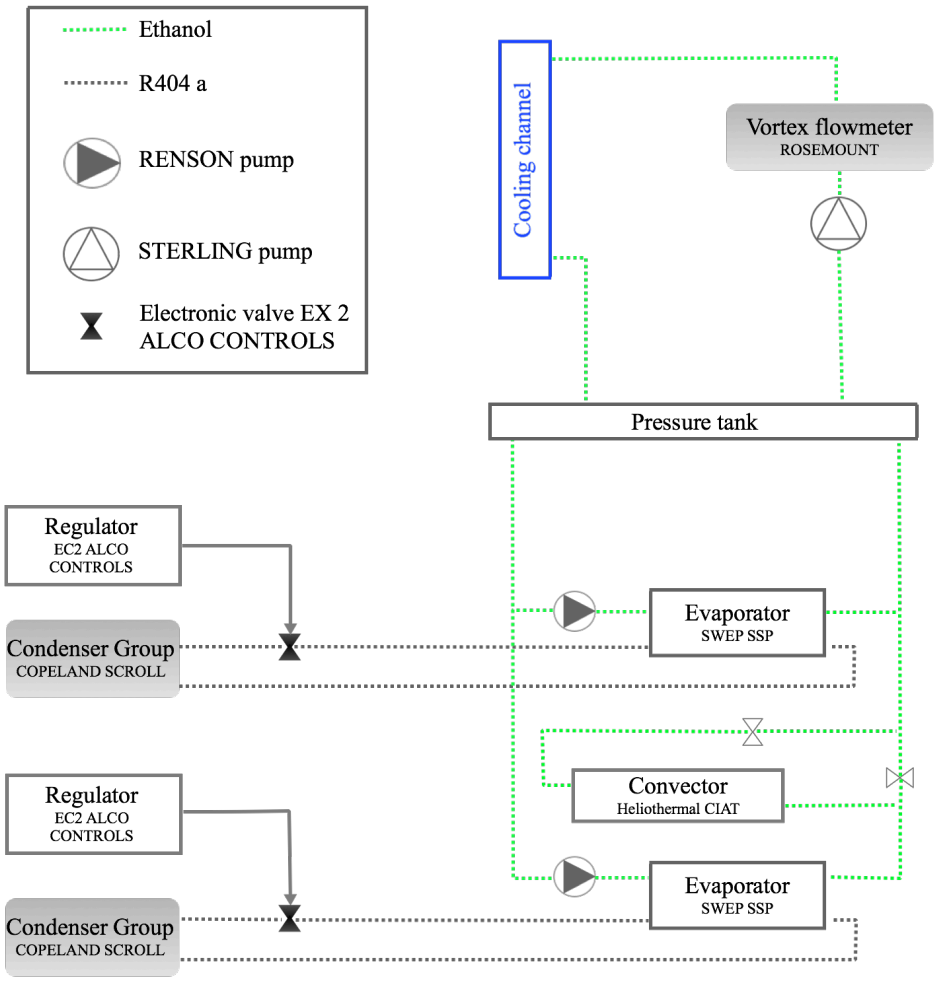

Figure II-3 Circuits of R404a and ethanol

II.1.1.2 Ethanol circuit

The ethanol circuit, illustrated in Fig. II-3, contains three pumps:

- two liquid ring pumps type RENSON AL25 of a maximal power of 1.2 kW at 2800 $tr.min^{-1}$;
- a third centrifugal pump STERLING type ZLND of 2.2 kW at 1450 $tr.min^{-1}$.

Both RENSON pumps allow the circulation of the ethanol in the evaporators and the heater while the STERLING pump ensures the circulation of the ethanol into the cooling channel. The cooled ethanol is introduced into a tank whose role is to stabilize the pressure for the main ethanol pump. The ethanol circuit comprises three heat exchangers: the two evaporators used to cool the ethanol arriving to the flow the refrigerant R404a and a coil heat exchanger (CIAT 2450 HELIO 3 WALL N1 R) illustrated in Figure II-4. This heat exchanger

allows three flow rates for the air, which serves to maintain the energy balance of the system. By heating a portion of the ethanol using air, the heater is used to control the temperature of the ethanol at the inlet of the cooling channel. Two manual valves (quarter turn (ALCO type BVA 138 RO124)) are used to control the flow rate through the heater (Fig. II-5). A servomotor type SAUTER AVM234S controlled by a controller 6100 WEST ensures the adjustment of the SAUTER MV43216 valve set on the circuit of the heater (Fig. II- 4 (b)).

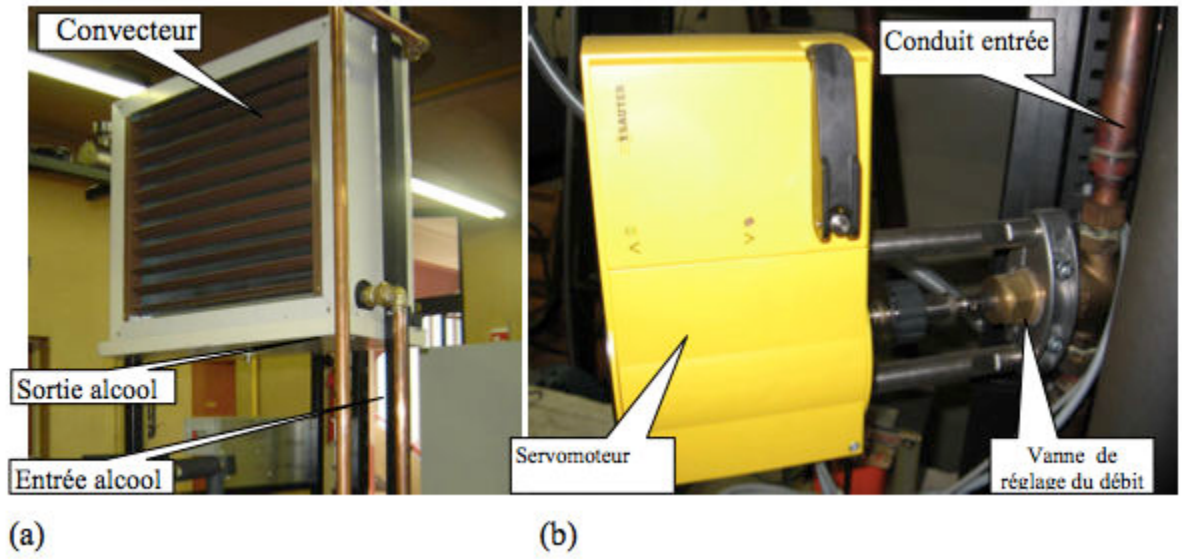

Figure II-4 Circuits of R404a and ethanol Ethanol heating system a) HELIOTHERME CIAT coil b) adjustment of the ethanol mass flow

The adjustment of this valve is made according to the temperature of the ethanol at the outlet of the pressure tank. Thus, a part of the ethanol is circulating through the heater and the other part circulating directly to the pressure tank. A vortex flow meter type 8800 ROSEMOUNT is used for measuring the mass flow of the ethanol circulating through the cooling channel. This flow meter outputs a 4-20 mA signal proportional to the mass flow rate. An expansion tank is provided for compensating the variations in the ethanol's volume due to temperature variations. This tank is connected to the outlet of the heater at the highest point of the installation.

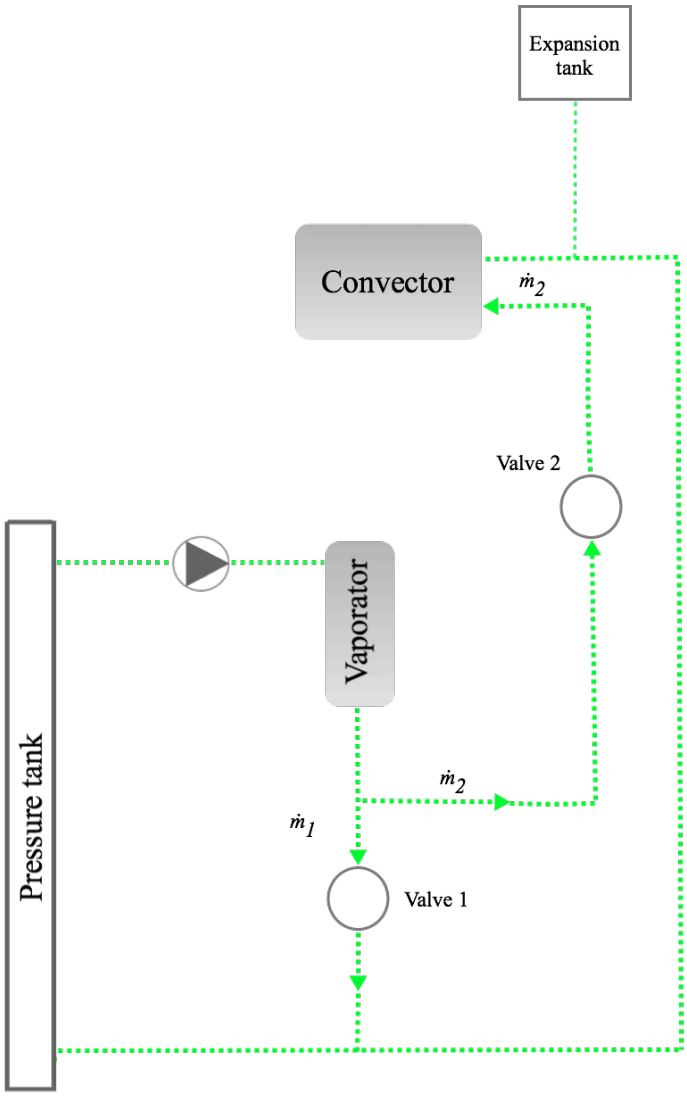

Figure II-5 Manual control valves of the ethanol charge through the heater (convector)

II.1.1.3 Two-phase secondary refrigerant circuit (also named PCME circuit)

The paraffin-in-water emulsion is circulated in the two-phase secondary refrigerant circuit, shown on Fig. II-6. The PCME circuit is mostly made out of partially transparent PVC tubes with an internal diameter of 56 mm and of two rectangular channels that are typical of plate heat exchangers. They represent the cooling section and the heating section of the circuit. The cooling channel provides the connection between the ethanol circuit and the circuit of the secondary refrigerant. A Coriolis mass flowmeter (Micro Motion) is used to measure the mass flow rate of the PCME. The circulation of the paraffin emulsion is ensured by a vortex pump (TURO EGGER-kind T21-32 HF4 LB1). A specific feature of this pump

lies in the retracted position of the wheel towards the stator, which provides a limitation of the contact between the fluid and the wheel to a maximum of 15% of the flow, thus avoiding high particles shear. The nominal power output of the pump is 2.2 kW and the flow rate adjustment of the PCME is provided by a DANFOSS frequency converter (type VL103), with a rotational speed of 600 to 3000 rot.min^{-1} (10 to 50 Hz).

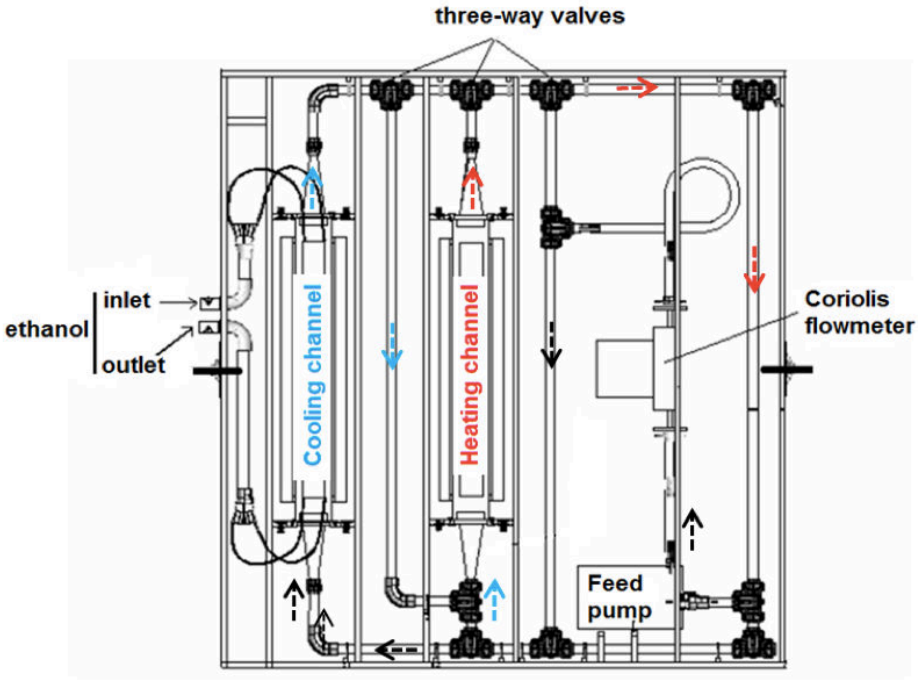

Figure II-6 Schematic of the PCME circuit

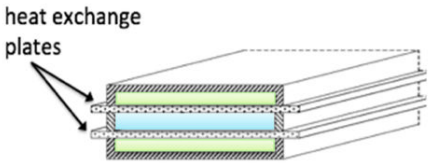

Figure II-7 Geometry of the cooling section

Cooling channel

The cooling section has three channels, shown schematically in Fig.II-7. Two steel plates and two polypropylene shells delimit the channel for the ethanol. Thus, the cooling section is 1000 mm long, 80 mm wide and 4 mm thick. The paraffin emulsion circulates between the two steel plates forming the central channel; it enters the bottom and exits through its upper part. This channel is formed by two stainless steel (304) plates 130 mm wide, 4.5 mm thick and 1110 mm long. The channel thickness is fixed at 6 mm by means of two spacers (6x3x1110 mm^3) made of polyethylene, which also provide the lateral sealing of

the channels. The inlet and outlet of the ethanol is made by 5 supply tubes (Fig. II-8) that are attached to the shells made of polypropylene for a uniform flow on the plates. The temperature of the ethanol conditions the plate heat exchanger during the cooling of the emulsion.

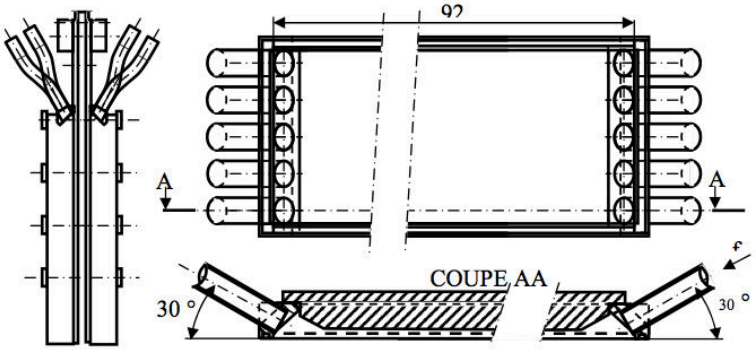

Figure II-8 Ethanol channel (El Boujaddaini, 2013)

The paraffin emulsion enters the channels through a copper convergent, which allows the adjustment of the section from a circular section (pipes) to a rectangular section without any change in the value of this section. The sizing of the convergent was performed using Fluent code in order to be sure to obtain a hydrodynamically established flow, at the beginning of the inlet of the cooling channel. The outlet of the cooling channel is made by a divergent with the same dimensions as those of the convergent (Fig. II-9). The convergent and divergent are attached to the channel by means of fixing steel plates placed on pins of stainless steel. The sealing between the convergent/divergent and both sides of the channel is performed by means of rubber seals.

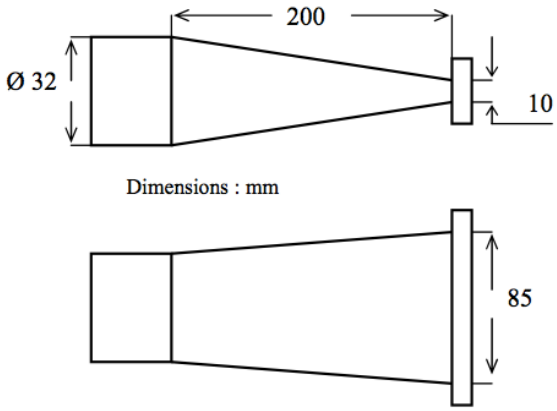

Figure II-9 Inlet convergent and outlet divergent for the cooling channel (El Boujaddaini, 2013)

Heating channel

The heating section has the same geometry and dimensions as the cooling section. Electric resistors are employed to heat the heating channel and temperatures along the channel are measured by K-type (copper-constantan), thermocouples in many points of the circuit. There are 18 resistors, ensuring a maximum power of 3.7 kW.

II.1.1.4 Measuring instruments

In this work, different physical quantities were measured; thus the following section presents a detailed description of all the measuring instruments used in order to measure these physical quantities.

1. Temperature measurements

Thirty-six thermocouples are necessary for each channel to measure nine local heat fluxes on each side of the plates that form the cooling channel. They are coupled one by one, in pairs, and placed on each side of the steel plate. Thus, one pair of thermocouples and the wall of the plate form a fluxmeter. Two other K-type thermocouples are used to measure the inlet and outlet temperature of the PCME in the cooling channel. Two thermocouples of the same type are placed on the ethanol circuit to measure the inlet and outlet temperatures of the ethanol. Figure II-10 shows the positioning of the thermocouples on the steel plates.

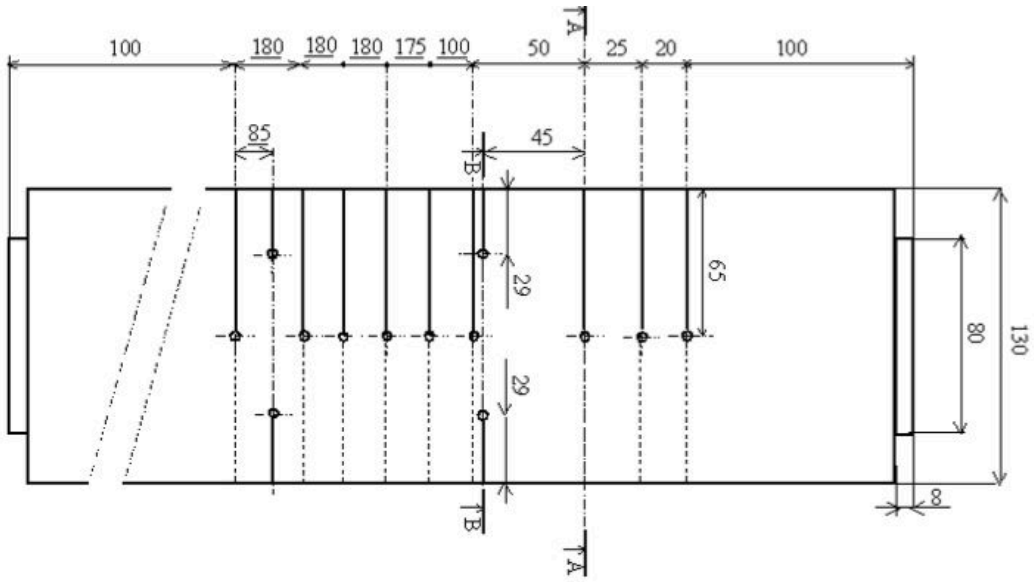

Figure II-10 Thermocouples position on the steel plates

The hot junction of the thermocouples is placed on the midline of the plate in a 25/100 mm deep cavity and 4 mm in diameter, using a 60/40 lead-tin solder with a thermal conductivity of 50 $Wm^{-1}. K^{-1}$.

The thickness of the tin pellet is sufficiently small (0.25 mm) to ensure that the measured temperature is that of the surface of the plate. The wires of the thermocouple are placed in grooves of 1x1 mm and then embedded in a two-component flowable epoxy resin, highly charged in aluminium powder (for temperatures between -30 and +95 °C).

2. Mass flow measurements

Measuring mass flow rates of the fluids in the installation is done using two flowmeters. The flow rate of the PCME is measured by a Coriolis effect mass flow meter (Micro Motion) placed just after the pup. Its measuring range is 0-5000 $kg.h^{-1}$. Its measuring accuracy, given by the manufacturer, is equal to ± 0.15%. It directly measures the mass flow without any correction. The mass flow of the ethanol in the cooling channel is measured with a vortex flowmeter ROSEMOUNT 8800, that measures the frequency of the vortex's detachment produced by a bar, placed perpendicularly to the fluid flow. The flowmeter converts the frequency into a 4-20 mA signal that is then converted into flow rate value by the central data acquisition. The measuring range of this flow meter is 0 - 7200 $kg.h^{-1}$.

3. Density measurements

The transmitter used to measure the mass flow of the PCME is equipped with a digital output (0-40 kHz) that provides a frequency proportional to the density of the fluid. Using an acquisition with the output values of the frequency and the corresponding values of the density displayed by the transmitter. Its calibration curve is displayed on Fig. II-11.

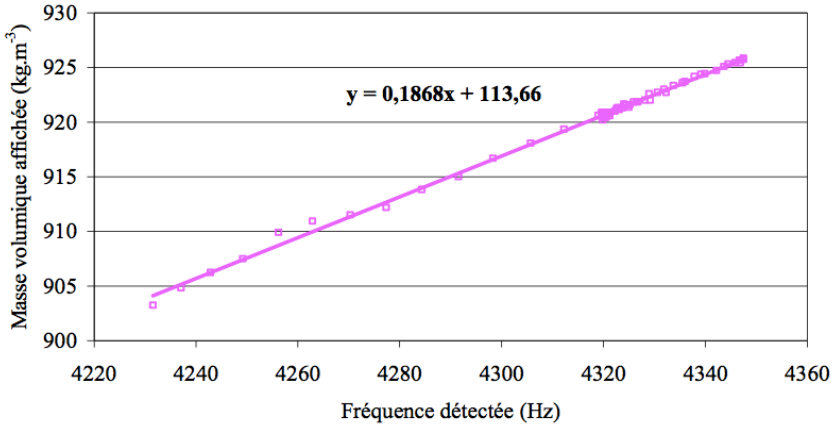

Figure II-11 Calibration curve for the density measurements

4. Electrical power measurements

A triode thyristor (“triac”; EUROTHERM TE200S) is used to adjust the electrical power of the resistors in the heating channel, depending on the temperature set on the controller. A PT 100 sensor is attached to the outlet of the heating channel, on the divergent. This sensor delivers a signal to a temperature controller WEST5010. This group of devices enables adjusting the PCME temperature at the outlet of the circuit. It also sets a constant electric power, thereby providing a constant heat flux on the plates of the heating channel.

5. Central data acquisition

The entire ensemble of the measured quantities described above is recorded by a data acquisition system, type Keithley 2750 with two cards for data acquisition, connected to a computer. A card with 40 channels (model 7708) is used for the acquisition of the temperatures. Initially, determination of temperature was carried out with a cold junction compensation based on the temperature of the card itself. After a calibration of the temperatures, a significant temperature gradient was observed on the card, causing large errors in the results. To overcome this problem, a cold junction compensation device was built during previous PhD thesis prepared on this setup. This box, thermally insulated, allows the cold junction compensation from the constant temperature measured by a PT sensor 100 placed in the box. The acquisition of the mass flow rates, density and electric power is made on the second card (model 7700) with 20 channels. The currents from the various sensors are converted to voltage using calibrated resistors of 47.12 Ω. Measurements of the power delivered to the electrical resistances are carried out by a HIOKI 3193 recorder which also allows reading the energy consumed by the integration over a time interval corresponding to the measurement acquisition period.

The acquisition system is connected to a laptop via a RS232 connection. The ExceLINXTM software delivered with the system allows the acquisition of data to an Excel file.

II.1.2 Rheology Setup

The experimental setup used for the rheology characterization is illustrated in Fig. II - 12. The measuring section is composed mainly of a copper tube with an inner diameter of 8 mm. The fluid is transported to the measuring section with a PQA60 Pedrollo Pump. Measurements of temperature, volume flow rate and differential pressure are used to characterize the rheological behaviour of the fluid.

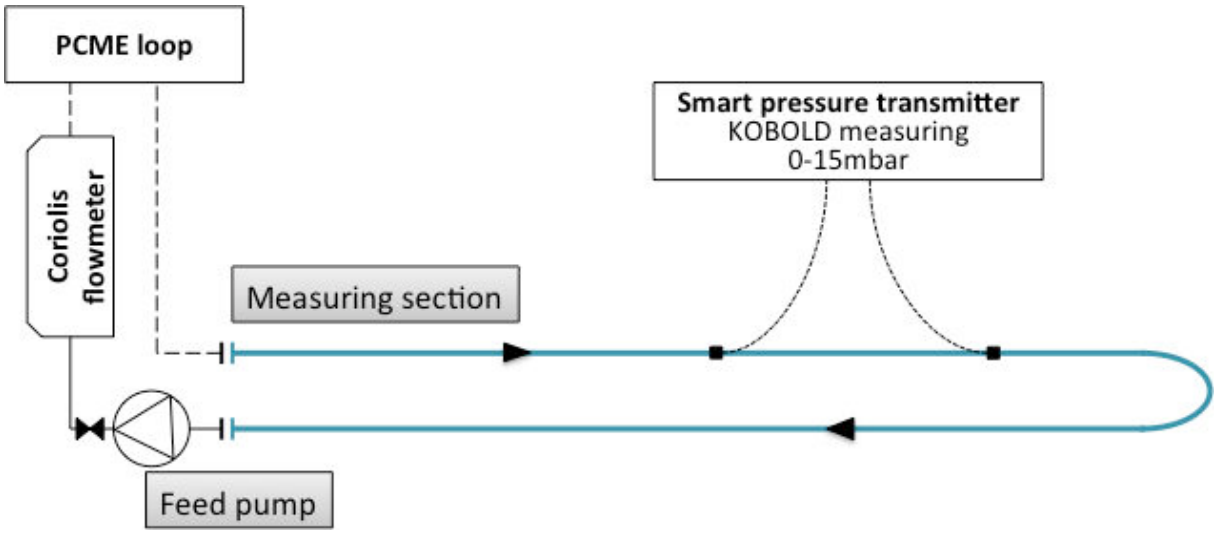

Figure II-12 Experimental setup for the rheology characterization

For measuring the differential pressure, a Kobold smart pressure transmitter is used. For values of 0 to 15 mbar this smart pressure transmitter operates with a standard error of ±0.075%. The volume flow is measured with a Micro motion Coriolis type flow meter with a standard error down to ±0.4% of the flow rate.

II.2 Other measuring instruments

As mentioned previously several additional instruments were used in order to perform different measurements for determining the thermophysical properties of the studied fluids.

II.2.1 Differential Scanning Calorimetry

Differential Scanning Calorimetry (DSC) is a thermo analytical technique used for measuring how physical properties of a sample change, along with temperature against time. The procedure involves measuring the amount of heat required to increase the temperature of a sample and reference. During experiments, both the sample and reference are maintained at nearly the same temperature. The difference in the input energy required to match the temperature of the sample to that of the reference is the amount of excess heat absorbed or released in the sample. Two such devices were used to determine the specific heat capacity and the phase change enthalpy of the tested fluids, but also to investigate their behaviour during heating and cooling. One of them was a Mettler Toledo DSC823e with a typical sample size of 10-20 mg and a typical heating/cooling rate of 1-2 $K.min^{-1}$. The second one is a

NETZSCH DSC204 with a sample of 18-22 mg and a heating rate of 1 $K.min^{-1}$. DSC measurements have this particular feature that allows the user to visualize the supercooling of the samples during their cooling. This feature must however be considered as only informative because DSC measurements and PCME in operation do not exhibit the same subcooling because of the differences in the sample sizes.

II.2.2 Analytical Balance

An analytical METLER Toledo XA 105 balance was used in order to estimate the density for the studied PCMEs.

II.2.3 Particle size distribution

In order to analyse the quality of emulsions, the particle size needs to be measured. A Beckman Coulter LS 13320 with Polarization Intensity Differential Scattering (PIDS) and Laser Diffraction was used for the measurements. The measuring range lies between 0.04 – 2000 µm which is in agreement with relevant standards (DIN ISO 9276, DIN ISO 9276-2, ISO/TR 13097).

II.2.4 Stability analysis

When applied in industrial setups, a very important parameter for the PCMEs is the shelf life and stability under thermal-mechanical loads. Therefore, the long-term stability of the PCME was investigated using a LUMiSizer centrifuge, which is capable of scattering light transmission through the sample. This centrifuge is able to analyse the emulsions for creaming and sedimentation phenomena. The major advantage of this instrument is that while most of the techniques focus on a single point of the sample, this one gives a global view over the entire sample from the bottom to the top. In Fig. II - 13 a schematic diagram of the centrifuge and the technology is presented. When the centrifuge is functioning, samples are exposed to up to 2300 times the gravitational acceleration. In order to obtain the lifespan at $g = 9.82\ m.s^{-2,}$ the measuring time is multiplied with the applied gravitational acceleration.

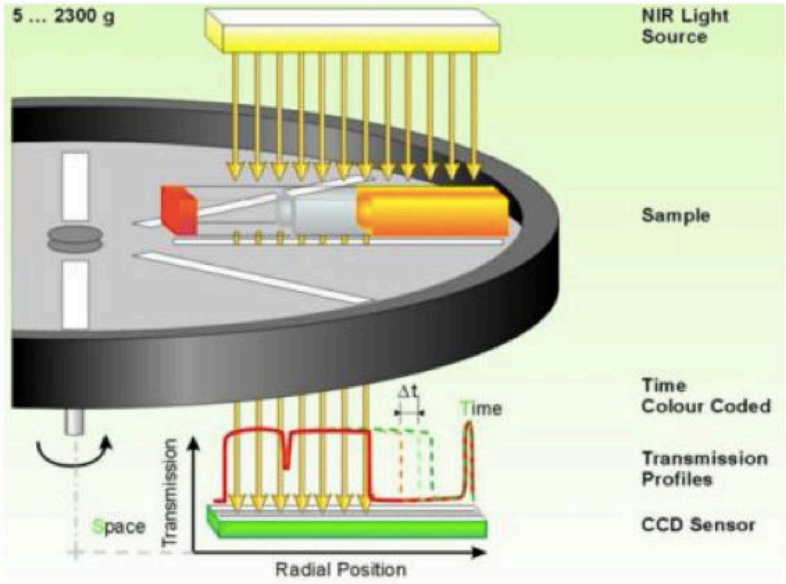

Figure II-13 Functional diagram of the LUMSizer (Sobisch and Lerche, 2008)

The intensity of the transmitted light is detected in space and time, resolved, and then converted into transmission profiles showing the evolution of the sample, as seen in Fig. II - 14. Results can be then translated into an instability-index (Detloff, 2013), which quantifies the shelf life of the PCME. Additional information on the definition and calculation of the instability index were also given by Detloff (2013) and Badolato et al. (2008).

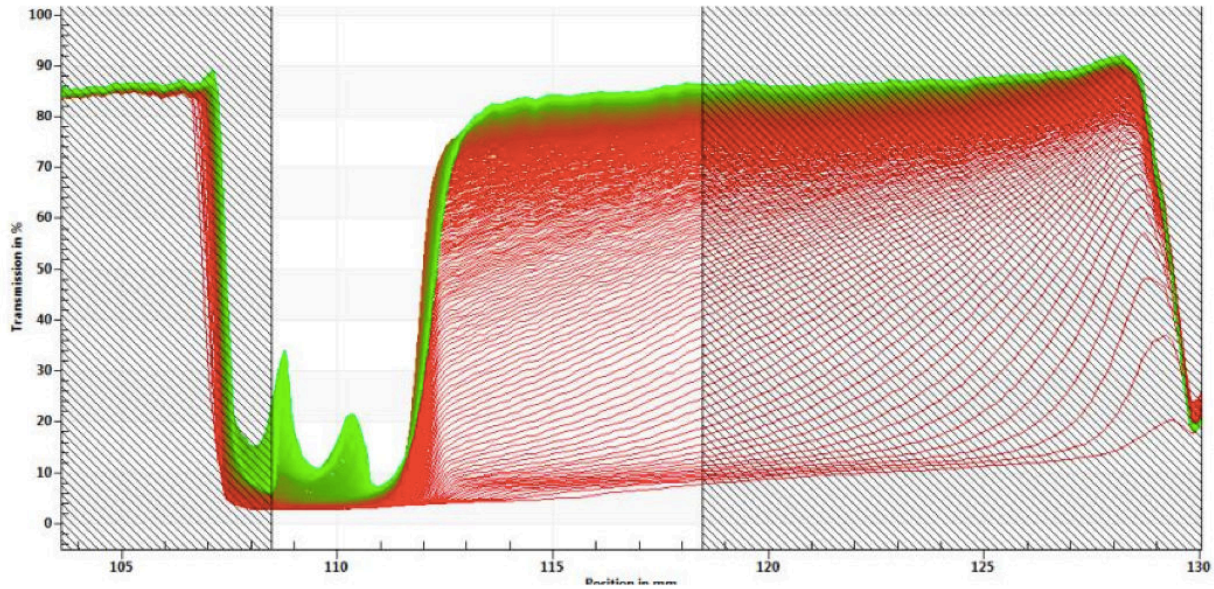

Figure II-14 Transmission-profile generated by the LUMiSizer for creaming during time. Only the unshaded section is used to calculate the instability index (Fischer et al., 2017)

For a PCME to be considered stable and with a long lifespan, the instability index should have low values. Fischer et al. (2017) consider that a sample is sufficiently stable as long as it does not exceed 10% from its maximal value, i.e. the final value of the instability index.

II.2.5 Conductivity analysis

Measurements for the thermal conductivity of the test fluid were performed using a flash method diffusivity meter in a company specialised in such measurements (Influtherm, Lyon).

II.2.6 Rheology analysis

Experiments were also performed using an Anton Paar Rheometer MCR 302 with a measuring cone CP50-1 (50 mm diameter, 1° angle). This device has an integrated Peltier element P-PTD200/Air that allows the change of the temperature in the sample. Tests were done for different temperatures between 1°C and 15°C for different shear rates. Additionally, the viscosity of the water was measured with the same procedure.

II.3 Experimental procedure

This subchapter deals with the method of determination of the local and average heat transfer coefficients during the flow of the investigated fluid along the cooling channel. This requires a detailed thermal analysis that is based on the mixed mean temperature of the fluid.

We also consider that it is better to present and define the test protocol to be followed before addressing these physical quantities.

II.3.1 Experimental procedure for the heat transfer analysis

II.3.1.1 Test protocol

Before starting the manipulations, the steps of the test protocol must be followed:

1. check liquid levels (PCME and ethanol) in the two circuits;
2. connect the laptop to the central data acquisition and start Excel ™ file for data acquisition;
3. turn on the measuring devices and let the central data acquisition on, for at least 15 minutes to check the status of thermocouples (without fluid circulation);
4. power up the control unit of the PCME circuit, as well as the one for the ethanol;

5. swap the auxiliary contactor 1 of the cabinet of the water circuit;
6. start the ethanol pump and the PCME pump for circulating fluids in the channels;
7. adjust the speed of the pumps and the three-way valves in order to establish the mass flow rates in the channels, then check the connection to the expansion tank;
8. start the condensing unit to cool the ethanol and therefore the PCME in the cooling channel;
9. adjust the manual valve to control the ethanol flow in the heater to control the temperature of the ethanol at the inlet of the cooling channel;
10. adjust the set point temperature of the PCME at the outlet of the heating channel or the thermal flux generated by the electrical resistances;
11. when all temperatures are established start the acquisition data for at least 2000s.

It is important to check the measuring instruments for the cold junction compensation of the thermocouples; therefore, a test campaign was performed at the beginning of the experiments. First test was performed at room temperature and without circulation of fluids to observe the temperature difference between one side and the other side of the instrumented steel plates.

The second test was performed with circulating fluids and was meant to verify the energy balance.

II.3.1.2 Mixed mean temperature of the fluid

"An experimental test consists of cooling the PCME in the cooling section of the experimental setup in order to analyse the evolution of the temperatures (inlet and outlet temperatures of the fluid, and inlet and outlet temperatures of the ethanol, as well as the wall temperatures of the heat exchanger) and to determine the mixed mean temperature of the fluid, that will ultimately allow to calculate the heat transfer coefficient during cooling.

As previously explained, the cooling channel is instrumented with a number of K-type thermocouples. Nine of them are located along each side of each steel plate forming the cooling channel, as depicted in Fig.15. In addition, two thermocouples (Z_4 and Z_1) are placed at the inlet and outlet of the cooling channel for measuring the inlet and outlet PCME's temperatures while, those denoted Z_2 and Z_3 are used to measure the inlet and outlet temperatures of the ethanol.

The temperatures of the fluid at the inlet and outlet of the cooling channel are such that: at the entrance of the channel (x_0 = 0), the mixed mean temperature of the fluid is $T_{m,0} = T_{Z4}$ (the fluid temperature measured by the thermocouple Z_4); at the outlet of the channel (x_9 = L), the mixed mean temperature of the fluid is $T_{m,9} = T_{Z1}$ (the fluid temperature measured by the thermocouple Z_1).

For location x_i on both sides of each heat exchange plate, the mixed mean temperature of the emulsion was calculated from an energy balance as:

$$T_{m,i} = T_{m,i-1} - \left(\frac{1}{\dot{m}c_p}\right)\frac{\varphi_{i-1} + \varphi_i}{2}(x_i - x_{i-1})a \qquad \text{(II-1)}$$

for i=1, $T_{m,0} = T_{Z4}$ at x_0=0 and for i=9 $T_{m,9}$=T_{Z1}.

where $\dot{m}$ is the mass flow rate of the emulsion, c_p its specific heat capacity, $\varphi_i$the heat flux through the plate at the axial location x_i and a the width of the channel.

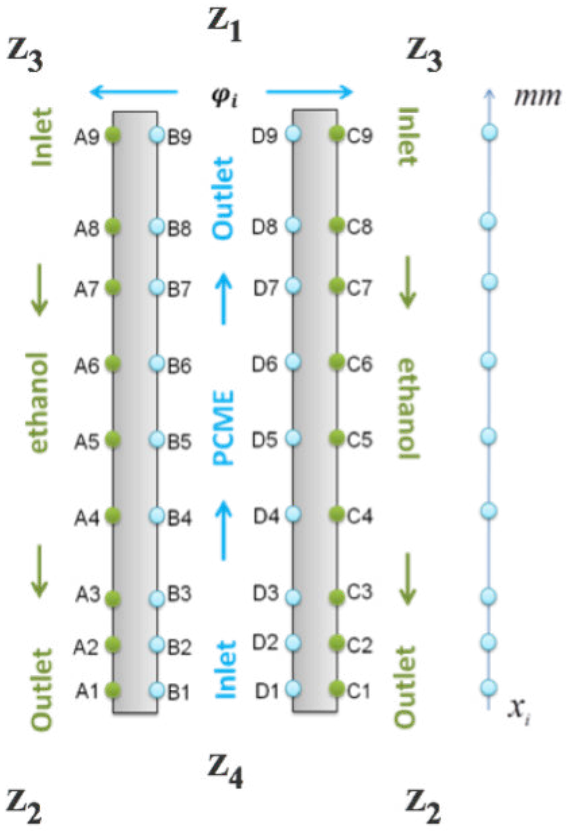

Figure II-15 Position of the thermocouples on the cooling channel

As previously mentioned, thermocouples are coupled by pairs and placed on both sides of the steel plates, one measuring the wall temperature on the side of the PCME and the other measuring the wall temperature on the side of the ethanol. From the thickness of the plate (e) and its thermal conductivity (λ_{steel}), the local wall heat flux $\varphi_i$at the axial location x_i is determined as:

$$\varphi_i = \frac{\lambda_{steel}}{e}\left(T_{w,PCME,i} - T_{w,ethanol,i}\right) \quad \text{(II-2)}$$

where $T_{w,PCME,i}$ is the wall temperature on the side of the PCME at the axial location x_i and $T_{w,ethanol,i}$ the wall temperature on the side of the ethanol at the same axial location.

II.3.2 Local heat transfer coefficients

Local heat transfer coefficients were determined by Eq. II-3, using the measured wall heat fluxes and the difference between the temperatures of the wall $T_{w,PCME,i}$ measured by each of the 9 thermocouples and the fluid temperatures calculated with Eq. II-1.

$$h_i = \frac{\varphi_i}{T_{m,i} - T_{w,PCME,i}} \quad \text{(II-3)}$$

where $T_{w,PCME,i}$ is the wall temperature at the location x_i. By the integration of the local heat transfer coefficients over the length of the cooling channel, the average heat transfer coefficient over the whole heat exchanger can be determined by:

$$h = \frac{1}{L}\int_0^L h(x)dx \cong \frac{1}{L}\left[\sum_{i=1}^{8}\frac{h_i + h_{i+1}}{2}(x_{i+1} - x_i) + h_9(L - x_9)\right] \quad \text{(II-4)}$$

where h is the average heat transfer coefficient, h_i the local heat transfer coefficient at the locationx_i, L the length of the cooling section and h_9 the ninth local heat transfer coefficient corresponding to the location x_9.

A typical time evolution of the inlet and outlet temperatures of the emulsion is depicted in Fig. II-16.

On the temperature curve during cooling, there is a decrease in the slope at approximately 1000 s. This variation of the curve seems to fit to the beginning of the paraffin crystallization at about 5 °C (which is the starting crystalizing temperature of the paraffin in water emulsion, as specified by the manufacturer).

During solidification, the density and the mass flow in the cooling channel have large variations. Cooling the PCME reveals the existence of three regions: in the first stage of time (until t=1000 s for the example of Fig. II-16), the emulsion is fully liquid. Then at the moment of subcooling break up, solidification starts, which sometimes gives birth to a small transient temperature increase (approximately 0.2 - 0.4 K on Fig. II-16).

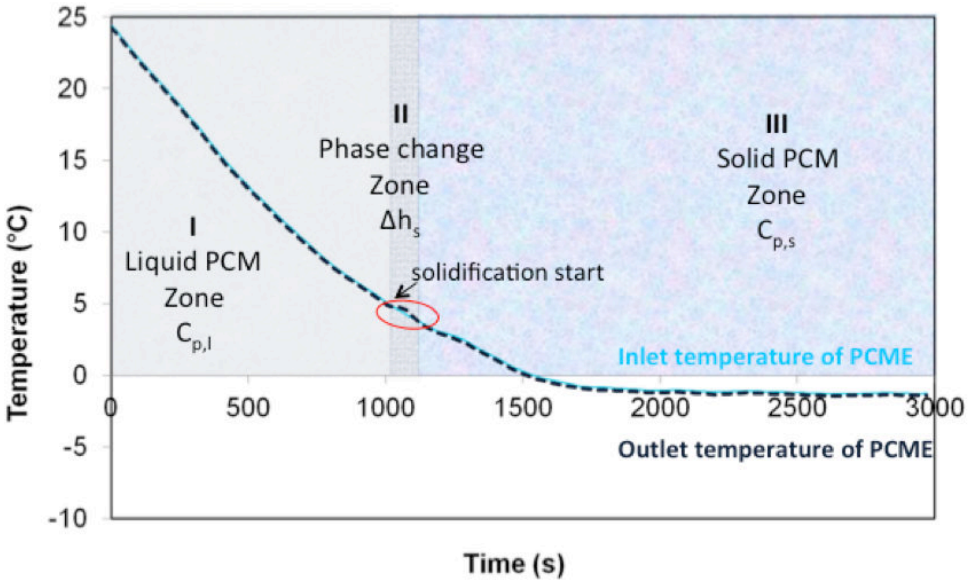

Figure II-16 Typical evolution of the inlet and outlet temperature of the PCME during cooling in the cooling channel

Then, once the paraffin is fully crystallized, the emulsion temperature decreases until a steady state is reached. In the present work, local heat transfer coefficients were determined first for each region followed then by the determination of the average heat transfer coefficient.

For every experiment, the PCME is cooled down gradually in the cooling channel starting from ambient temperature. The cooling of the PCME and of ethanol starts simultaneously. Thus, the time evolution of their temperatures is almost parallel. The minimum temperature approach between them is about 2 K, when steady flow regime is reached. For each set of measurements, the mixed mean temperature of the emulsion can be determined and thus the local heat transfer coefficient for every points of measurement."

II.3.3 Experimental procedure for the rheology analysis

"The PCME sample has a melting temperature of 6°C and a freezing temperature between 2 and 5°C. Measurements with variable shear rate were conducted for different temperature values between 1°C and 15°C to study the rheology of the emulsion when the PCM is solid, during its transition and when it is in liquid phase. A laminar flow was maintained for the entire set of measurements. The experimental test for the rheological characterization of the fluid consists in cooling down the emulsion to the desired temperature. Then shear rates are varied using a manual valve. Tests were performed for a variable mass flow rate between 5 and 80 kg.h-1 corresponding to a differential pressure between 5 and 15 mbar. Such paraffin emulsions are usually considered to be rheofluidifiant (Huang *et al.*, 2009, Huang *et al.*, 2010, Huang and Petermann, 2015). The non-Newtonian behaviour can be described using the Herchel- Bulkley model:

$$\tau = \tau_0 + K\dot{\gamma}^n \tag{II-4}$$

where K is the consistency coefficient of the fluid, n degree of the non-Newtonian behaviour, τ the shear stress, τ_0 the minimal shear stress and ,$\dot{\gamma}$ the shear rate. For a Newtonian fluid, e.g. water, n is equal to 1. If the fluid is pseudoplastic, n<1. If is $\tau_0$negligible then Eq. II-4 becomes:

$$\tau = K\dot{\gamma}^n \tag{II-5}$$

For a pipe flow, shear stress and shear rate are defined as (Rabinowitsch):

$$\tau = \frac{D\Delta p}{4L} \tag{II-6}$$

$$\dot{\gamma} = \frac{3n+1}{4n}\frac{8u_d}{D} \tag{II-7}$$

D is the pipe diameter, L is the distance between the pressure tapings, Δp the differential pressure, and $u_d$the velocity.

This procedure was used especially for small shear rates up to 150 s^{-1}. Further experiments were performed to determine the effect of the temperature on the viscosity for

shear rates above 150 s^{-1}. For these experiments the Anton Paar Rheometer MCR 302 described in section II.2.6."

This chapter presents the experimental setup used for the experimental analysis of the PCME in terms of heat transfer and rheology. The experimental setup with its measurement and acquisition systems together with the other additional measuring instruments presented in this chapter, the protocol of use and the calculations procedures facilitate:

- *the analysis of the PCME during cooling into the cooling channel;*
- *the determination of the mixed mean temperature of the PCME, the local heat transfer coefficients and the average heat transfer coefficient;*
- *the determination of the rheological behaviour of the PCME before phase change of the paraffin droplets, during phase change and after phase change;*
- *the determination of the thermophysical properties and viscosity for the PCME;*

The elements presented in this chapter enabled us to produce a set of results on the PCME that are original and reliable. These results are necessary to get a better understanding of PCMEs and to fully characterize them in order to establish guidelines design for industrial applications.

CHAPTER III

This chapter essentially aims at presenting the results of the experimental campaign concerning the determination of the thermodynamical properties and heat transfer characteristics of the PCME-V1, PCME-V2 and PCME-V3. Correlations for the dimensionless Nusselt number are presented and compared with those already existing in the literature for Phase Change Slurries. In addition, rheology results are presented for the

III. Experimental results

The experimental study on the installation presented in the previous chapter was carried out for 3 versions of the emulsion, presented in Table 8.

Table 8 PCME versions tested for this thesis

Version	Paraffin	Surfactant		Observations
PCME-V1	30 wt.%	<3 wt.% surfactant		-
PCME-V2	30 wt.%	3 wt.% surfactant		different type of surfactant in comparison to PCME-V1
PCME-V3	30 wt.%	3 wt.% surfactant	before ageing	same surfactant as PCME-V2
			after ageing	
		5 wt.% surfactant	before ageing	
			after ageing	

III.1 PCME-V1

The first version of the phase change material emulsion tested during this research consists of 30 wt.% paraffin (tetradecane $C_{14}H_{30}$), water and less than 3 wt.% of surfactant. The phase change temperature for the tetradecane is 6 °C. The thermal performance and the rheological behaviour were studied and the results are presented below.

III.1.1 Evaluation of the thermophysical and transport properties for the PCME-V1

Density

Using the METLER Toledo scale, the density of the PCME-V1 was estimated to be equal to 925 kg m^{-3} at 20°C. In addition, its time dependence during cooling was investigated using the Coriolis flowmeter with a measuring accuracy of ±0.15%, as given by the manufacturer. This dependence can be caught on Fig. III-1 that represents the time evolution of the PCME temperature and density during cooling experiment. It somewhat represents the relationship between the density and the temperature corresponding to the protocol described in Section II.3

All measured quantities shown in Fig. III - 1 are recorded by the data acquisition system during one experiment and then plotted against time. A relative strong increase in the density of the PCME is noticeable when the phase change occurs at approximately 4 °C.

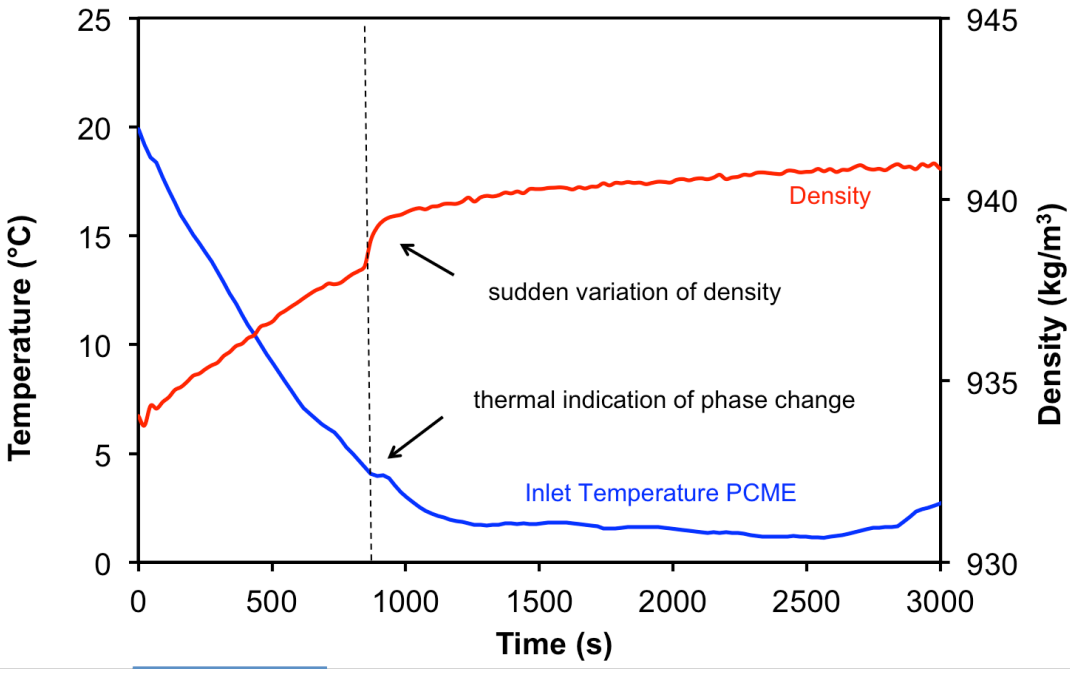

Figure III-1 Evolution of the density during cooling of the PCME-V1 in the cooling channel

($\dot{m} = 211 kg/h$)

Thermal Conductivity

Measurements for the thermal conductivity of the PCME-V1 were performed using a flash method diffusivitymeter. Several tests were performed and the average thermal conductivity of the PCME was found to be equal to 0.31 W m^{-1} K^{-1}±3% at a temperature of 24.2 °C.

Viscosity

The rheological behaviour of the studied emulsion was established using a rotation rheometer, type Physica MC301 with cone and plate geometry. The diameter of the cone is 50 mm and the angle is 1°. The stress ramp tests for the paraffin emulsion were conducted in a temperature range of 3 - 25 °C as indicated in Table 9.

The analysis showed a Newtonian behaviour: for a given temperature, the viscosity is constant (independant of the shear rate), i.e. the shear stress varies linearly with the shear rate. The results are shown in Fig. III - 2, by plotting the viscosity versus the shear rate.

Table 9 Viscosity variation with the temperature

Temperature (°C)	3	5	10	15	20	25
Viscosity (mPas)	12.8	12.1	10	8.3	7	6

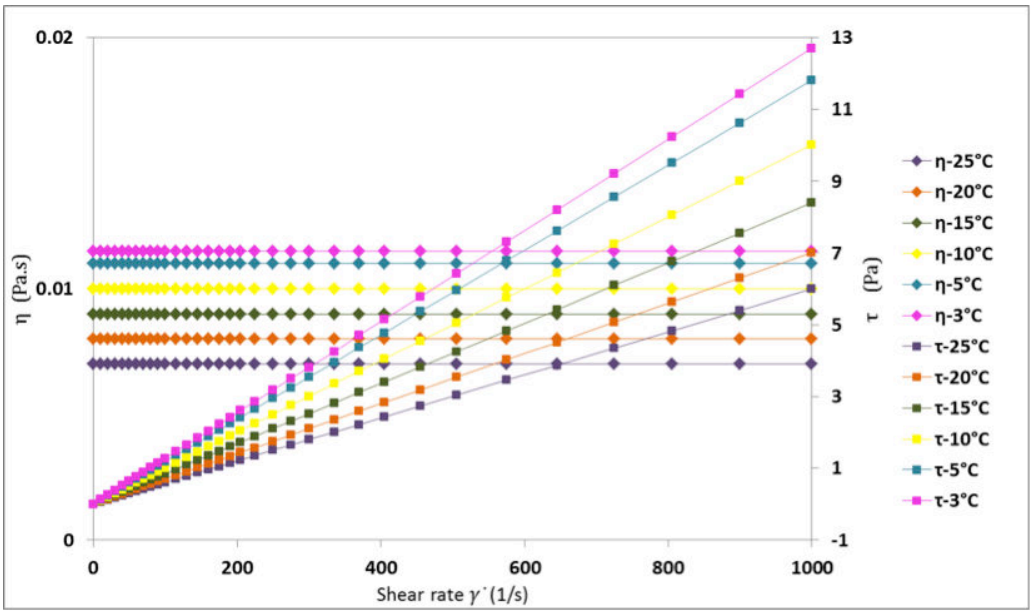

Figure III-2 Viscosity of the PCME-V1 containing 30 wt.% paraffin versus shear rate

It is known that the viscosity can be very dependent on the type of the surfactant used. Because the manufacturer has not specified, nor the type or the concentration of the surfactant used, it is not possible to confirm whether this Newtonian behaviour is due to the presence of the surfactant or not.

III.1.2 Study of the local heat transfer for the PCME-V1

III.1.2.1 Temperature of the PCME – V1 in the cooling channel

Figure III - 3 illustrates the evolution of the inlet and outlet temperature of the PCME – V1 during cooling in the cooling channel. The temperature of the ethanol is optionally represented. At the beginning of the test, the PCME – V1 temperature in the system was 19.9 °C (room temperature in May). Cooling of the ethanol and paraffin emulsion takes

place simultaneously. The flat section in the evolution of the ethanol temperature at 570 seconds is due to the set point temperature of the ethanol. For these experiments, temperature of the ethanol was initially set at 5 °C and then at -5 °C, thus cooling of the paraffin emulsion was done in a progressive manner and slowly, so that the stability of the emulsion was not affected. The flat section in the evolution of the PCME temperature at approximately 900 seconds coincides with the phase change of the paraffin at 4°C.

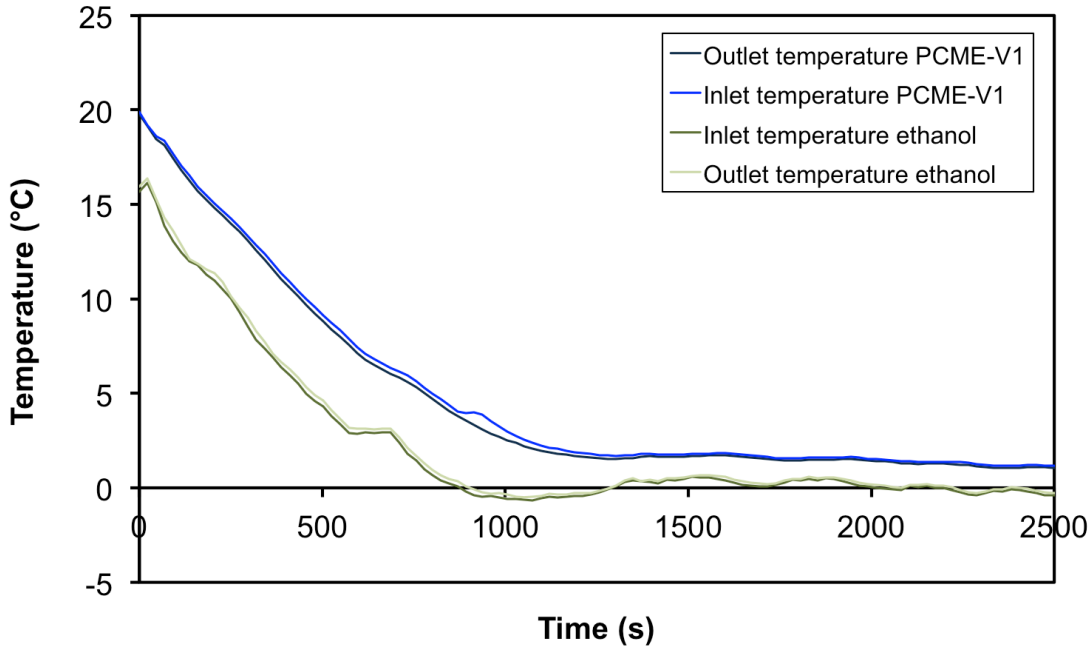

Figure III-3 Evolution in time of the inlet and outlet temperatures of the PCME -V1 and ethanol, during cooling into the cooling channel

III.1.2.2 Evolution of the PCME-V1 mass flow during cooling in the cooling channel

On Fig. III-4 the evolution of the mass flow rate is represented for the PCME-V1 during cooling in the cooling channel. The emulsion is in laminar flow during its cooling, with an initial mass flow rate of 597 $kg.h^{-1}$.

Because of the increase in viscosity of the carrier fluid (water) during cooling, the mass flow rate of the emulsion decreases fairly linearly until the end of the phase change, from 597 $kg.h^{-1}$ to 440 $kg.h^{-1}$, when its tendency is to remain constant during the rest of the test.

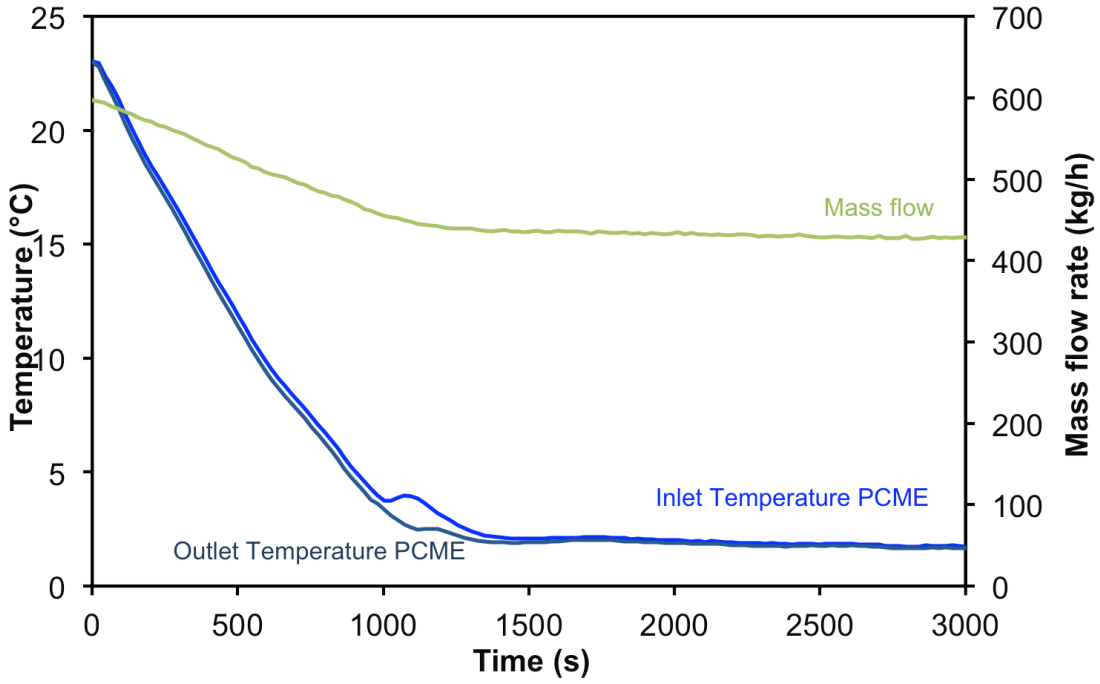

Figure III-4 Evolution of the PCME-V1 mass flow during the cooling into the cooling channel

III.1.2.3 Evolution of the local and average heat transfer coefficient during cooling in the cooling channel

Six tests were conducted on the PCME-V1 during its cooling in the cooling channel. Local heat transfer coefficients were determined for different Reynolds numbers. On Fig. III - 5, the local heat transfer coefficients during the cooling of the paraffin emulsion are represented as a function of the distance from the inlet (x) and for different values of the Reynlods number. The evolution of the heat transfer coefficient can be expressed in terms of Nusselt number ($Nu = \frac{hD_h}{\lambda}$) with $D_h = 0.0111$ m and $\lambda = 0.31$ $W.m^{-1}K^{-1}$ as measured with the flash method (Section III.1.1).

The evolution of the local Nusselt number is displayed on Fig. III - 6. A strong decrease in the heat transfer coefficient can be observed in the inlet zone of the channel. For x > 200 to 300 mm, the value of the local heat transfer coefficient levels off at an approximately constant value. This significant decrease at the entrance of the measurement section is related to the establishment of the thermal boundary layer, which is relatively short, in the present case. The temperature gradient of the emulsion along the channel is situated between 0.1 and 0.3 °C.

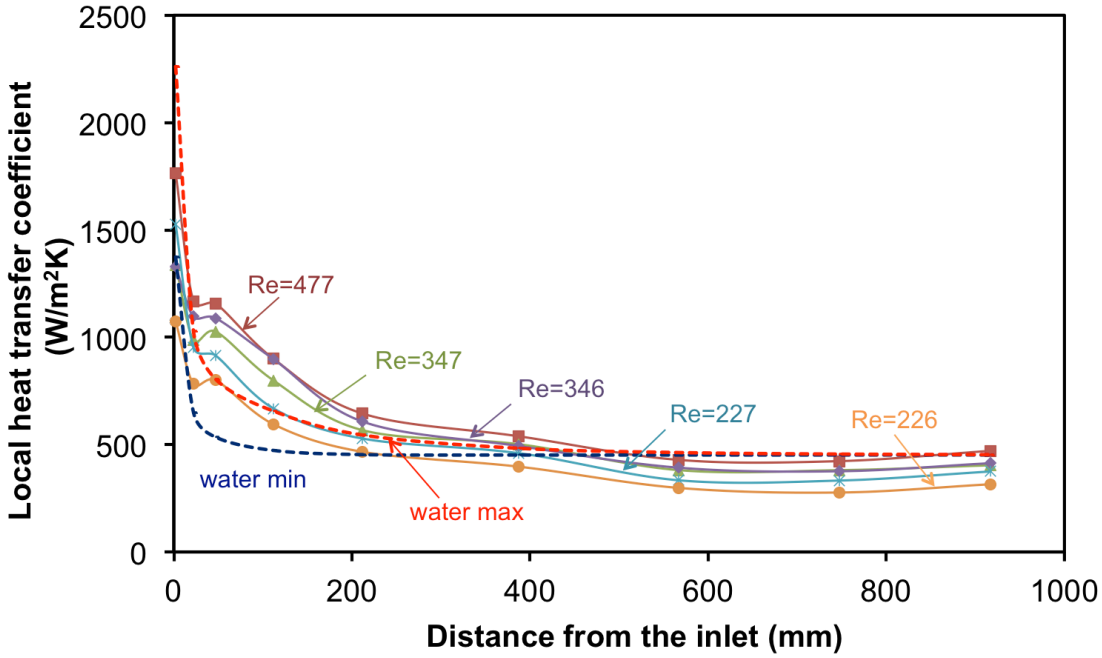

Figure III-5 Evolution of the local heat transfer coefficients along the cooling channel during the cooling of the PCME-V1 for different Reynolds numbers

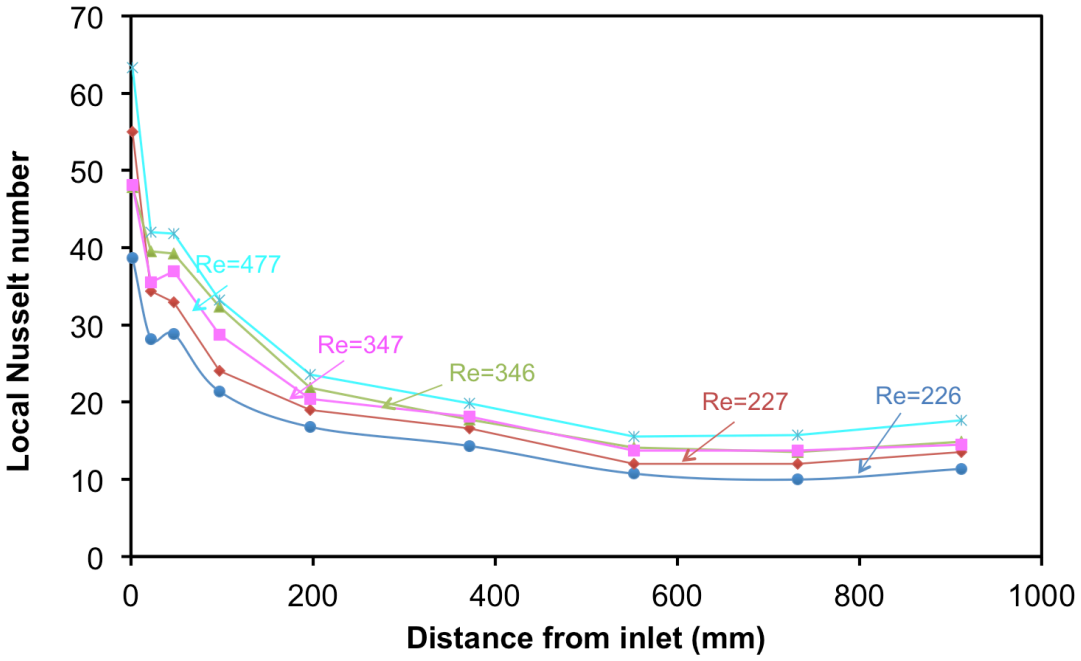

Figure III-6 Evolution of the local Nusselt number, along the channel, for the PCME - V1 for a laminar flow

For the studied range of Reynolds numbers, heat transfer coefficients for the fully developed zone can reach 300 up to 430W/m²K. The integration of the local heat transfer coefficients over the entire length of the heat exchanger, allows the calculation of the average heat transfer coefficient. A correlation between the local Nusselt number, the Reynolds

number, the Prandtl number and the dimensionless axial position $x^* = \frac{x}{D_h}$ has been determined, as illustrated as an example in Fig. III - 7 for Re=477. To establish correlations, as the Prandtl number variations are weak, because the paraffin concentration is constant, its exponent has been assumed constant and equal to 0.33. In addition, this value is usually used for heat transfer in laminar flows (Arsenyeva *et al.*, 2015).

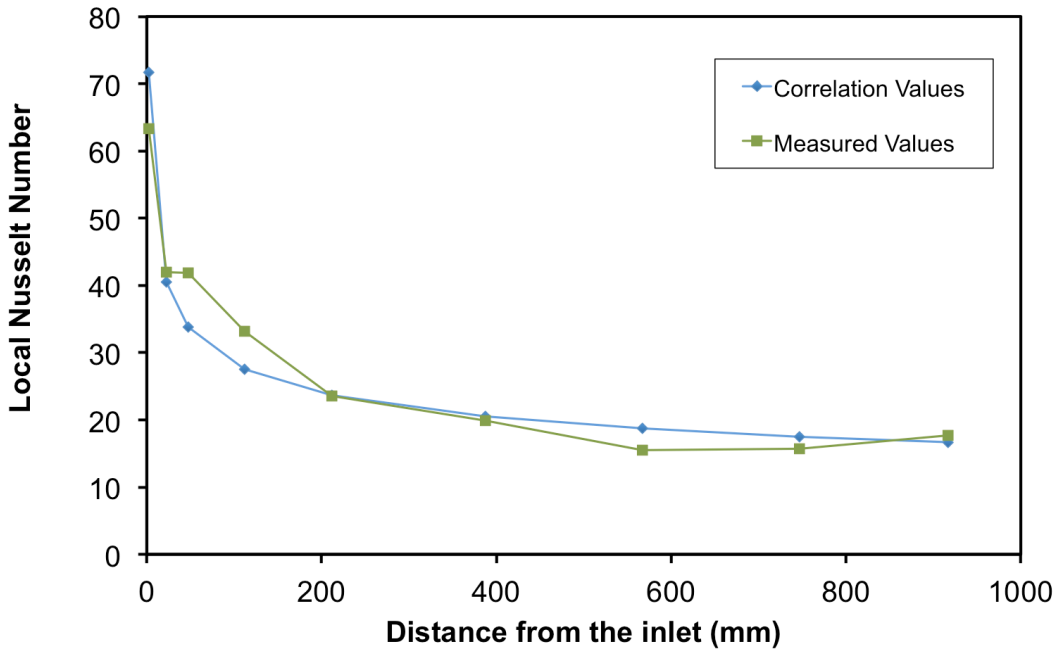

Figure III-7 Evolution of the average Nusselt number for the PCME - V1 in a laminar flow, during cooling in the cooling channel, Re=477

For a mass fraction of 30 wt.% paraffin, the following correlation (valid for $200 \leq Re \leq 500$ and $Pr \leq 160$) was obtained:

$$Nu(x) = 0.37\,\mathrm{Re}^{0.427}\mathrm{Pr}^{0.33}\,x^{*-0.238} \qquad \text{(III-1)}$$

A correlation between the average Nusselt number, Reynolds number and the Prandtl number could also be obtained for the cooling of the paraffin emulsion (Eq. III - 2) for $200 \leq Re \leq 500$ and $Pr \leq 160$:

$$Nu = 0.2784\,\mathrm{Re}^{0.431}\mathrm{Pr}^{0.33} \qquad \text{(III-2)}$$

III.2. PCME-V2

The second version of the phase change material emulsion tested consists of 30 wt.% paraffin (tetradecane $C_{14}H_{30}$), water and 3 wt.% surfactant. The design phase change temperature for the PCME - V2 is 6 °C. As in the case of the first tested paraffin emulsion, thermal performances and rheological behaviour were studied and the results are presented below.

III.2.1 Evaluation of the thermophysical and transport properties for the PCME-V2

Heat Capacity

The specific heat capacity of the emulsion was tested using two devices. The first one is a SETARAMC80II calorimeter. The temperature scanning rate was 0.25 K/min and the sample mass was 1.3610 g. The sample was initially heated up to a temperature of 40 °C, held for 10 minutes at this temperature and then cooled down. The second device is a NETZSCHDSC204 differential scanning calorimeter. A sample of 22.96 mg of paraffin emulsion was cooled down to -10 °C and kept at this temperature for 10 min to allow stabilisation and then heated up to 35 °C, with a heating rate of 1 K/min.

The latent heat capacity of the emulsion is 35.43 kJ/kg within the range temperature of 4 -12 °C. The latent heat capacity of the emulsion Δh_{cp} in kJ/kg is expressed as the paraffin weight fraction X_p multiplied by the heat of fusion of the paraffin Δh_p, in the temperature range. The total heat capacity of a paraffin emulsion Δh_e includes not only the latent heat capacity Δh_{cp}, but also the sensible heat capacity of the water, as follows:

$$\mathbf{\Delta h_e = \Delta h_{cp} + \Delta h_w = X_p \Delta h_p + X_w c_{p,w} \Delta T} \quad \text{(III-3)}$$

where $c_{p,w}$ is the specific heat capacity of water, X_w is the water mass fraction, and ΔT the range temperature of 4 – 12°C. In our case, the emulsion has a total heat capacity of 58.94 kJ/kg with 30 wt.% paraffin, which is about 2 times higher than that of water, which, from an applicative point of view, would be a minimum required (Huang *et al.*, 2009). Fig. III-8 illustrates the evolution of the specific heat capacity for the PCME-V2 vs. temperature during cooling of the sample performed with the SETARAM calorimeter.

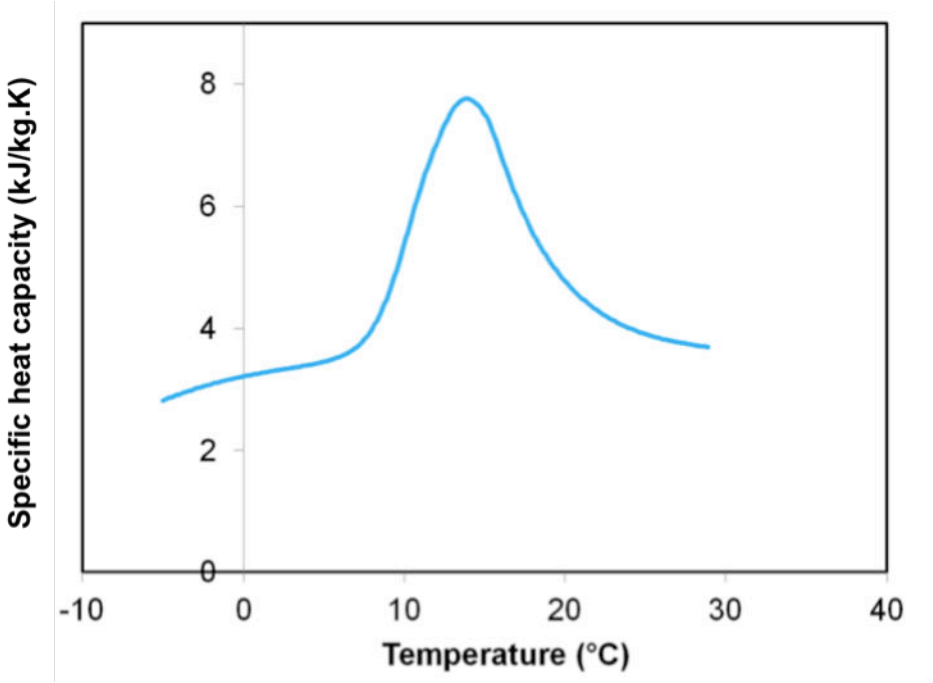

Figure III-8 Specific heat capacity of the emulsion during cooling of the sample

Thermal conductivity

Repeated tests were performed using a flash diffusivitymeter and the average thermal conductivity of the PCME was found to be equal to 0.38 W m^{-1} K^{-1}±3% at a temperature of 29°C.

Density

Using the METLER Toledo scale, the PCME - V2 density was estimated to be equal to 969 kg m^{-3} at 25.9 °C. As for the first version of the PCME, its time dependence during cooling was investigated using the Coriolis flowmeter. Fig.III - 9 shows the time evolution of the PCME - V2 temperature and density during cooling operation. As previously observed, for the PCME - V1, a relative strong increase in the density of the PCME - V2 is noticeable when the phase change occurs at approximately 5 °C.

Mass flow rate

In Figure III-10, the evolution of the mass flow rate for the PCME – V2 is represented during cooling in the cooling channel. The emulsion is in laminar flow during its cooling, with an initial mass flow rate of 967 kg.h^{-1}.

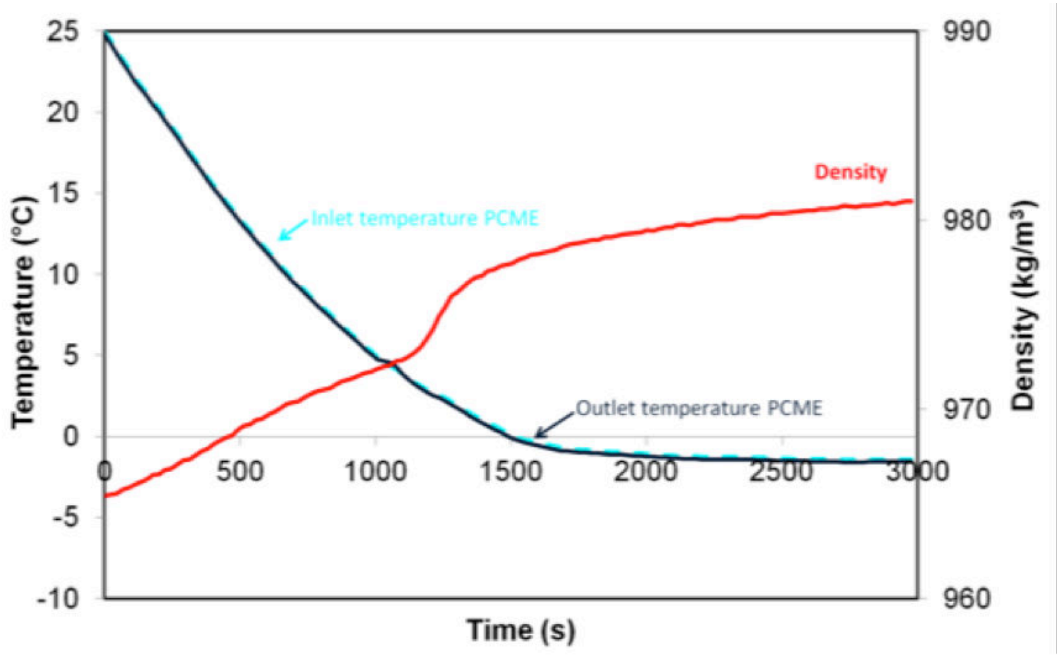

Figure III -9 Evolution of the PCME - V2 density during cooling in the cooling channel

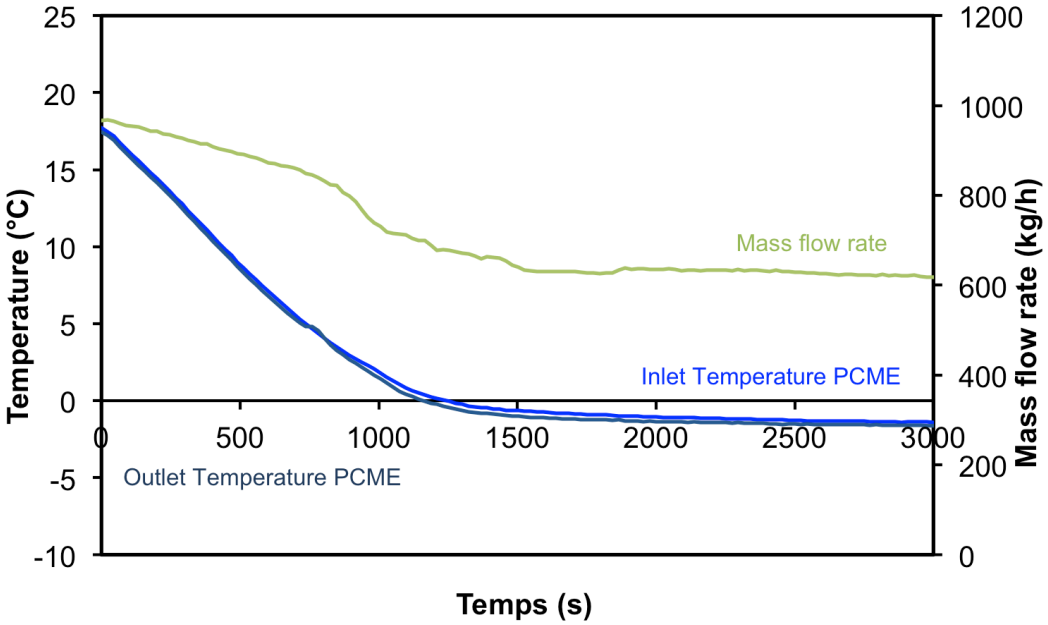

Figure III-10 Evolution of the PCME-V2 mass flow rate during cooling into the cooling channel

As in the case of the PCME-V1, because the viscosity of the carrier fluid (water) increases during cooling, the mass flow rate of the emulsions decreases to the beginning of the phase change of the paraffin from 967 kg.h^{-1} to 824 kg.h^{-}1, when it has a low sudden decrease, which corresponds to the solidifying temperature of the paraffin. As already

mentioned for the PCME-V1, this decrease is due to the sudden increase of the viscosity of the paraffin emulsion when the phase change of the paraffin droplets occurs.

Viscosity

The stress ramp tests for the viscosity of the PCME – V2 were conducted in a temperature range of 2 – 25 °C. Results for 5 different temperatures are reported in Table 10.

Table 10 Variation of the viscosity with the temperature for the PCME - V2

Temperature [°C]	2	4	6	10	25
Viscosity [mPa.s]	7.31	6.63	6.35	5.52	3.40

It was observed that for a given temperature, the viscosity is constant with the shear rate, i.e. the shear stress varies linearly with the shear rate, which corresponds to a Newtonian behaviour. Different authors such as Dai and Sun, 1997, Zhang *et al.*, 2016 reported that the viscosity can be very dependent on the type of surfactant used.

For the same reasons as with PCME-V1, it is not possible to confirm whether this Newtonian behaviour is due to the presence of the surfactant or not.

III.2.2 Evolution of the local and average heat transfer coefficient during cooling in the cooling channel

As for the previous phase change material emulsion, PCME-V1, different tests were conducted on the PCME-V2 during cooling into the cooling channel. Local heat transfer coefficients were determined for seven different Reynolds numbers.

On Fig. III - 11, the local heat transfer coefficients during the cooling of the paraffin emulsion are represented as a function of the distance from the inlet x and for different values of the Reynolds number. Similar to the first tested version of PCME, this one presents a strong decrease in the heat transfer coefficient along the entry length of the channel, which is related to the establishment of the thermal boundary layer. Interestingly, it takes more length for the heat transfer coefficient to stabilize at a constant value, about 600 mm over a total length of 1000 mm, in comparison to PCME-V1. The temperature difference of the emulsion along the channel remains between 0.1 K and 0.3 K.

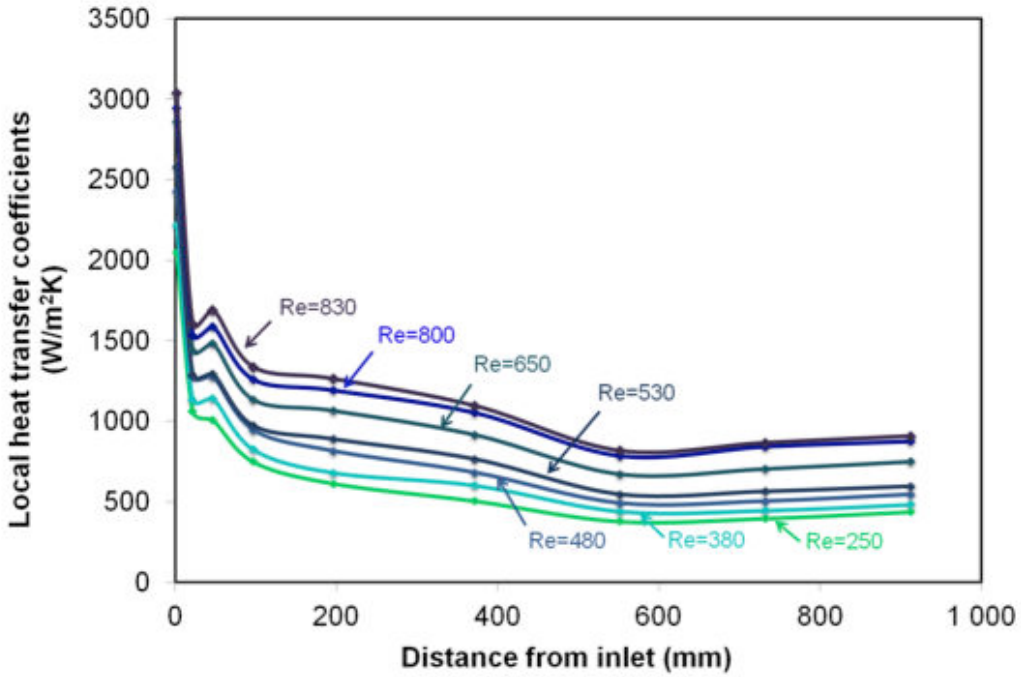

Figure III-11 Evolution of the local heat transfer coefficient along the channel during cooling of the emulsion for different values of the Reynolds number

As can be observed on the figure, the values of the Reynolds number for this second emulsion are between 250 and 830. PCME-V2 validates the increasing trend of the heat transfer coefficients with the Reynolds number. Therefore, the first Reynolds numbers on the figure are as low as for the first version of the emulsion; PCME-V1 and the others are higher. The evolution of the average heat transfer coefficient as a function of the Reynolds number, during cooling under laminar flow is displayed on Fig. III - 12.

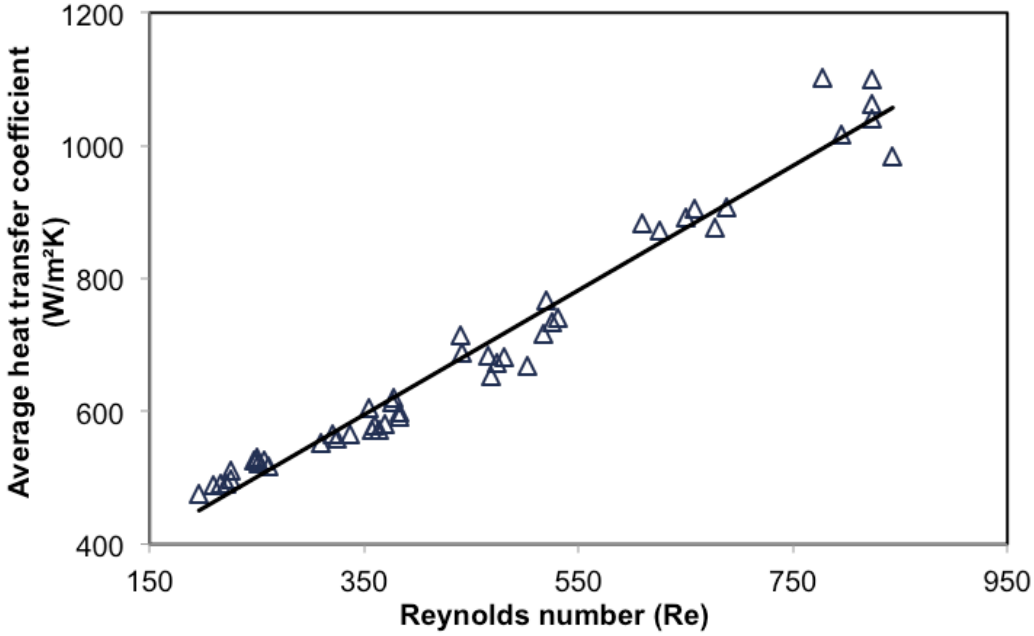

Figure III -12 Evolution of the average heat transfer coefficient integrated along the length of the channel for different values of the Reynolds number

As indicated in the figure, an increase in the average heat transfer coefficient values up to 1100 W/m^2K can be observed for the studied range of Reynolds numbers. The heat exchange is improved progressively as the Reynolds number increases.

Therefore, a new correlation was established, as in the case of PCME-V1, taking into consideration the same definitions for the Reynolds number, the Prandtl number and dimensionless axial position.

For a mass fraction of 30% paraffin, for $200 \leq Re \leq 900$ and for $Pr \leq 160$ this correlation is written:

$$Nu(x) = 0.28\,\mathrm{Re}^{0.427}\mathrm{Pr}^{0.33}\left(\frac{x}{x+D_h}\right)^{-0,59} \qquad \text{(III-4)}$$

Fig. III - 13 represents the deviation between the calculated and the experimental values of the Nusselt number for the present correlation and for that developed by Ionescu *et al.* (2008), who studied stabilized ice slurry using the same test bench.

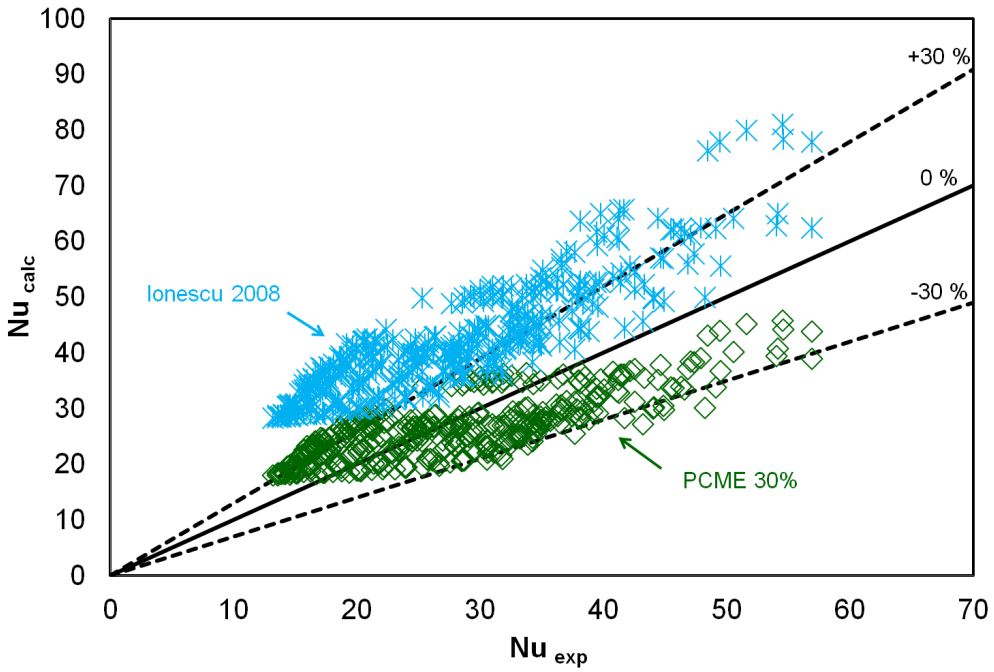

Figure III -13 Calculated vs. experimental Nusselt number for a constant wall temperature and a laminar flow in the cooling channel. Correlation used is given by Eq. III-3

Fig. III - 14 represents the evolution of the average Nusselt number as a function of the Reynolds number, as well as the values calculated by the correlations proposed by Ionescu *et al.* (2008), El Boujaddaini *et al.* (2013) and Vasile *et al.* (2016). It is noticeable that none of these correlations satisfactorily predicts the experimental results. This is the reason why a new

correlation between the average Nusselt number, Reynolds number and Prandtl number is proposed as follows:

$$Nu = 0.13\mathrm{Re}^{0.56}\mathrm{Pr}^{0,33} \quad \text{(III-5)}$$

Its form is the same as the previously mentioned correlations because the trends of evolution do not differ much from one case to another, but the constant and exponents were adjusted to better fit the current experimental results. This correlation is valid for 200 ≤ Re ≤ 900 and Pr≤160 and a paraffin concentration of 30%.

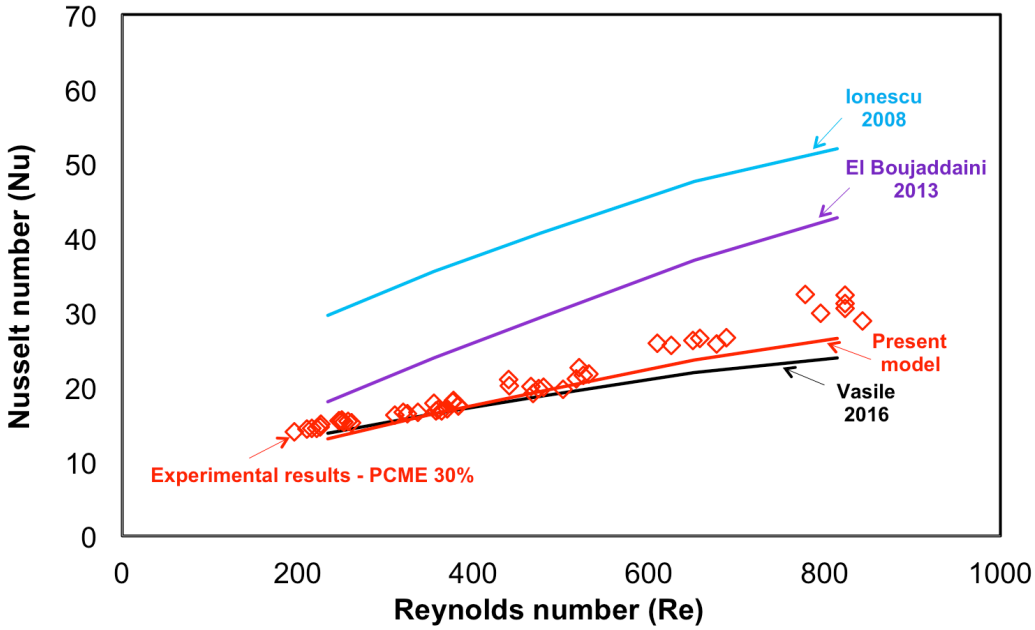

Figure III-14 Average Nusselt number vs. Reynolds number for the emulsion for a laminar flow in the cooling channel

III.3. PCME-V3 (3 wt.% and 5 wt.%)

The third version of the phase change material emulsion tested consists of 30 wt.% paraffin (tetradecane $C_{14}H_{30}$) and water. It was delivered in two batches, one containing 3 wt.% of surfactant, identical to the PCME – V2 and the other one containing 5 wt.% of surfactant. The design phase change temperature for the PCME – V3 is 6 °C. The major difference compared with the first version of PCME tested previously, lies in the type of surfactant used. As for the two tested paraffin emulsions, PCME-V1 and PCME-V2, the thermal performances and rheological behaviour for the PCME-V3 were studied and the results are presented below. As already mentioned, the PCME – V3 with 3 wt.% surfactant

has the same formulation as PCME – V2. Therefore, further tests were performed in order to complete the analysis and to check the compatibility of the results previously obtained.

Since the same PCME is studied, but with different concentration in surfactant, results are presented in comparison between the two of them.

III.3.1. Evaluation of the thermophysical and transport properties for the PCME-V3

Heat Capacity

As for the PCME-V1 and PCME-V2 the specific heat capacity of the PCME-V3 was tested using two devices. For the PCME-V3 with 3 wt.% surfactant before ageing, the temperature scanning rate was 0.25 K/min and the sample mass was 2.7549 g. The same temperature scanning rate was used for a mass of 2.8815 g of PCME-V3 with 3 wt.% surfactant after ageing. The specific heat capacity was tested in the same conditions for a mass of 2.8833 g of PCME-V3 with 5 wt.% surfactant before ageing and a mass of 2.8380 g of PCME-V3 with 5 wt.%. Same testing conditions as for the first two versions of PCME were applied for the samples of PCME-V3.

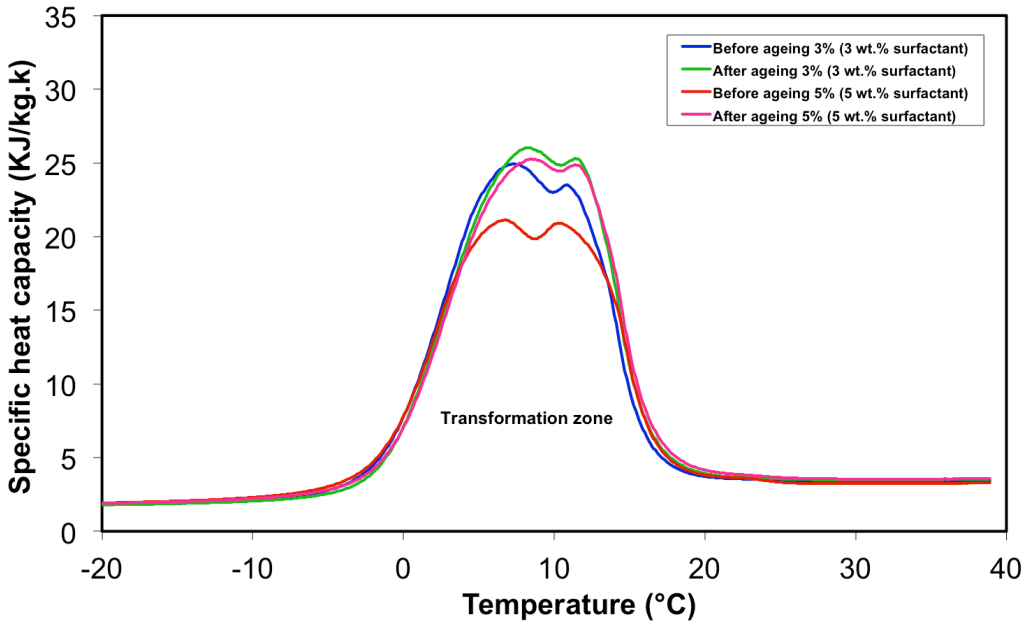

Figure III -15 Specific heat capacity of the emulsion (4 types of the PCME-V3) during cooling of the sample

The PCME-V3 was the tested using the second device as the two previous versions of PCME. The samples of 18.03 g for the PCME with 3 wt.% surfactant before ageing, 18.99 g for the PCME with 3 wt.% surfactant after ageing, 18.58 g for the PCME with 5 wt.% surfactant before ageing and 18.97 g for the PCME with 5 wt.% were cooled down to -20 °C and kept at this temperature for 10 min to allow stabilisation and then heated up to 39 °C, with a heating rate of 1 K/min.

Fig. III - 15 illustrates the relationship between the specific heat capacities for all 4 types of the PCME - V3 vs. temperature during cooling of the sample performed with the SETARAM calorimeter. Total heat capacity of the PCME – V3 remains two times higher than that of water.

Thermal conductivity

Conductivity for the PCME – V3 was measured using a flash method diffusivity meter. After repeated tests, the average thermal conductivity for the PCME – V3 with 3 wt.% before ageing was found to be equal to 0.38 W m^{-1} K^{-1}±3% at a temperature of 25 °C and for the PCME – V3 with 3 wt.% after ageing was 0.43W m^{-1} K^{-1} ± 3% at the same temperature. For the PCME – V3 with 5 wt.% before ageing, an average thermal conductivity of 0.32 W m^{-1} K^{-1} ± 3% at a temperature of 25 °C was found, while for the PCME – V3 with 5 wt.% after ageing was 0.39 W m^{-1} K^{-1} ±3% at the same temperature. Both PCMEs with 3 wt.% and 5 wt.% of surfactant increased their conductivities during testing, up to 0.43 W m^{-1} K−1 the PCME – V3 with 3 wt.% surfactant and 0.39 W m^{-1} K^{-1} for the PCME – V3 with 5 wt.% surfactant.

Density

Using the same device as previously, a METLER Toledo scale, the density was estimated to be equal to 924 kg m^{-3} for the PCME – V3 with 3 wt.% surfactant at 23 °C and 898 kg m^{-3} for the PCME – V3 with 5 wt.% surfactant at the same temperature. As in the case of conductivity, after ageing, density of the PCMEs had increased. The new values for the density of the PCMEs were estimated to be 980 kg m^{-3} for the PCME – V3 with 3 wt.% surfactant at 23 °C and 937 kg m^{-3} for the PCME – V3 with 5 wt.% surfactant at the same temperature.

Fig. III - 16 shows the time evolution of the PCME – V3 density during a cooling operation. In this case, the density was recorded by the data acquisition system during one experiment and then plotted against time.

Unlike the first two tested versions of PCME where density presented a relative strong increase when the phase change occurred, in this situation, the density shows no major changes when the phase change should occur, at approximately 6 °C. One can notice on Fig. III-16, that both densities, for the 3 wt.% surfactant versions of the PCME and 5 wt.% surfactant follow the same trend of evolution in time. This specific evolution with no major changes during the presumed phase change remains similar for all tests performed for different Reynolds numbers, for both PCME – V3 (3 wt.% and 5 wt.% surfactant).

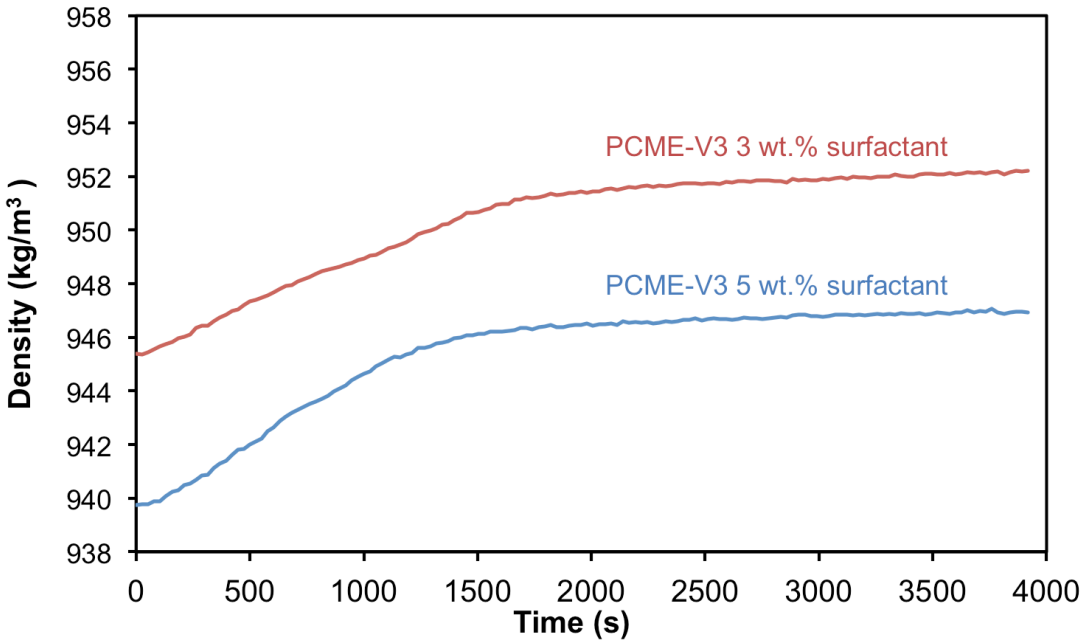

Figure III -16 Evolution of the PCME - V3 density during cooling in the cooling channel for Re=589

Mass flow rate

In Figure III-17, the evolution of the mass flow rate for the PCME – V3, for both 3 wt.% surfactant and 5 wt.% surfactant, is represented during cooling in the cooling channel. One can observe that as for the two other PCMEs tested, PCME-V1 and PCME-V2, the evolution of the mass flow rate during cooling is decreasing.

For the PCME – V3 with 3 wt.% surfactant, the sudden decrease in the mass flow (when phase change occurs) takes place quicker. This behaviour was observed for all test

performed on these two versions of PCME – V3, which can be related to s smaller supercooling degree.

Viscosity

The stress ramp test with PCME - V3 with 3 wt.% surfactant were conducted at different temperatures. Results for a temperature of 1.5 °C are shown in Fig. III-18 and Fig. III-19. Coefficients n and K were obtained by plotting the curves.

$$\tau = K\dot{\gamma}^n \tag{III-6}$$

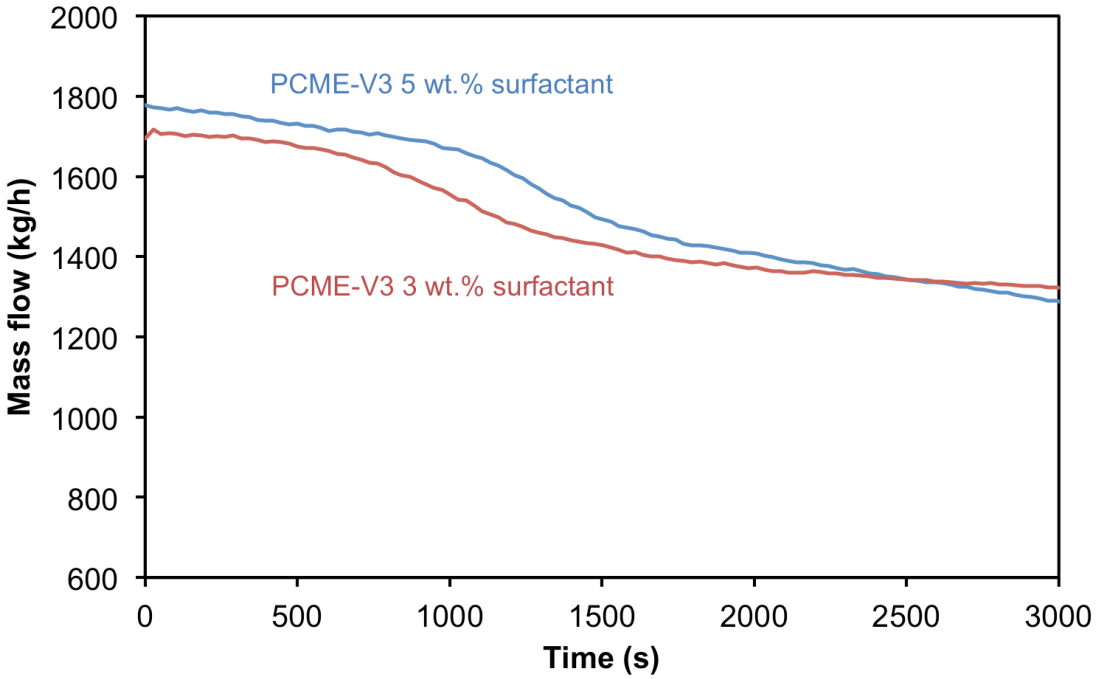

Figure III-17 Evolution of the PCME - V3 mass flow during cooling into the cooling channel for Re=737

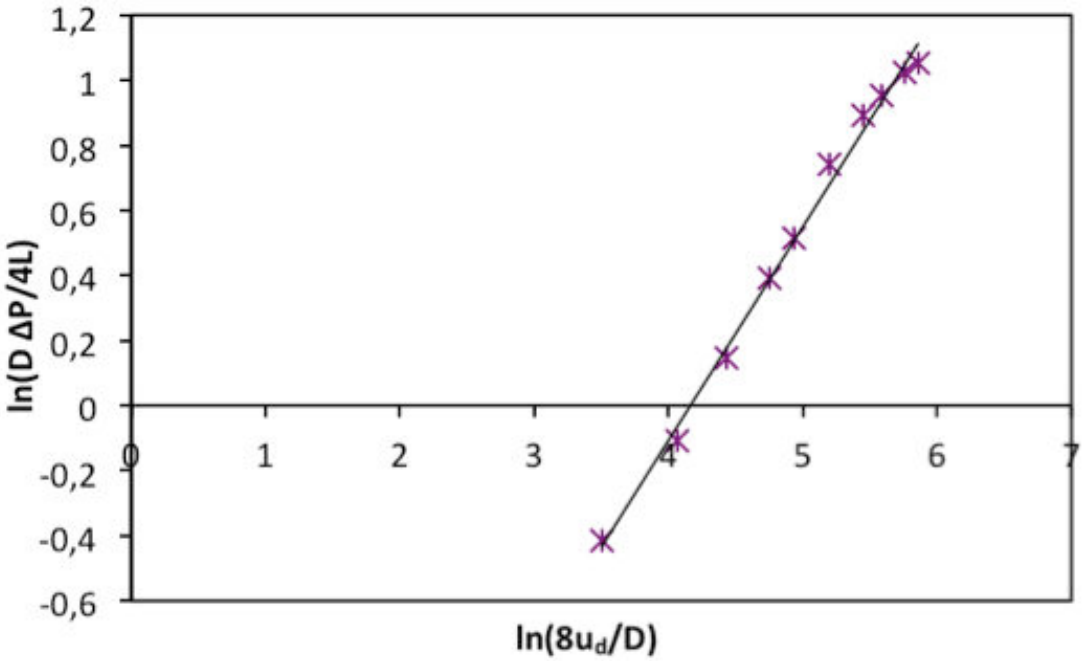

Figure III -18 Example graph for obtaining the coefficient n for the PCME - V3 with 3 wt.% surfactant at 1.5°C

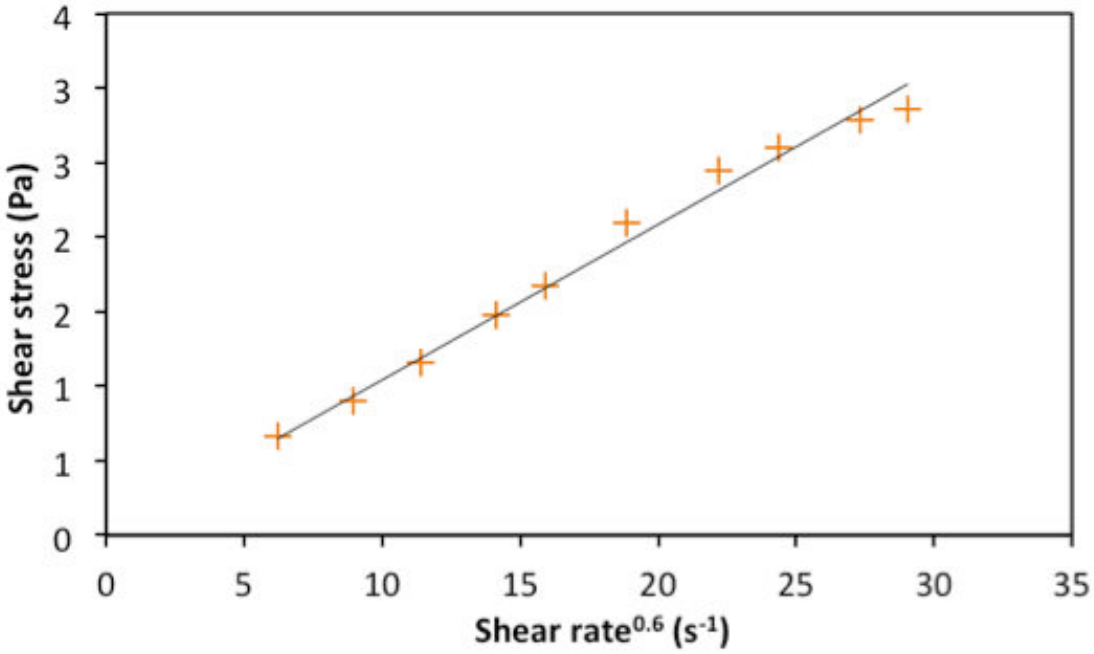

Figure III -19 Consistency coefficient K for the PCME - V3 with 3 wt.% surfactant at 1.5°C

All results show a pseudoplastic behaviour for the PCME-V3 with $n = 0.6 - 0.7$ The coefficient K was then plotted against the temperature, as seen in Fig. III-20. A decrease of the K value is observed with the increase of the temperature.

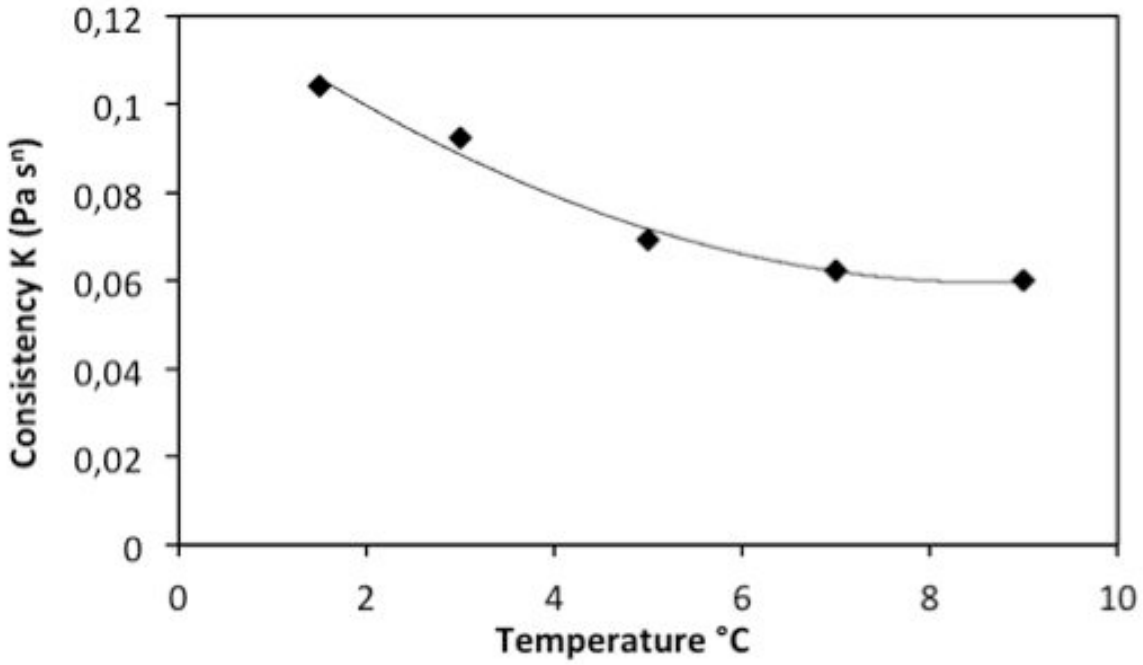

Figure III-20 Consistency coefficients K for the PCME - V3 with 3 wt.% surfactant for different temperatures

Further results are presented in Fig.III-21 by plotting the shear stress versus the shear rate for both laminar and turbulent flows. Experimental results on the viscosity are illustrated in Fig.III-22.

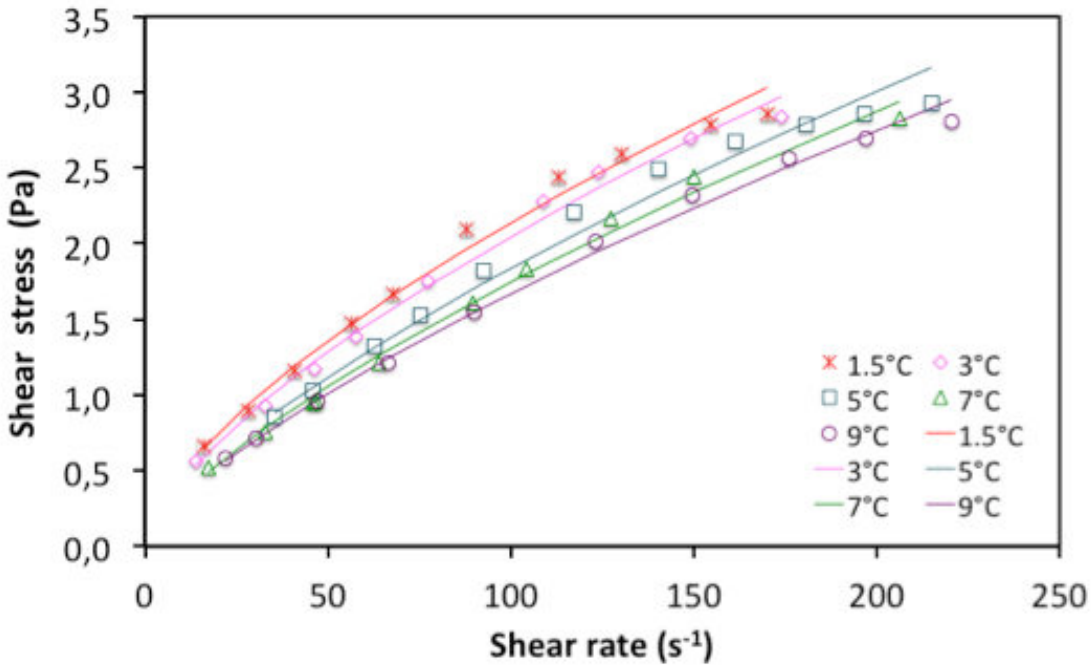

Figure III-21 Shear stress of the PCME - V3 with 3 wt.% surfactant versus shear stress at 1.5°C, 3°C, 5°C, 7°C and 9°C and the corresponding trend lines according to (II-5)

Curves showing the viscosity for all temperatures vs. the shear rate are shown on Fig. III-22. With the increase in the shear rate, a decrease in viscosity can be observed. This kind

of behaviour is known as “shear thinning”. At low shear rates, this effect is quite visible while it is less evident at higher shear rates. It was found that the rheology characteristics of the fluid could be described by the power law fluid model (Fig. II-5).

Further experiments were performed to determine the effect of the temperature on the viscosity. For these measurements an Anton Paar Rheometer MCR 302 was used, presented in Chapter II. For both PCMEs – V3 with 3 wt.% surfactant and 5 wt.%, the dynamic viscosity was measured at 5 different temperatures between 2 °C and 20 °C as we can see in Fig. III - 24, Fig. III-25 and Fig. III-26. Additionally, the viscosity of the water was measured with the same procedure.

The rheological behaviour was determined for two samples of the PCME – V3 with 3 wt.% surfactant. The first sample tested was the PCME – V3 with 3 wt.% surfactant before ageing in the heat transfer experimental setup and the second one was the PCME – V3 with 3 wt.% after ageing in the heat transfer experimental setup to simulate ageing. The second sample was circulated continuously, 24 hours a day, during 45 days.

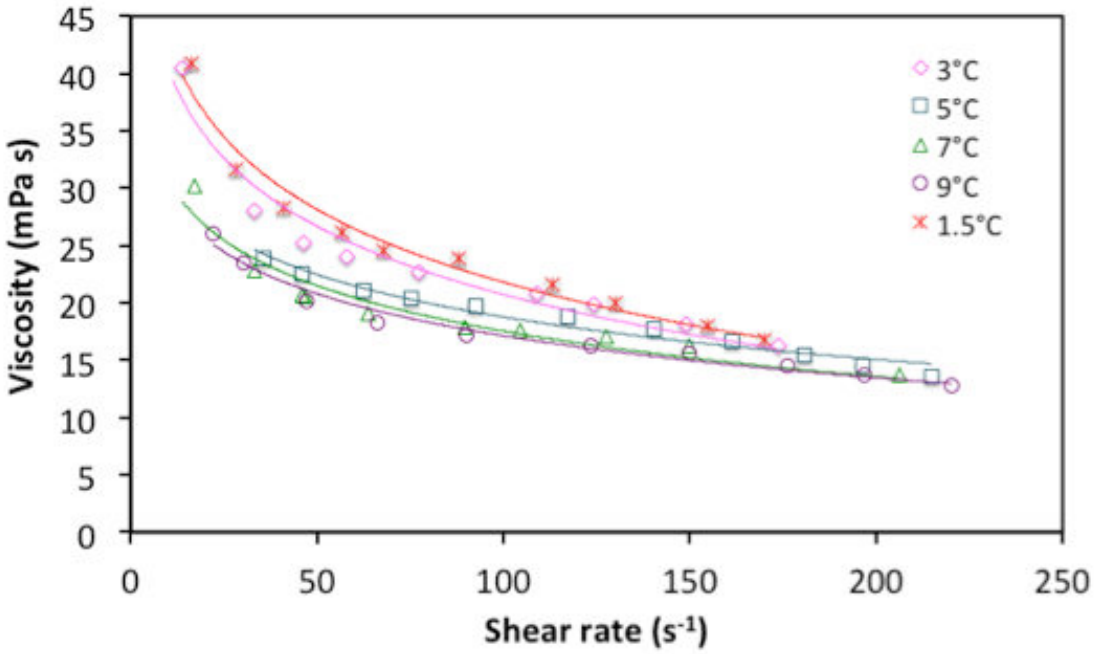

Figure III -22 Viscosity curves versus shear rates at 1.5°C, 3°C, 5°C, 7°C and 9°C

During that period of time, 60 heating/cooling cycles were imposed to the PCME. The main objective for this test was to see the effect of ageing on the viscosity of emulsion during or after being employed within an application.

Because of lack of availability, only one sample of the PCME – V3 with 5 wt.% surfactant was tested, the one before being employed in the heat transfer experimental setup.

Fig. III-23 clearly indicates a decrease of the viscosity at higher temperatures for the PCME – V3 with 3 wt.% surfactant. This is caused by the decreasing viscosity of the continuous phase and by changing from solid to liquid once the melting point of the paraffin droplets is exceeded. One can also observe that the viscosity decreases with the increase of the shear rate, which is in accordance with the previous results presented above.

Fig. III-24 shows the results for the PCME – V3 with 3 wt.% surfactant after ageing, in the heat transfer experimental setup. The same decrease of the viscosity for higher temperatures can be observed. It should be noted the high decrease in the viscosity for the second tested sample, the PCME – V3 with 3 wt.% surfactant after ageing. For example, in the case of the first sample, before ageing, the viscosity value between 2 and 20°C is up to 45 mPas while for the second sample after ageing, the viscosity value for the same temperature range is up to 20 mPas. Compared to water which has a Newtonian behaviour (n=1), as seen in Fig. III-24 and Fig. III-25, the PCME – V3 with 3 wt.% surfactant is approaching a Newtonian behaviour for temperatures superior to 15°C. For temperatures inferior to 15°C the emulsion is maintaining the shear-thinning behaviour.

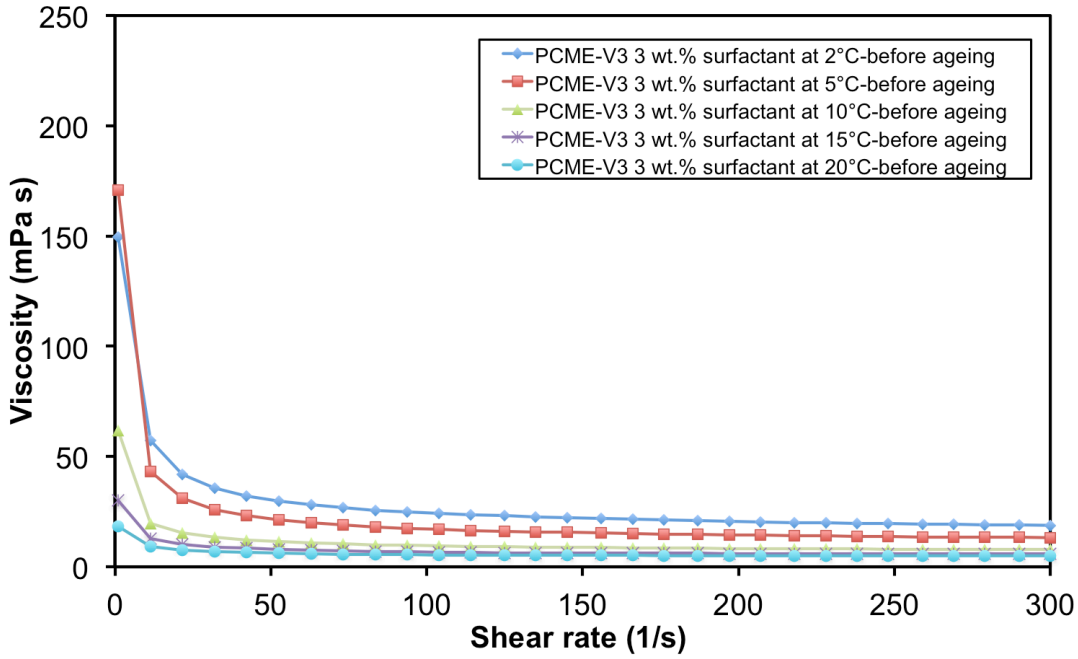

Figure III-23 Evolution of the viscosity for the PCME - V3 with 3 wt.% surfactant before ageing for different shear rates at 2°C, 5°C, 10°C, 15°C and 20°C

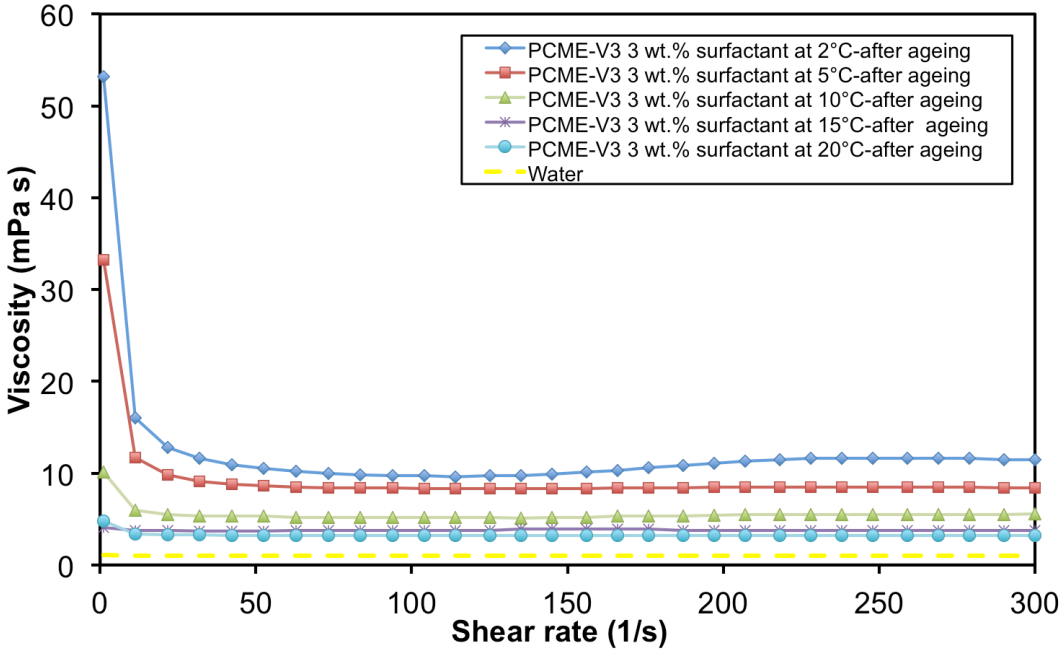

Figure III-24 Evolution of the viscosity for the PCME - V3 with 3 wt.% surfactant after ageing for different shear rates at 2°°C, 5C, 10°C, 15°C and 20°C

Regarding the PCME – V3 with 5 wt.% surfactant, same series of tests were performed. The flow behaviour index and the consistency coefficient were determined for four different temperatures, namely 1°C, 5°C, 10°C and 15°C, as displayed on Figs. III-25 and III-26.

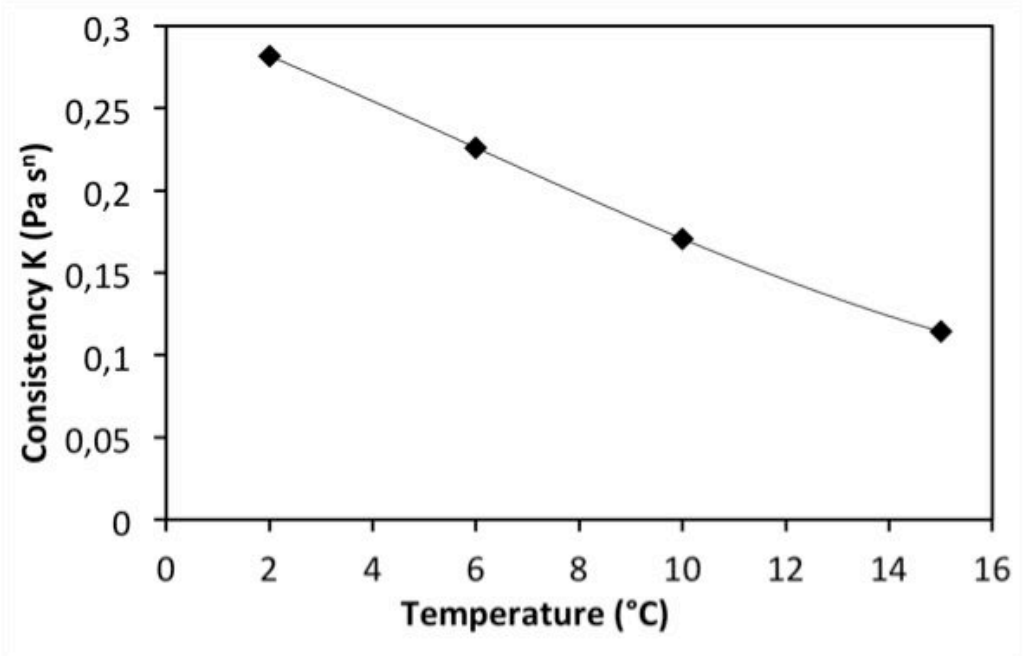

Figure III-25 Consistency coefficient for different temperatures for the PCME-V3 with 5 wt.% surfactant

The entire set of tests shows the same shear thinning behaviour as for the PCME –V3 with 3 wt.% surfactant ($n < 1$) with a flow behaviour index (n) ranging from 0.60 to 0.94.

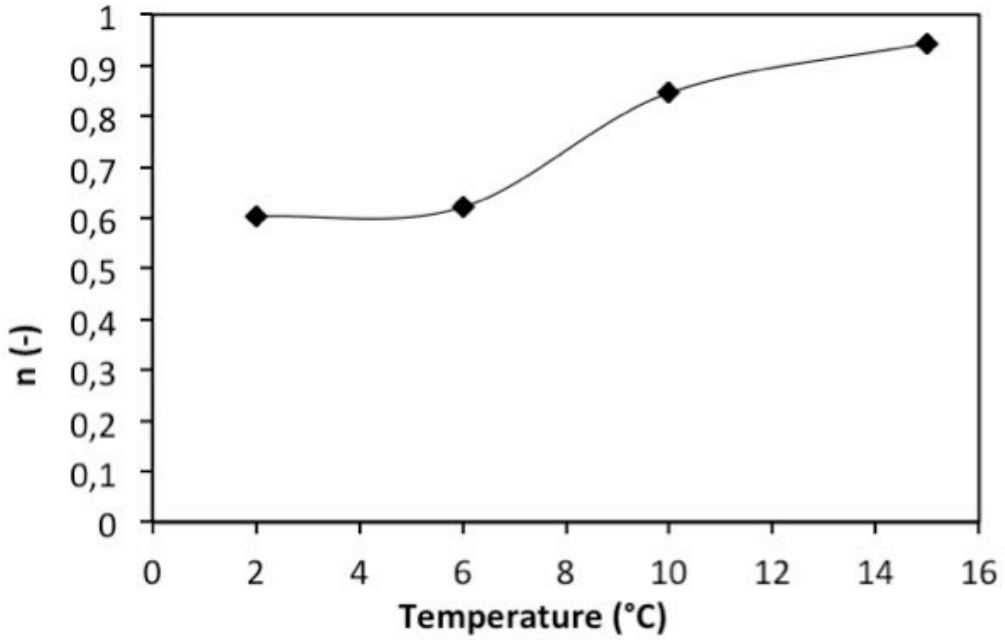

Figure III-26 The flow behaviour index for different temperatures for the PCME - V3 with 5 wt.% surfactant

The latter parameter increases with the temperature. K decreases when the temperature increases. This trend of evolution of K is in agreement with results of the literature, while to the author's knowledge, no clear evolution of n with the temperature was reported so far. The results can be presented in a more detailed manner by plotting the shear stress as a function of the shear rate, as seen in Fig. III-27.

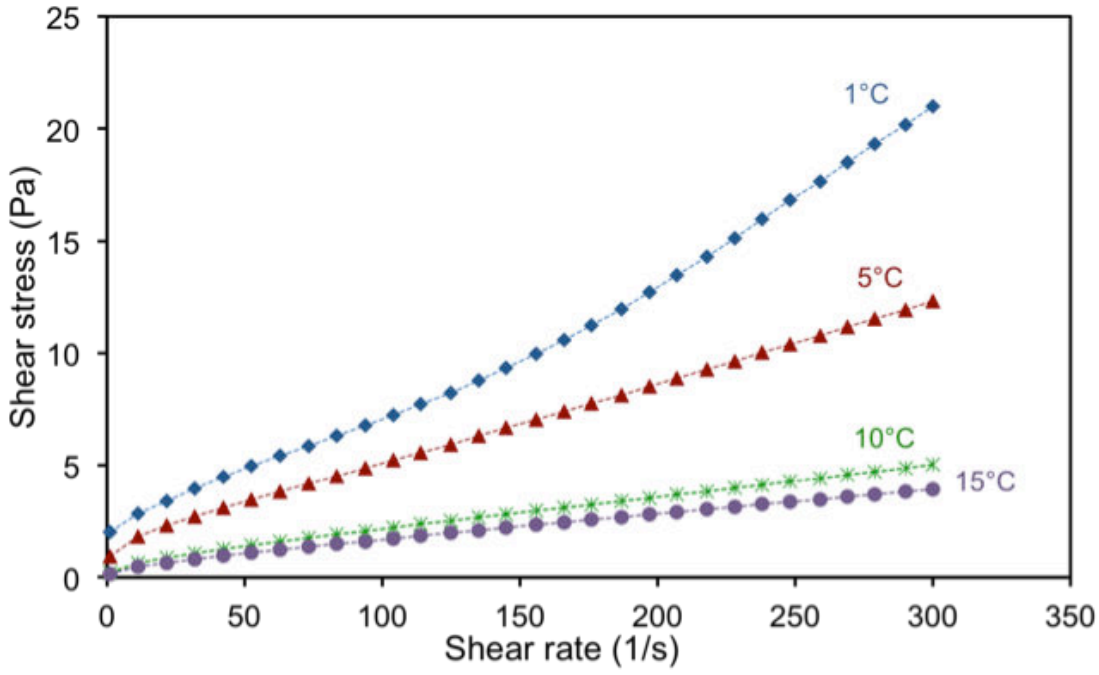

Figure III -27 Shear stress vs. shear rate for different temperatures for the PCME - V3 with 5 wt.% surfactant

The relationship between the shear stress and the shear rate for different temperatures is non-linear with greater visibility for very low temperatures, as same as for the PCME – V3 with 3 wt.% surfactant.

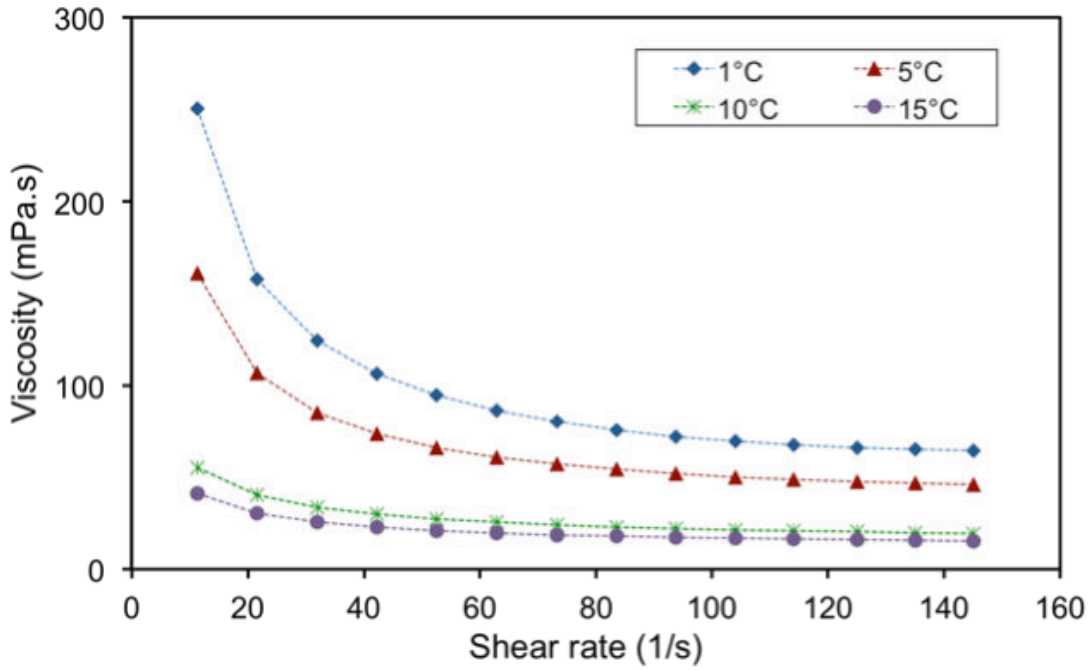

Figure III-28 Viscosity vs. shear rate for different temperatures for the PCME - V3 with 5 wt.% surfactant

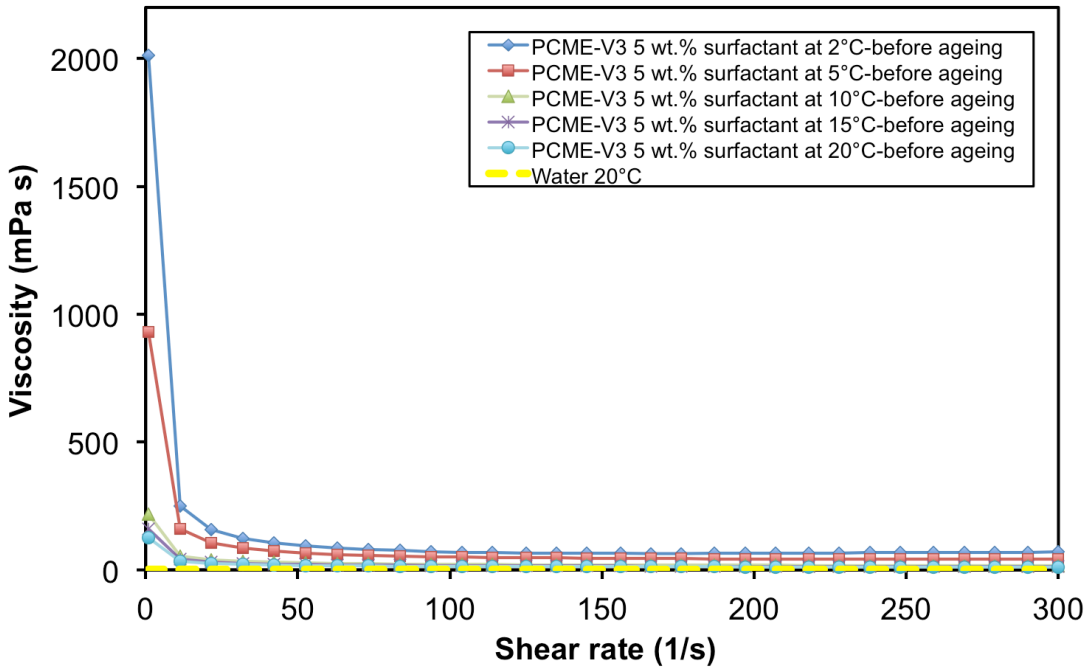

Figure I-29 Evolution of the viscosity for the PCME - V3 with 5 wt.% surfactant for different shear rates at 2°C, 5°C, 10°C, 15°C and 20°C

For temperatures close to or above the phase change temperature of the paraffin (6°C), the relationship between the shear stress and the shear rate is quite linear. Fig. III-28 shows the viscosity against the shear rate: it clearly indicates a strong decrease of the viscosity when increasing the shear rate for the highest tested temperatures. For values of the shear rates beyond 120 s^{-1}, the viscosity tends to level off whatever the temperature.

Fig. III-29 shows the viscosity vs. the shear rate for the PCME – V3 with 5 wt.% surfactant before ageing in the heat transfer experimental setup. Unfortunately, because of the lack of material and time, the PCME – V3 with 5 wt.% surfactant after being tested was not investigated in terms of rheology. Nevertheless, results obtained for the available sample show the influence of the surfactant concentration on the viscosity. Thus, compared to the PCME – V3 with 3 wt.%, the viscosity is greater up to 4 times, due to the addition of surfactant by only 2 wt.%.

Most importantly is that in the range of shear rates from 50 to 100 s^{-1}, which corresponds to a potential industrial application, viscosity does not change appreciably.

Particle size distribution and stability under thermal-mechanical loads

Stability of the emulsion is highly influenced by the droplet size (Fischer and Scheid, 2006; Schuchmann, 2012). As already mentioned in Chapter 1 (Section I.2.4.2 Surfactants), droplet size will suffer modifications by adjusting the amount of surfactant. PCMEs with smaller droplets are in general more stable. The particle size distribution of PCME-V3 was specifically analysed to establish any link with its stability. Fig. III-30 shows the volume density distribution of the droplets for two samples of PCME – V3, the one with 3 wt.% before ageing in the heat transfer experimental setup and the one after ageing in the same experimental setup.

We can observe that after ageing the volume density distribution of the PCME can change. Small differences were observed before ageing and after ageing for the PCME with 3 wt. % surfactant.

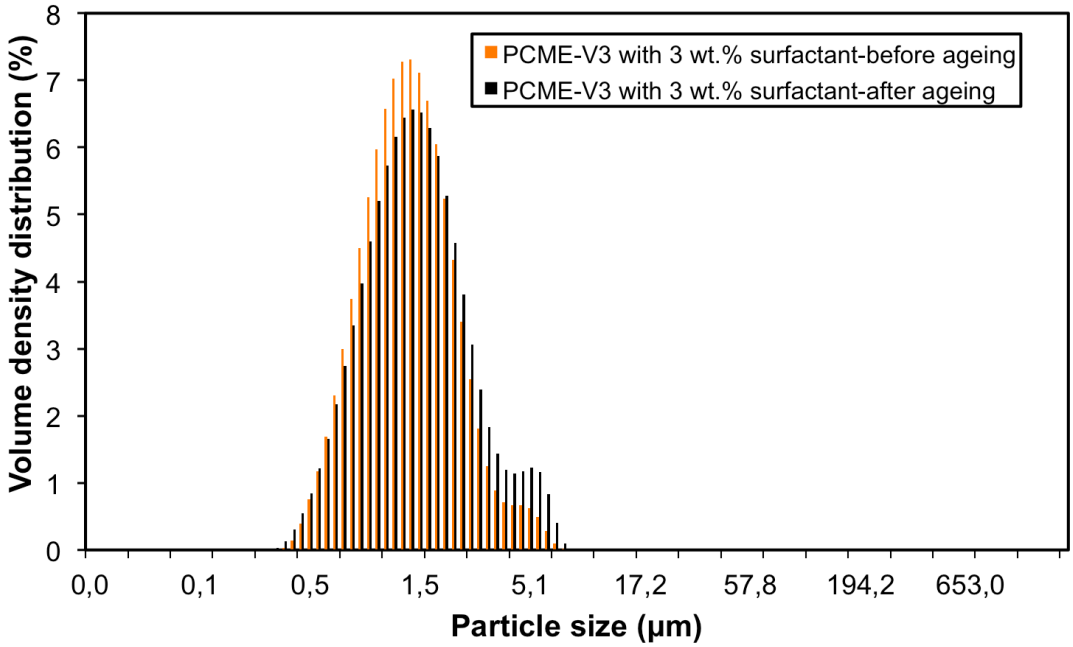

Figure III-30 Volume density distribution as function of the particle size for the PCME – V3 with 3 wt.% surfactant

Fig.III-31 shows the volume density distribution as a function of the particle size for all samples of PCME – V3. All particle size distribution tests were done twice for more accuracy and one can observe on this figure, first results for sample 1 of the PCME – V3 with 3 wt.% surfactant before ageing and second results for sample 2 of the same emulsion.

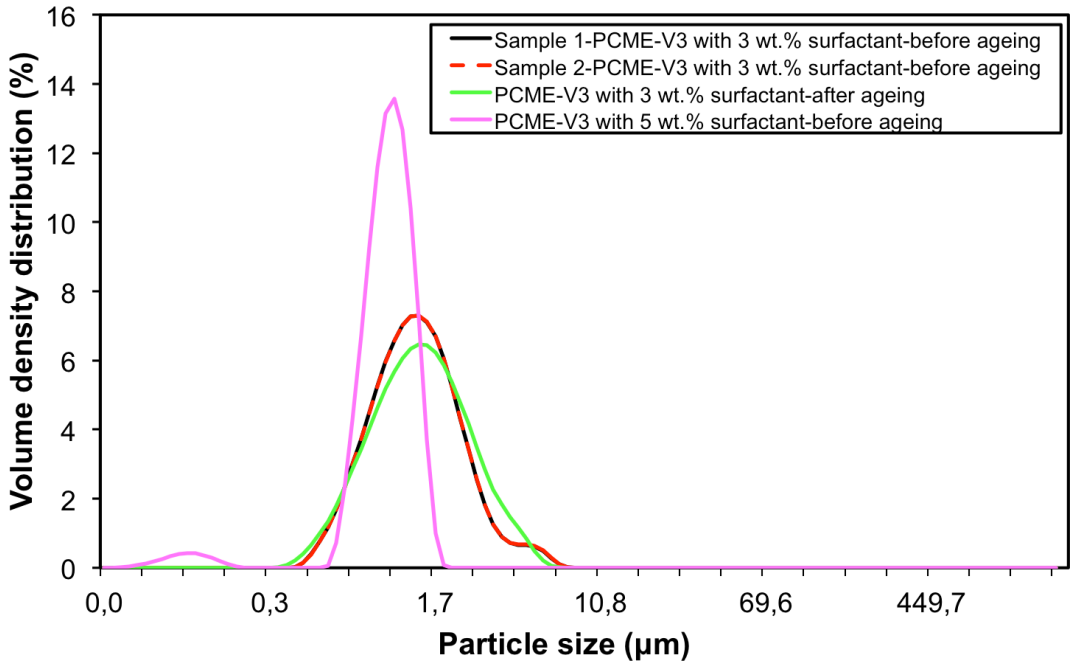

Figure III-31 Volume density distribution as function of the particle size for the PCME - V3

As shown in Fig.III-31, an increase in the surfactant content reduces the mean particle size as well as the maximum droplet size. Comparing the PCME – V3 with 3 wt.% surfactant before and after ageing, one can observe that after ageing the volume density distribution does not present major differences, but the maximum droplet size is slightly reduced after ageing. That means that in time, by continuously being pumped, the paraffin droplets tend to get smaller and therefore maintain or even increase the stability of the emulsion.

The stability under thermal–mechanical loads as already mentioned was examined during the heat transfer tests. The PCME – V3 with 3 wt.% surfactant was circulated continuously, 24 hours a day during 45 days. During that period of time, 60 heating/cooling cycles were imposed to the PCME. A small amelioration, i.e. a decrease in the supercooling degree was observed, which could be attributed to a coalescence phenomenon. Otherwise, the average heat transfer coefficients during cooling were calculated after the testing period and no significant changes were observed. The emulsion remained in dispersion after the testing period. The stability of the emulsion was not affected by the testing.

Depending on its use and application a PCME can have different requirements for stability and therefore a different minimally required mean droplet size.

For practical application, the shelf life of the PCME can also be an important feature. Therefore, to determine the long-term stability of the PCMEs, a centrifuge with possibility to scatter transmission through the probe was applied. A centrifuge (LUMiSizer presented in Chapter 2) capable of accelerating the creaming and sedimentation was used to test the PCMEs. PCMEs samples were exposed to up to 2300 times the gravitational acceleration g. The lifespan at $g = 9.81 ms^{-2}$ was then calculated by multiplying the measuring time with the applied gravitational acceleration within the centrifuge.

Twelve samples of PCME were prepared for the test as seen in Fig.III-32, 4 samples of PCME – V3 with 3 wt.% surfactant before ageing, 4 samples of PCME – V3 with 3 wt.% surfactant after ageing and 4 samples of PCME – V3 with 5 wt.% surfactant before ageing.

During the process, transmission profiles were generated; they are presented in Fig. III-34. These transmission profiles indicate the creaming or sedimentation phenomena over the samples.

An instability-index, that quantifies the shelf life of the PCME, can be then calculated from the obtained data (Detloff *et al.*, 2013). The stability index is calculated depending on the industrial application of the emulsion. Low values of the instability index indicate stability and a long lifespan.

Figure III-32 Samples of PCME - V3 before being tested with the LUMiSizer

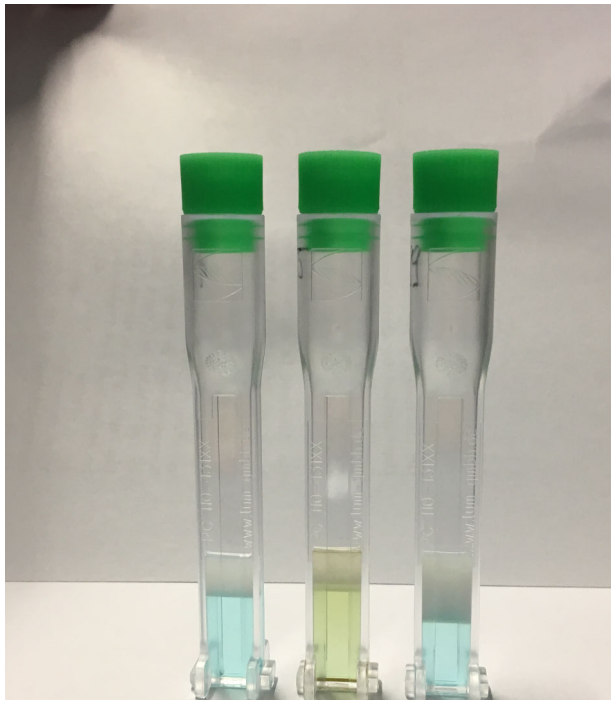

Figure III-33Tested samples with the LUMiSizer of the PCME -V3 with # wt.% surfactant before being tested in the heat transfer setup, the PCME - V3 with 3 wt.% surfactant after being tested in heat transfer setup and the PCME - V3 with 5 wt.% surfactant before being tested in the heat transfer setup

Figure III-34 Transmission profile for the PCME - V3 with 5 wt.% surfactant (a)

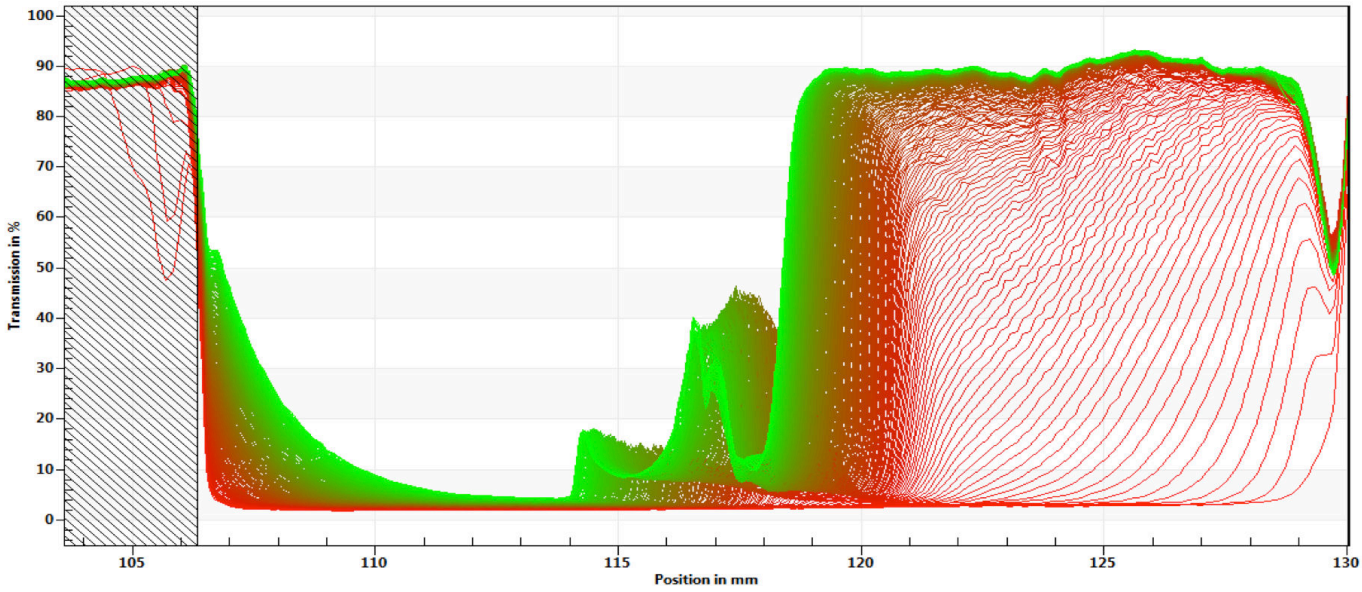

Figure III-35 Transmission profile for the PCME - V3 with 5 wt.% surfactant (b)

III.3.2. Evolution of the local and average heat transfer coefficient during cooling in the cooling channel

Heat transfer analysis carried out on the two versions of PCME - V3 with 3 wt.% surfactant and 5 wt.% surfactant aimed at check by the heat transfer capacity of these emulsions. For this reason, a heat transfer evaluation of the emulsion with 5 wt.% surfactant, a more stable emulsion due to the excess of 2 wt.% of surfactant but more viscous was done. The main purpose of the study was to determine if the PCME with 5 wt.% surfactant could be more advantageous in terms of heat transfer, despite the high viscosity in comparison to the PCME with 3 wt.% surfactant.

Different tests were conducted on the PCME-V3 during cooling into the cooling channel. Local heat transfer coefficients were determined for seven different Reynolds numbers.

On Fig. III - 36, the local heat transfer coefficients during the cooling of the PCME – V3 are represented as a function of the distance from the inlet x and for different values of the Reynolds number.

A strong decrease in the heat transfer coefficient along the entry length of the channel, can be observed on the figure, which is similar to the first results obtained on the previous tested PCMEs, V1 and V2. Interestingly to observe is that it takes more length for the heat transfer coefficient to stabilize at a constant value. This particular evolution was not seen in the first emulsion tested, PCME – V1 but noticed on the second emulsion, PCME – V2. The temperature difference of the emulsion along the channel remains between 0.1 K and 0.3 K.

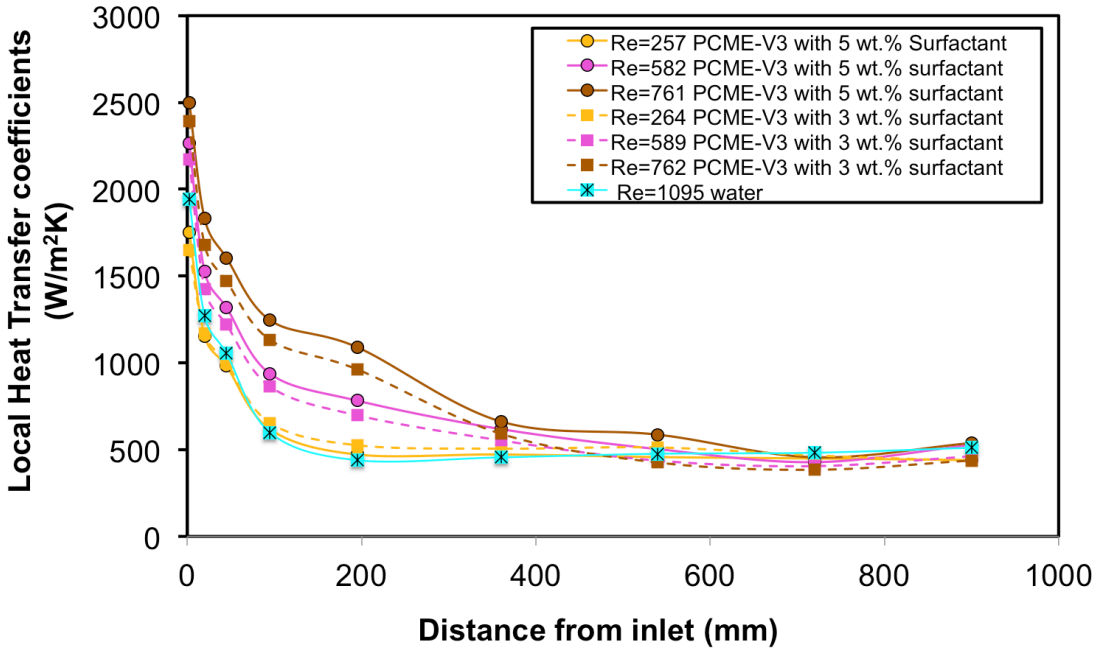

Figure III-36 Evolution of the local heat transfer coefficients during cooling in the cooling channel of the PCME - V3 for different Reynolds numbers

We can observe on the figure that heat transfer coefficients for the PCMEs have higher values in comparison with water tested for a laminar flow.

The local heat transfer coefficients at the entry of the channel are somewhat greater with PCME – V3 with 5 wt.% surfactant than with 3 wt.% surfactant but they tend to stabilize at approximately the same constant value.

The PCME-V3 was the tested using the second device as the two previous versions of PCME. The samples of 18.03 g for the PCME with 3 wt.% surfactant before ageing, 18.99 g for the PCME with 3 wt.% surfactant after ageing, 18.58 g for the PCME with

5 wt.% surfactant before ageing and 18.97 g for the PCME with 5 wt.% were cooled down to -20 °C and kept at this temperature for 10 min to allow stabilisation and then heated up to 39 °C, with a heating rate of 1 K/min.

Fig. III - 15 illustrates the relationship between the specific heat capacities for all 4 types of the PCME - V3 vs. temperature during cooling of the sample performed with the SETARAM calorimeter. Total heat capacity of the PCME – V3 remains two times higher than that of water.

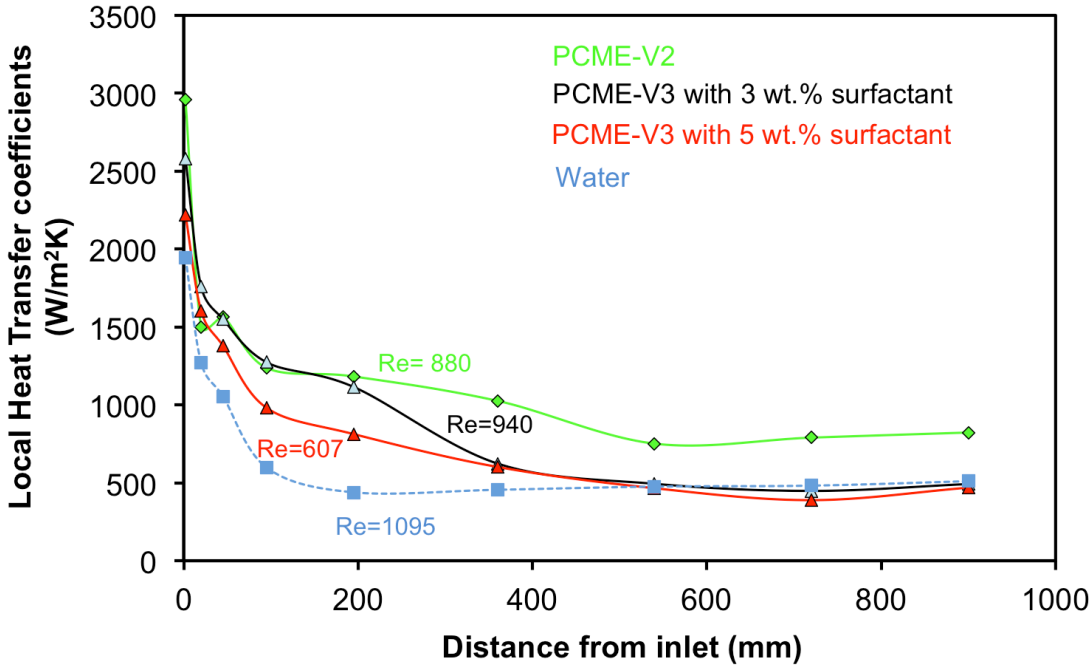

Figure III-37 Evolution of the local heat transfer coefficients during cooling in the cooling channel of the PCMEs for a laminar flow

Fig. III-37 illustrates the evolution of the local heat transfer coefficients of the emulsions during cooling in the cooling channel for a laminar flow. Local heat transfer coefficients for water under the same operating conditions are also presented in the figure.

We can observe, that even though PCME – V3 with 3 wt.% and PCME – V2 have the same formulation and approximately the same thermophysical properties, as already showed in this chapter, the evolution of the heat transfer coefficient is slightly different. Comparing Fig. III-36, Fig. III-37 and Fig. III-11, values for the heat transfer coefficients for the PCME – V2 are higher than for the PCME – V3 with 3 wt.% surfactant, for the same Reynolds number. This decrease in the heat transfer for the PCME – V3 with 3 wt.% may be caused by

the production procedure or by the storage conditions of the PCME – V3 with 3 wt.% surfactant until provided by the manufacturer.

Integration of the local heat transfer coefficients along the entire heat exchanger length leads to the average heat transfer coefficient. The evolution of the average heat transfer coefficient as a function of the Reynolds number, during cooling under laminar flow is displayed on Fig. III - 38.

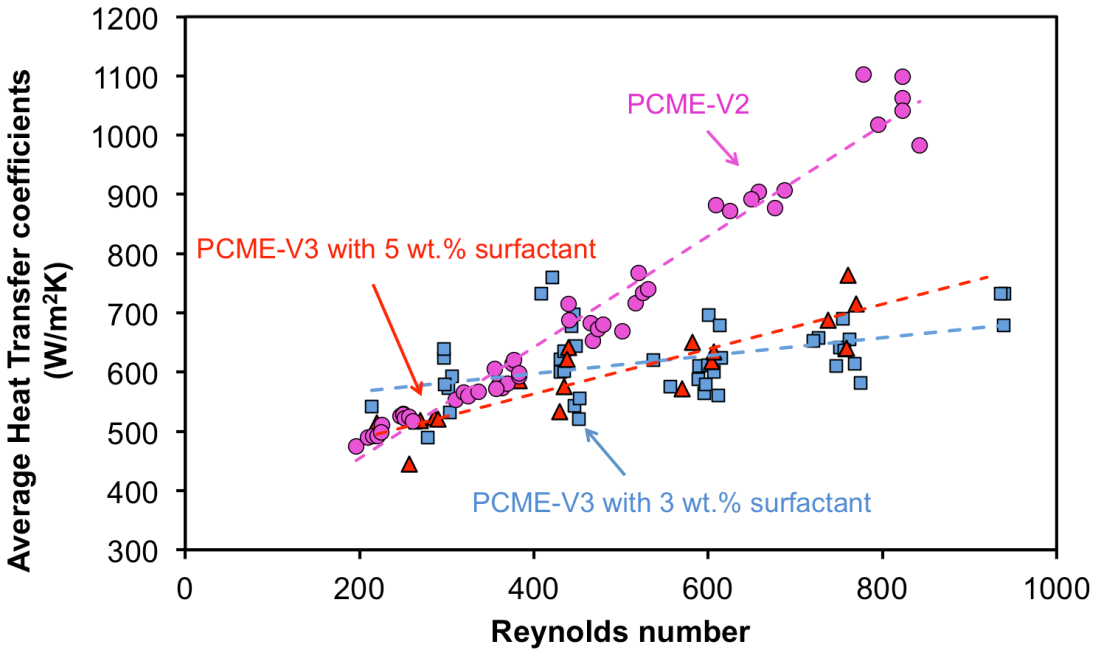

Figure III-38 Values for the average heat transfer coefficient in the studied Reynolds number range

As indicated in Fig. II-38, for the PCME – V3 the average heat transfer coefficients can reach up to 732 $W.m^{-2}$ K^{-1} for the studied range of Reynolds numbers. The heat exchange is improved progressively as the Reynolds number increases, as for the other previous tested paraffin emulsions. Still, for Reynolds numbers greater than 500, PCME –V2 has greater values for the local heat transfer coefficients. Comparing the three evolutions of the local heat transfer coefficients on the figure and following the results obtained in terms of thermophysical properties and rheological behaviour we consider that for the PCME – V3 phase change occurred partially or not at all.

The present chapter reports on an experimental study of the rheological and heat transfer characteristics of a 30 %wt. paraffin emulsion that can be used as a two-phase secondary refrigerant. Three types of paraffin emulsion were tested; PCME-V1, PCME-V2 and PCME-V3. Conclusions on this chapter fall into 3 categories: conclusions on thermophysical properties, heat transfer behavior of the PCME and rheological behavior of the PCME.

- ***Thermophysical properties***

Thermophysical properties were determined and presented for all three versions of the PCME.

The total heat capacity of the emulsion was investigated experimentally and for all tested types of PCME, the total heat capacity is two times higher than that of water. Such a value is very promising for industrial applications.

Thermal conductivity measurements showed an average thermal conductivity of 0.31 W $m^{-1}K^{-1}$ for PCME-V1 at a temperature of 24.2 °C while for the PCME-V2 it was found to be 0.38 W $m^{-1}K^{-1}$ at 29 °C. For the PCME-V3 with 3 wt. % surfactant before ageing the conductivity was found to be 0.38 W $m^{-1}K^{-1}$ at a temperature of 25 °C and for the PCME-V3 with 3 wt. % surfactant after ageing, the conductivity was found to be equal to 0.43 W $m^{-1}K^{-1}$ at the same temperature. The PCME-V3 with 5 wt. % surfactant before ageing showed an average thermal conductivity of 0.32 W $m^{-1}K^{-1}$ at a temperature of 25 °C, while the PCME-V3 with 5 wt.% surfactant after ageing was 0.39 W $m^{-1}K^{-1}$ for the same temperature. The process of ageing thus leads to an increase in the thermal conductivity.

Density was estimated to be 925 kg m^{-3} at 20 °C for the PCME-V1, 969 kg m^{-3} at 25.9 °C for the PCME-V2, 924 kg m^{-3} at 23 °C for the PCME-V3 with 3 wt.% surfactant before ageing and 898 kg m^{-3} at the same temperature for the PCME-V3. As for the density during or after ageing, density of the PCME increased. Results after ageing showed a density of 980 kg m^{-3} at 23 °C for the PCME-V3 with 3 wt.% surfactant and 937 kg m^{-3} at the same temperature for the PCME-V3 with 5 wt.% surfactant.

The evolution of the density all along a process of progressive cooling of the emulsions was investigated. PCME-V1 and PCME-V2 showed a relative strong increase in the density when the phase change occurs. Unlike the PCME-V1 and PCME-V2, PCME-V3 showed no major changes in the density during phase change.

Heat Transfer behavior

A complete characterization of the PCME was performed for a laminar flow inside a rectangular channel typical of plate heat exchangers. The experimental results were used to determine the local Nusselt number and the average Nusselt number integrated over the length of the heat exchanger. For the PCME-V1, a correlation between the local Nusselt number, the Reynolds number, the Prandtl number and the dimensionless axial position was determined.

$$Nu(x) = 0.37\,\mathrm{Re}^{0.427}\mathrm{Pr}^{0.33}\,x^{*-0.238}$$

Furthermore, for the PCME-V1 a second correlation was determined between the average Nusselt number, Reynolds number and the Prandtl number.

$$Nu = 0.2784\,\mathrm{Re}^{0.431}\mathrm{Pr}^{0.33}$$

Experimental results for the PCME-V2 showed a similar behaviour in terms of heat transfer but with slightly improved thermal performance. Therefore, new correlations were proposed for the local Nusselt number and the average Nusselt number.

$$Nu(x) = 0.28\,\mathrm{Re}^{0.427}\mathrm{Pr}^{0.33}\left(\frac{x}{x + D_h}\right)^{-0,59}$$

$$Nu = 0.13\,\mathrm{Re}^{0.56}\mathrm{Pr}^{0,33}$$

For Reynolds numbers higher than 500, the average heat transfer coefficients for the PCME-V3 are higher with 5 wt.% than with 3 wt.% surfactant. For the lowest Reynolds numbers, no clear clue could confirm whether phase change had occurred or not.

Nevertheless, even though phase change might not have occurred the heat transfer coefficients are not dramatically low – they still remain comparable with those observed for 3 wt.% surfactant.

For all three types of PCME, it was found that heat transfer coefficients increased with the Reynolds number. Regarding the relatively short thermal boundary layer establishment, the interest in the global heat transfer coefficient for the heat exchanger sizing rather than the local heat transfer coefficient is confirmed. The correlations proposed to predict the number of Nusselt for this type of flow are adequate and constitute a first tool for the design of heat exchangers that use this type of two-phase secondary refrigerant.

- ***Rheological behavior***

Experimental tests showed that PCME-V1 exhibited a Newtonian behavior. Because the manufacturer has not specified, nor the type or concentration of the surfactant used, this Newtonian behavior cannot be interpreted with respect to formulation or composition.

The second version of the emulsion, PCME-V2 was also tested from a rheological point of view. The results show a Newtonian behaviour such as the first of emulsion, PCME-V1. This version also presented high values for viscosity compared to the viscosity of water for the same temperature values.

The third version of the emulsion was tested much more thoroughly from the point of view of the viscosity. For the PCME-V3, tests showed a shear thinning behavior ($n < 1$) with a flow behavior index (n) ranging from 0.60 to 0.94. The latter parameter increases with the temperature. K decreases when the temperature increases. This trend of evolution of K is in agreement with results of the literature, while to the author's knowledge; no clear evolution of n with the temperature was reported so far. Results clearly indicate a strong decrease of the viscosity when increasing the shear rate for the highest tested temperatures. For values of the shear rates beyond 120 s^{-1}, the viscosity tends to level off whatever the temperature.

But for the third type of emulsion PCME-V3 with 3 wt. % surfactant, the experimental results showed a non-Newtonian behaviour from a rheological standpoint.

A number of other conclusions on this chapter were given by testing the stability of the emulsion and by investigating the particle size distribution for the PCME-V3. A decrease in the supercooling degree was observed for higher Reynolds numbers, which could be attributed to a coalescence phenomenon. In spite of this change in the supercooling degree before phase change is triggered, the average heat transfer coefficients during cooling were not significantly different from those obtained before the ageing tests. Visual observations revealed that the emulsion remained in dispersion after the testing period.

CHAPTER IV

Design guidelines help researchers; engineers, operations and maintenance personnel understand the basic characteristics of these types of fluids (PCMEs) and increase their knowledge in selection and sizing. Heat transfer is the most important and therefore need deep investigations in order to suggest accurate design guidelines.

IV. Theoretical evaluation for the use of PCME

IV.1 Introduction

In the present section a theoretical performance metric is suggested in order to assess the benefits obtainable by using PCMEs. The primary purpose of this chapter is to evaluate the trade-offs between the PCMEs composition, thermophysical characteristics, heat transfer capacity and practical applications. Thus providing design guidelines for their use in the industry. In order to make the process of decision making in the choice of fluid for a given application easier, three critical key parameters are defined and explained together with the most representative non dimensional-numbers. The main objective is to be able to determine the most suitable fluid for a given application.

IV.1.1 Analysis on the three key parameters of a PCME

Previous work as described in Chapter 1 and the present experimental work have reasonably characterized the use of paraffin droplets within a carrier as coolant. These studies show that from an application stand point all resumes to three critical key parameters: the increased heat capacity of the PCME during phase change, the increased viscosity after the phase change and the heat transfer coefficient which is comparable to that of water. Therefore in this section we focused on these three key parameters, presented in Table IV – 1.

Taking into consideration that the average heat transfer coefficients are almost or even comparable with those for water, PCME could easily replace water in industrial applications. Even though it gives birth to higher energy pump consumption by means of high viscosity during and after phase change, special pumps can be used and the loss can be replaced by the winning from the heat transport capacity, given by the product between the mass flow and specific heat capacity, $\dot{m} \times c_p$. For the PCME the heat transport capacity is much more higher in comparison to water due to the increase of the heat capacity during phase change of the droplets.

Table 11Description of key parameters of a PCME

Key parameter	Name	Description
$\dot{m} \times c_p$.	heat transport capacity	heat transport capacity much more higher for PCME due to the increase in the c_p during phase change of the paraffin droplets from liquid to solid
η	viscosity	high viscosity implying an increase in the pumping power
h	average heat transfer coefficient	not very high but comparable to water

IV.2 Most representative non-dimensional numbers

In order to treat the heat transfer performance of the PCME, three non-dimensional numbers are introduced. The Colburn factor (J) is used as a first approach to describe the heat transfer performance of the PCME. Since J is proportional to Nusselt number, whose method of calculation depends upon Reynolds number, J is also dependent upon the Reynolds number. Different surfaces geometries in designing heat exchangers give rise to different J factor trends with the Reynolds numbers. The optimal surface depends upon the Reynolds number of interest, therefore upon the Colburn factor. Even though this analogy is known to be valid for a turbulent flow, the author used just to verify the already shown results on the use of the PCME-V3.

$$J = \frac{Nu_{PCME}}{\mathrm{Re}_{PCME}\,\mathrm{Pr}_{PCME}^{1/3}} \qquad \text{(IV-1)}$$

Furthermore, in order to compare the heat transfer performance of the PCME to that of water a non-dimensional number H is introduced, as presented by Yu *et.al*, 2010. Since water and the tested PCMEs can be reproduce by Eq. III-4 for the laminar flow, the figure of merit can be therefore obtained based on Eq. III-4.

For the laminar flow, the following equation for evaluation of heat transfer enhancement can be generated from Eq. III-4 based on the constant flow velocity basis:

$$H = \frac{h_{PCME}}{h_w} = \left(\frac{\lambda_{PCME}}{\lambda_w}\right)^{0.67} \left(\frac{Cp_{PCME}}{Cp_w}\right)^{0.33} \left(\frac{\rho_{PCME}}{\rho_w}\right)^{0.56} \left(\frac{\eta_{PCME}}{\eta_w}\right)^{0.23} \quad \text{(IV-2)}$$

The non-dimensional number H is a function of the thermophysical properties of the PCME and water. Hence, the heat transfer enhancement of the PCME in comparison with water depends on different parameters as temperature, PCME concentration and the PCME composition. If H > 1, the PCME is beneficial in the process of heat transfer.

The third non-dimensional number N for the rate of net heat exchange between the two fluids of the heat exchanger is adopted in order to compare the ratio of the PCME to that of water. It is defined as it follows:

$$N = \frac{NTU_{PCME}}{NTU_w} = \frac{\dot{m}_w Cp_w}{\dot{m}_{PCME} Cp_{PCME}} \frac{h_{PCME}}{h_w} \quad \text{(IV-3)}$$

Concerning this non-dimensional number N, the interpretation of its value varies and it depends on the deployment of the PCME. If one reports to this non-dimensional number, from the heat transfer point of view, then larger NTU values indicate that the highest limit was reached for heat transfer whereas smaller values of NTU indicate more opportunities for heat transfer. In this case the non-dimensional number N should have values higher than 1, in order for the PCME to be beneficial for the heat exchanger design.

If one refers to N from the heat transport capacity point of view, then the optimal value of N should be around 0.5 in order for the PCME to be advantageous. Under the assumption that the PCME mass flow and water mass flow are identical, with a higher specific heat capacity c_p, identical heat transfer coefficients and the same heat transfer surface, N might be around 0.5 or lower. This result delivers a great advantage. Therefore, N should be below 1 to show an advantage from this point of view.

A third perspective on the non-dimensional number N could be related to the assumption of identical temperature difference of water and PCME. In this case, NTU must be identical, then N is equal to 1 and the required mass flow of PCME can be reduced due to the c_p of the PCME, which is larger than that of water. This will be an advantage as well.

IV.3 Application to the present data

A first approach to describe the heat transfer performance of the PCME is using the Colburn factor (J), defined previously. Result obtained for the PCME-V2, PCME-V3 with 3 wt. % surfactant and PCME-V3 with 5 wt. % surfactant are illustrated in Fig. IV – 1.

One can observe that for the version PCME-V2, the evolution of the Colburn factor is slightly different from its evolution for the PCME-V3. This difference can be given by the composition of the emulsion. From the description of the producer, regarding the PCME composition, between PCME-V2 and PCME-V3, the type of surfactant used gives the difference. For smaller Reynolds number from 200 to 400, PCME-V3 has a better heat transfer performance, while for higher Reynolds number, above 400, PCME-V2 seems more appropriate with an increased heat transfer performance.

The results in terms of H and N, for the studied PCMEs are presented in Fig. IV – 2, Fig. IV – 3 and Fig. IV – 4. One can observe that for all versions of emulsion the variation of the 2 non-dimensional numbers is roughly the same, with small differences, for Reynolds numbers between 200 and 300.

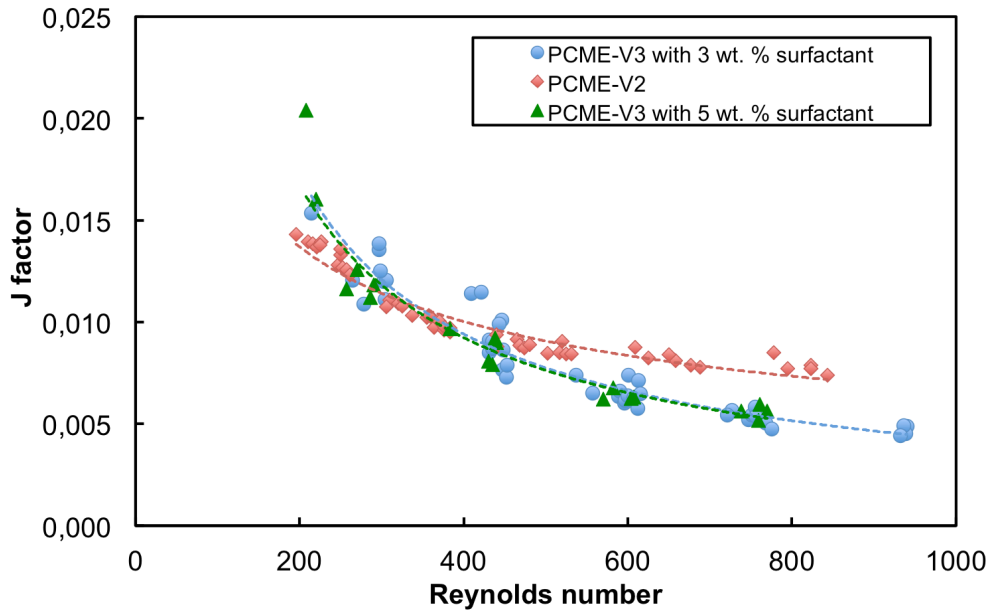

Figure IV-1 Effect of the Reynolds on the J number for PCME-V2, PCME-V3 with 3 wt. % surfactant and PCME-V3 with 5 wt. % surfactant

The results in terms of H, for different Reynolds numbers between 250 and 625 for the PCME-V2, 300 and 747 for the PCME-V3 with 3 wt. % surfactant, 220 and 737 for the PCME-V3 with 5 wt. % surfactant show the same variation and the values obtained are

maintained around 1.01 for PCME-V2, 1.08 for PCME-V3 3 wt. % surfactant and 1.09 for PCME-V3 with 5 wt. % surfactant.

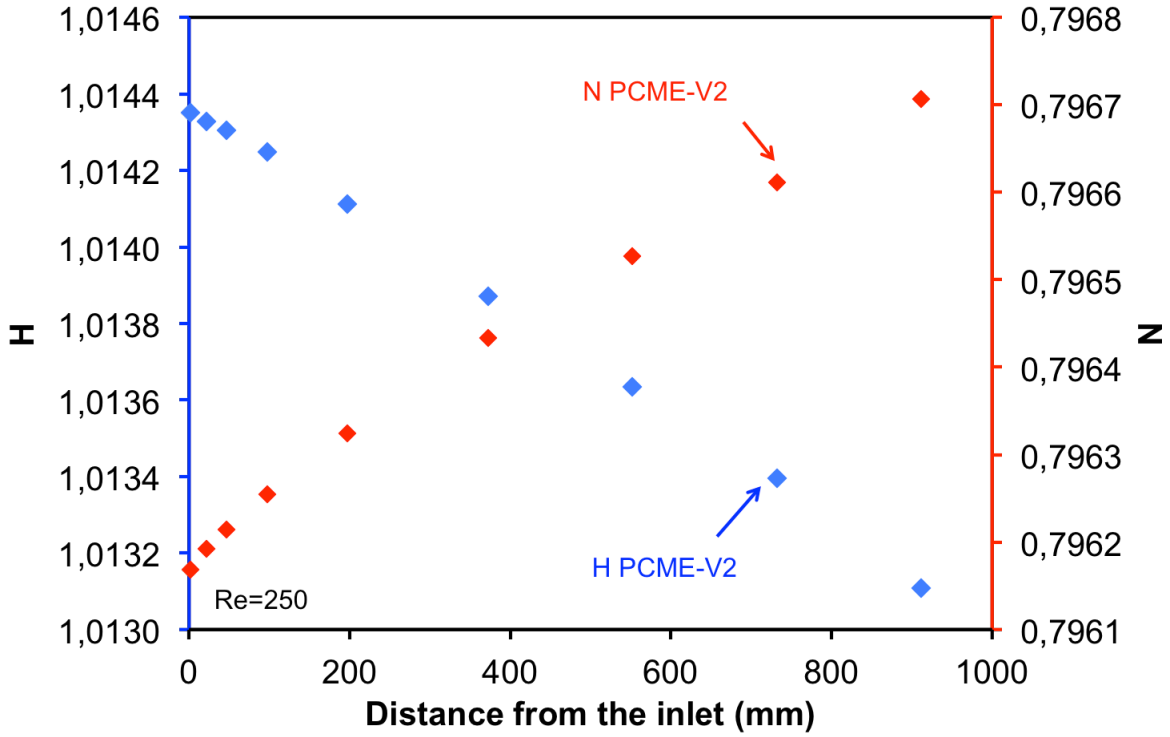

Figure IV-2 H number and N number for the PCME-V2 as a function of the distance from the inlet (Re=250)

This result can be considered expected taking into account the fact that H is based on the thermophysical properties of the emulsion, the differences between the three versions of PCME being given by the type of surfactant used in the composition. This evolution can also be better visualized in Fig. IV – 5. For all three versions of the PCME, the H is higher than 1, which shows beneficial heat transfer performance.

The results for the third non-dimensional number N, for different Reynolds numbers between 250 and 625 for the PCME-V2, 300 and 747 for the PCME-V3 with 3 wt. % surfactant, 220 and 737 for the PCME-V3 with 5 wt. % surfactant show different variations. Values tend to decrease with the increase in the Reynolds number, 0.79 to 0.52 for PCME-V2, 0.53 to 0.34 for PCME-V3 3 wt. % surfactant and 0.91 to 0.31 for PCME-V3 with 5 wt. % surfactant. The entire set of results for N can be observed in Fig. IV- 6.

As previously mentioned, number N gives birth to different possible points of view, depending on the use of the PCME. If we consider the same mass flow for the PCME as for the water, same heat transfer coefficients and same heat transfer surface, with a higher c_p for the PCME, the number N might be 0.5 or even have values lower than 0.5 which clearly

delivers a great advantage in terms of heat transport capacity. Therefore, from this point of view, number N should be inferior to 1, as one can observe furthermore in the figures below.

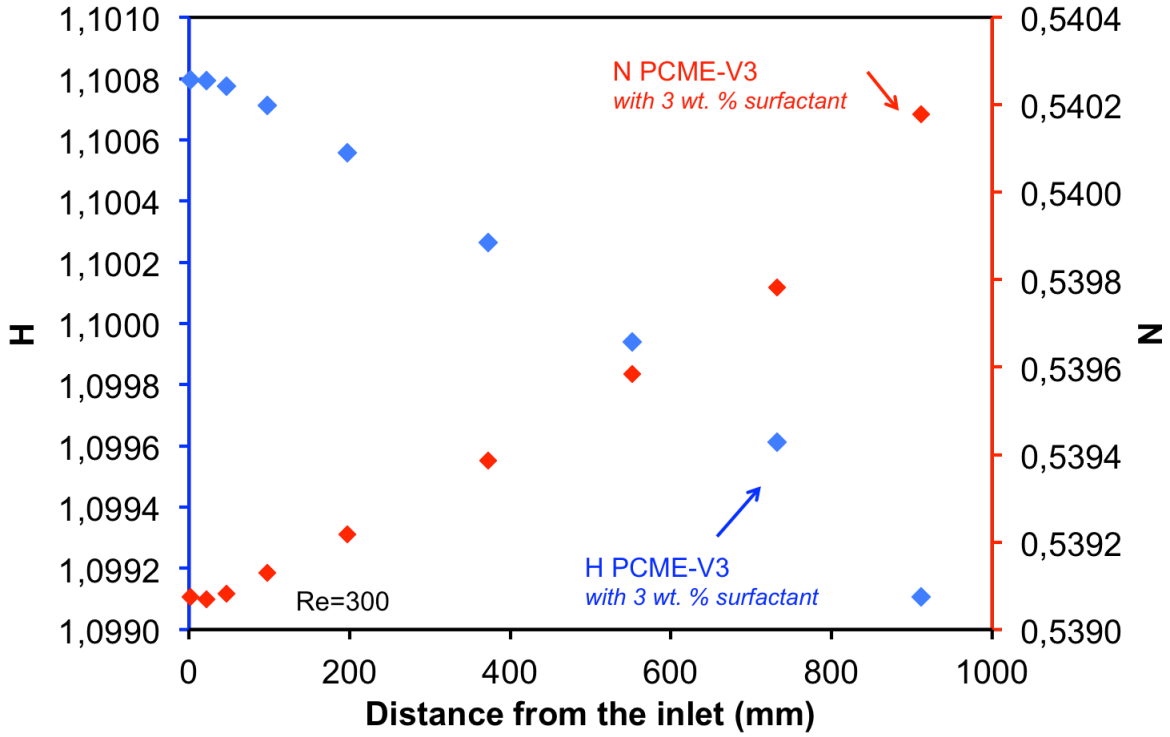

Figure IV-3 H number and N number for the PCME-V3 with 3 wt. % surfactant as a function of the distance from the inlet (Re=300)

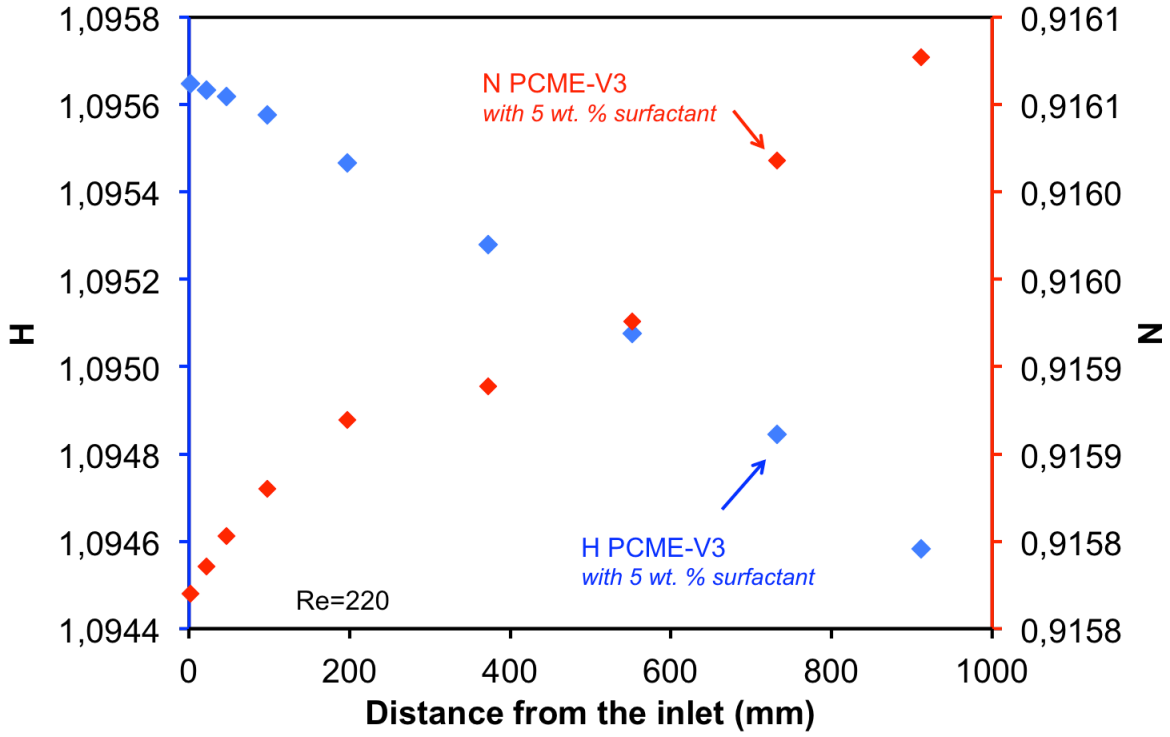

Figure IV-4 H number and N number for the PCME-V3 with 5 wt. % surfactant as a function of the distance from the inlet (Re=220)

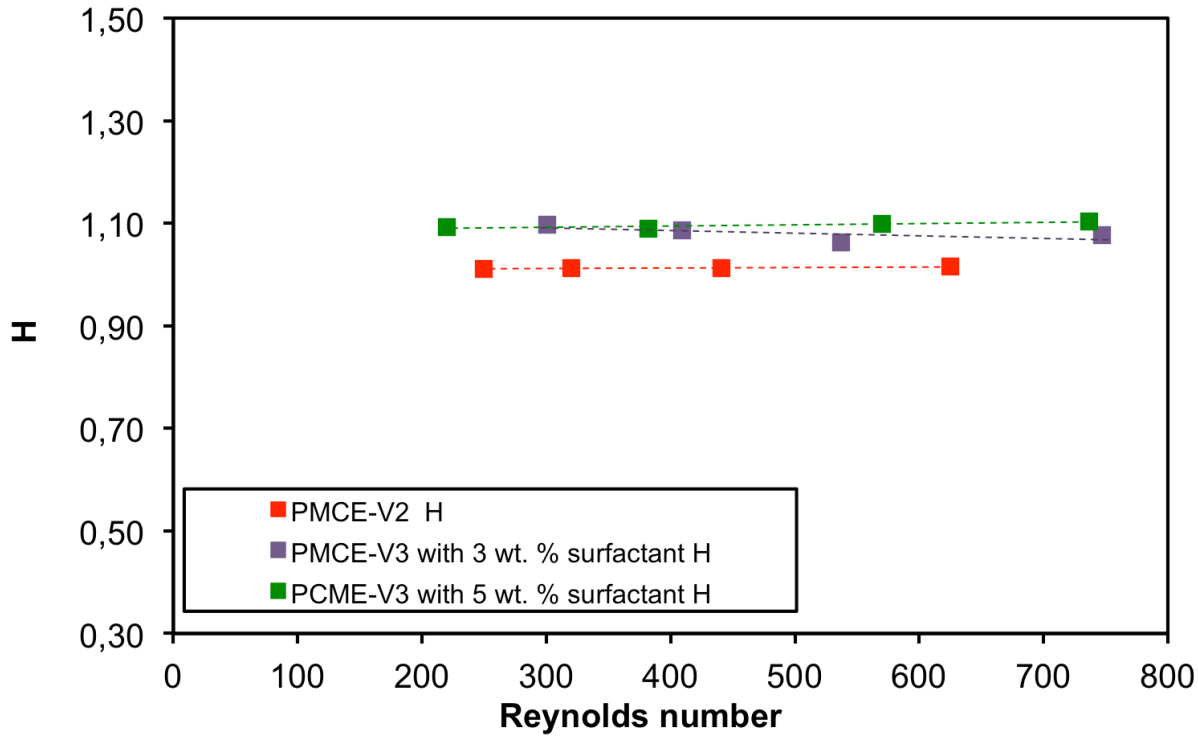

Figure IV-5 H number for PCME-V2, PCME-V3 with 3 wt. % surfactant and PCME-V3 with 5 wt. % surfactant for different Reynolds numbers

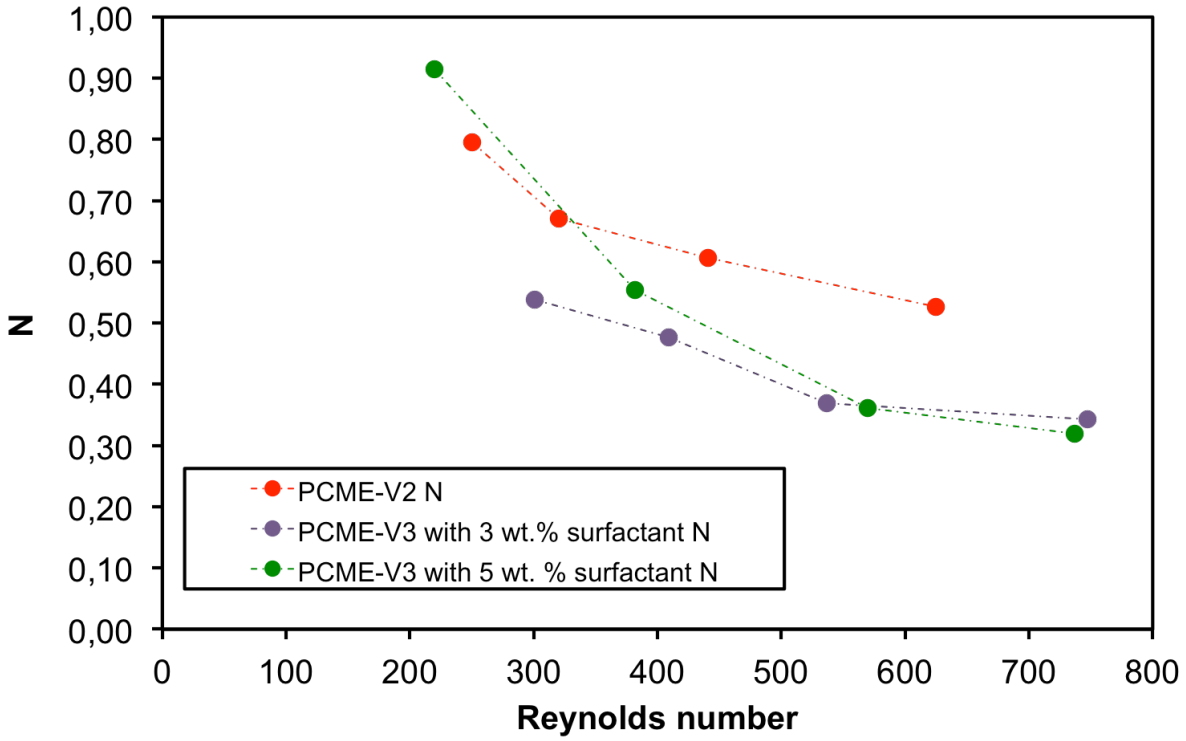

Figure IV-6 N number for PCME-V2, PCME-V3 with 3 wt. % surfactant and PCME-V3 with 5 wt. % surfactant for different Reynolds numbers

If same temperature difference for water as for PCME is considered, the NTU should be the same, therefore the number N equal to 1, and the required mass flow of PCME can be reduced since the c_p of the PCME is 2 times larger than the one of water. This will be of an advantage as well for the PCME. The interpretation of the results show indicate more opportunities in terms of heat transfer since N is smaller than 1 but great heat transport capacity. Furthermore, by analysing Fig. IV-4, one can observe the results on the impact of the concentration in surfactant on the number N. Even though one might consider that the fluid is beneficial in terms of heat transfer, since N is almost equal to 1, the heat transport capacity of the fluid decreases with the increase in the surfactant concentration.

The N should have been calculated for the same values for the mass flow of water as those of the emulsion. Due to the lack of experimental values for water at the same rates, a single Reynolds value was used for water.

As consequence, results can be misleading, the results validated experimentally are the first values for N, at Reynolds numbers, 250 for PCME - V2, 300 for PCME - V3 with 3 wt. % surfactant and 220 for PCME - V3 with 5 wt. % surfactant.

When using a PCME as coolant for industrial applications, three key factors are identified as being necessarily studied. From an application point of view, the increased heat transport capacity of the PCME together with the heat transfer coefficients to those of water are very attractive but the increased viscosity tends to affect this benefit by generation of higher energy pump consumptions. It is advisable to maximize the use of the latent heat capacity of the PCME.

Furthermore, the Colburn factor was investigated for the PCME-V2, PCME-V3 with 3 wt. % surfactant and PCME-V3 with 5 wt. % surfactant. Results show that the Colburn factor is affected by the composition of the PCME, precisely by the type of surfactant used within the composition.

Two non-dimensional numbers are theoretically proposed to evaluate the performance of the PCME for industrial applications. H number represents the ratio for the heat transfer coefficient of the PCME over water. It is used to compare the heat transfer performance of the emulsion in comparison to that of water. N number denotes the ratio of the net heat exchange between the two fluids of the heat exchanger when using PCME to when using water. Results for N number are slightly misleading since for water the same Reynolds number was used. H number presents values above 1, which show the heat transfer enhancement of the PCME over water for laminar flow.

This chapter represents an attempt by the author to approach a more complete characterization of this type of fluid that can be used as a guideline in the design of PCME applications.

Conclusions and Perspectives

The main objective of this thesis comprises a literature review of the state of technology of secondary refrigerants, the methodologies used for determination of their thermophysical and an analysis of the heat transfer behaviour and theological behaviour for the PCME use as heat transfer fluid. These contributions are summarized below.

Contributions

This doctoral thesis was made in the current context, increasingly discussed globally, to keep a balance between energy consumption and environmental protection.
Strong environmental concerns related to ozone depletion potential of CFCs forced the search for alternative solutions for cooling applications. PCMEs have the potential to provide strong benefits both environmentally and economically in secondary refrigerant systems. The main objective of this work is to contribute to a better knowledge of the flows and heat transfers of a PCME, in a channel of a rectangular section simulating a plate heat exchanger.

A literature review regarding refrigeration production was introduced as a necessary background for the experimental results presented in this thesis. Single-phase refrigerants and two-phase secondary refrigerants were presented. Their thermal and rheological behaviour were exposed.
This review focused, on one hand, on the elaboration and fabrication of the PCMEs. On the other hand, this review focused on the analysis of thermophysical properties, which is a key factor in the development of paraffin emulsions.

To better understand the thermal and rheological behaviour of the PCMEs an experimental setup was used for the experimental analysis. The experimental setup with its measurement and acquisition systems, together with other additional measuring instruments presented, the protocol of use and the calculations procedures facilitate:

- the analysis of the PCME during cooling into the cooling channel;
- the determination of the mixed mean temperature of the PCME, the local heat transfer coefficients and the average heat transfer coefficient;

- the determination of the rheological behavior of the PCME before phase change of the paraffin droplets, during phase change and after phase change;
- the determination of the thermophysical properties and viscosity for the PCME;
- the stability of the PCME under thermal mechanical loads.

Three types of paraffin emulsion were tested; PCME-V1, PCME-V2 and PCME-V3. All of them contain 30 % wt. paraffin mass concentration (tetradecane) and different surfactant concentrations.

A set of results on the PCME was then presented that is original and reliable. These results are necessary to get a better understanding of PCMEs and to fully characterize them in order to establish guidelines design for industrial applications.

Conclusions are divided into 3 categories: conclusions on thermodymical properties, heat transfer behavior of the PCME and rheological behavior of the PCME.

- **Thermodynamical properties**

Thermodynamical properties were tested and presented for all three versions of the PCME.Total heat capacity of the emulsion was investigated experimentally and for all tested types of tested PCME is two times higher than that of water which is very promising for industrial applications.

Investigations on the thermal conductivity showed an average thermal conductivity of 0.31 W $m^{-1}K^{-1}$ for PCME-V1 at a temperature of 24.2 °C while for the PCME-V2 it was found to be 0.38 W $m^{-1}K^{-1}$ at 29 °C. For the PCME-V3 with 3 wt. % surfactant before ageing the conductivity was found to be 0.38 W $m^{-1}K^{-1}$ at a temperature of 25 °C and for the PCME-V3 with 3 wt. % surfactant after ageing 0.43 W $m^{-1}K^{-1}$ at the same temperature. The PCME-V3 with 5 wt. % surfactant before ageing showed an average thermal conductivity of 0.32 W $m^{-1}K^{-1}$ at a temperature of 25 °C, while the PCME-V3 with 5 wt.% surfactant after afeing was 0.39 W $m^{-1}K^{-1}$ for the same temperature. Results show that during testing in an experimental setup, the PCME increases its conductivity.

Regarding the density, this one was estimated to be 925 kg m^{-3} at 20 °C for the PCME-V1, 969 kg m^{-3} at 25.9 °C for the PCME-V2, 924 kg m^{-3} at 23 °C for the PCME-V3 with 3 wt.% surfactant before ageing and 898 kg m^{-3} at the same temperature for the PCME-V3. As for the density during or after ageing, density of the PCME increased. After ageing, results

showed a 980 kg m^{-3} at 23 °C for the PCME-V3 with 3 wt.% surfactant and 937 kg m^{-3} for the same temperature for the PCME-V3 with 5 wt.% surfactant. Time dependence of the density was also investigated for the PCME. PCME-V1 and PCME-V2 showed a relative strong increase in the density when the phase change occurs. Unlike the PCME-V1 and PCME-V2, PCME-V3 showed no major changes in the density during phase change.

- **Heat Transfer behavior**

In terms of heat transfer, investigations aimed to perform a complete characterization of the PCME for a laminar flow inside a rectangular channel typical of plate heat exchangers. The experimental results were used to determine the local Nusselt number and the average Nusselt number integrated over the length of the heat exchanger. For the PCME-V1 a correlation between the local Nusselt number, the Reynolds number, the Prandtl number and the dimensionless axial position has been determined.

$$Nu(x) = 0.37\,\mathrm{Re}^{0.427}\mathrm{Pr}^{0.33}\,x^{*-0.238}$$

Furthermore, for the PCME-V1 a second correlation has been determined between the average Nusselt number, Reynolds number and the Prandtl number.

$$Nu = 0.2784\,\mathrm{Re}^{0.431}\mathrm{Pr}^{0.33}$$

Experimental results for the PCME-V2 showed a similar behaviour in terms of heat transfer but with slightly improved performances. Therefore new correlations have been proposed for the local Nusselt number and the average Nusselt number.

$$Nu(x) = 0.28\,\mathrm{Re}^{0.427}\mathrm{Pr}^{0.33}\left(\frac{x}{x+D_h}\right)^{-0,59}$$

$$Nu = 0.13\,\mathrm{Re}^{0.56}\mathrm{Pr}^{0,33}$$

For Reynolds numbers higher than 500, the average heat transfer coefficients for the PCME-V3 are higher with 5 wt.% than with 3 wt.% surfactant. For the lowest Reynolds numbers, showed no clear clue could confirm whether phase change had occurred or not.

Nevertheless, even though phase change might not have occurred the heat transfer coefficients are not dramatically low – they still remain comparable with those observed for 3 wt.% surfactant.

For all three types of PCME it was found that heat transfer coefficients are higher for a higher Reynolds number. Regarding the relatively short thermal boundary layer establishment, the interest in the global heat transfer coefficient for the heat exchanger sizing rather than the local heat transfer coefficient is confirmed. The correlations proposed to predict the number of Nusselt for this type of flow are adequate and constitute a first tool for the design of heat exchangers that use this type of two-phase secondary refrigerant.

- **Rheological behavior**

The rheological behavior of PCME is a controversy one. The purpose of the investigations was to determine the behavior of the three tested versions of PCME and to what extent it is affected by the concentration of surfactant added in their composition. Experimental tests showed that PCME-V1 exhibited a Newtonian behavior. Because the manufacturer has not specified, nor the type or concentration of the surfactant used, this Newtonian behavior cannot be interpreted with respect to formulation or composition.

The second version of the emulsion, PCME-V2 was also tested from a rheological point of view. The results show a Newtonian behavior such as the first of emulsion, PCME-V1 and with high values for viscosity compared to the viscosity of water for the same temperature values.

The third version of the emulsion was tested much more thoroughly from the point of view of the viscosity precisely to try a better understanding of the rheological behavior of these fluids. For the PCME-V3, the entire set of tests shows a shear thinning behavior ($n < 1$) with a flow behavior index (n) ranging from 0.60 to 0.94. The latter parameter increases with the temperature. K decreases when the temperature increases. This trend of evolution of K is in agreement with results of the literature, while to the authors' knowledge; no clear evolution of n with the temperature was reported so far. Results clearly indicate a strong decrease of the viscosity when increasing the shear rate for the highest tested temperatures. For values of the shear rates beyond 120 s^{-1}, the viscosity tends to level off whatever the temperature.

After the experimental tests, we assumed that for the first two types of emulsion PCME-

V1 and PCME-V2, the manufacturer used a concentration less than 4 wt. % in surfactant. But for the third type of emulsion PCME-V3 with 3 wt. % surfactant, the experimental results showed a non-Newtonian behavior from a rheological standpoint. Following discussions with the emulsion producer, he confirmed that for the manufacture of the third type of emulsion PCME-V3, another type of surfactant was used. Fact also confirmed by the results obtained in terms of heat transfer for the PCME-V3.

A number of other conclusions are given by testing the stability of the emulsion and investigation of the particle size distribution for the PCME-V3. A decrease in the supercooling degree was observed for higher Reynolds numbers, which could be attributed to a coalescence phenomenon. In spite of this change in the supercooling degree before phase change is triggered, the average heat transfer coefficients during cooling were not significantly different from those obtained before the ageing tests. Visual observations revealed that the emulsion remained in dispersion after the testing period

When approaching the PCME from a practical point of view, as coolant for industrial applications, three key factors are identified as being necessarily studied. Taking in consideration this point of view, the increased heat transport capacity of the PCME together with the heat transfer coefficients comparable to those of water are very attractive but the increased viscosity tends to affect this benefit by generation of higher energy pump consumptions. It is advisable to maximize the use of the latent heat capacity of the PCME.

Precisely to follow up on future investigations from a practical point of view, it was attempted to establish factors with the purpose to offer some guidelines. The Colburn factor was investigated for the PCME-V2, PCME-V3 with 3 wt. % surfactant and PCME-V3 with 5 wt. % surfactant. Results show that the Colburn factor is affected by the composition of the PCME, precisely by the type of surfactant used within the composition.

Two non-dimensional numbers are then proposed to evaluate the performance of the PCME for industrial applications. H number represents the ratio for the heat transfer coefficient of the PCME over water. It is used to compare the heat transfer performance of the emulsion in comparison to that of water. N number denotes the ratio of the net heat exchange between the two fluids of the heat exchanger when using PCME to when using water. Results for N number give birth to several discussions on its more advantageous values for the

practical use. H number presents values above 1, which show the heat transfer enhancement of the PCME over water for laminar flow.

This work represents an attempt by the author to approach a more complete characterization of this type of fluid that can be used as a guideline in the design of PCME applications.

Perspectives

The correlations proposed to predict the number of Nusselt for this type of flow are adequate and constitute a first tool for the design of heat exchangers that use this type of two-phase secondary refrigerant. A perspective of further work would be to extend the analysis to other paraffin concentrations and turbulent flow in order to approach a practical utilization of these fluids in the cooling field.

It is appropriate, in this case, to know more precisely the quantitative improvement of the heat exchanges (because of the high speeds of the refrigerant fluid, the residence time in the exchangers is minimised) by a better design of these exchangers to ensure the total phase change of the paraffin.

Another future work should be focused on testing PCME with different types of surfactant in the attempt to find a compromise between the degree of subcooling and the viscosity so that the stability of the emulsion is not affected. A study on the thermal storage will be useful in order better understand the behaviour of a PCME in a system of production and use of cold, as well as its stratification in particular. Therefore, study of natural convection in a tank for latent thermal energy storage systems could be considered a future perspective for PCMEs.

Another future perspective could be a case study of practical use of PCMEs on an existing building and comparison with conventional air-conditioning systems.

List of References

Allouche. J. Synthesis of organic and bioorganic nanoparticles: an overview of the preparation methods. In Nanomaterials: A Danger or a Promise? Springer London, p. 27-74, 2013.

Americas. I. The HLB Sytem: A time saving guide to surfactant selection. Chemmmunique, Wilmington, DE, USA, 1987.

Arsenyeva, O., Klemeš, J., Tovazhnyanskyy, L., Kapustenko, P. Compact Heat Exchangers for Energy Transfer Intensification: Low Grade Heat and Fouling Mitigation. 1st ed. CRC Press, 2015.

Awad. T., Hamada. Y., Sato, K. Effects of addition of diacylglycerols on fat crystallization in oil-in-water emulsion. European Journal of Lipid Science and Technology 103, p. 735–741, 2001.

Badolato. G. G., Aguilar. F., Schuchmann. H. P., Sobisch. T., Lerche. D. Evaluation of Long Term Stability of Model Emulsions by Multisample Analytical Centrifugation. in Surface and Interfacial Forces – From Fundamentals to Applications (eds. Auernhammer, G. K., Butt, H.-J. & Vollmer, D.), Springer Berlin Heidelberg, p. 66–73, 2008.

Barber. R. W., Emerson, D. R. A numerical study of low Reynolds number slip flows in the hydrodynamic development region of circular and parallel plate ducts. Deresbury Laboratory Technical Reports, DL-TR-2000-02, Warrington, Angleterre, p. 48, 2000.

Ben Lakhdar. M.A., Guilpart, J., Lallemand, A. Experimental study and calculation method of heat transfer coefficient when using ice slurries as secondary refrigerant. Int. J. of Heat and Technology, Vol. 17, p.49-55, 1999.

Bo. H., Gustafsson, E. M. Setterwall. F. Tetradecane and hexadecane binary mixtures as phase change materials (PCMs) for cool storage in district cooling systems. Energy 24(12), p. 1015-1028, 1999.

Boyd. J., Parkinson. C., Sherman. P. Factors affecting emulsion stability, and the HLB concept. Journal of Colloid and Interface Science 41, p. 359–370, 1972.

Chang. Q. H. H. Z. L. Preparation of high wax emulsion and investigation on affecting factors [J]. Advances in Fine Petrochemicals, p. 4-13, 2007.

Chen. B., Wang. X., Zhang. Y., Xu. H., Yang. R. Experimental research on laminar flow performance of phase change emulsion. Applied Thermal Engineering 26, p. 1238–1245, 2006.

Choi. M., Cho. K. Effect of the aspect ratio of rectangular channels on the heat transfer and hydrodynamics of paraffin slurry flow. International Journal of Heat and Mass Transfer 44, p. 55–61, 2001.

Clarksean. R. Development of a PCM slurry and examination of particle statics. In: Egolf P.W., Sari O., editors. Proceeding of the phase change material and slurry scientific conference & Business Forum, Yverdon-Ies-Bains, Switzerland, p. 173-186, 2003.

Cullum. D. C. Surfactant types; classification, identification, separation. In Introduction to Surfactant Analysis, Springer Netherlands, p. 17-41, 1994a.

Cullum. D. C. Introduction to surfactant analysis. Springer Netherlands, 1994b.

Dai. Y., Sun. Y. Study of viscosity problem of paraffin wax emulsion. Journal Petrochem Univ. 10, p. 48-50, 1997.

Davies. J. T., Rideal. E. K. Interfacial phenomena (2nd ed). Academic Press, New York, 1961.

Degner. B.M., Chung. C., Schlegel. V., Hutkins. R., McClements. D.J. Factors influencing the freeze-thaw stability of emulsion-based foods: freeze-thaw stability of food emulsions? Comprehensive reviews in food science and food safety 13, p. 98–113, 2014.

Delgado. M., Lázaro. A., Mazo. J., Zalba. B. Review on phase change material emulsions and microencapsulated phase change material slurries: Materials, heat transfer studies and applications. Renewable and Sustainable Energy Reviews 16, p. 253–273, 2012.

Delgado. M., Lázaro. A., Mazo. J., Peñalosa. C., Dolado. P., Zalba. B. Experimental analysis of a low cost phase change material emulsion for its use as thermal storage system. Energy Conversion and Management 106, p. 201–212, 2015.

Detloff. **T., Sobisch. T., Lerche. D.** Instability index, T4, p. 1-4, 2013.

El Boujaddaini, M., Mimet, A. and Haberschill, P. 2013. Forced Convective Heat Transfer Study of Paraffin Slurry Flowing in a Vertical Rectangular Channel. International Journal of Fluid Mechanics Research, 40(5), 405-419

Elgafy. A., Lafdi. K. Effect of carbon nanofiber additives on thermal behavior of phase change materials. Carbon 43, p. 3067–3074, 2005.

El Rhafiki. T., Kousksou. T., Jamil. A., Jegadheeswaran. S., Pohekar. S.D., Zeraouli. Y. Crystallization of PCMs inside an emulsion: supercooling phenomenon. Solar Energy Materials and Solar Cells 95, p. 2588–2597, 2011.

Eunsoo. C., Cho. Y. I., Lorsch. H. G. Forced convection heat transfer with phase-change-material slurries: Turbulent flow in a circular tube. International Journal of Heat and Mass Transfer 37, p. 207–215, 1994.

Ionescu, C., Haberschill, P., Kiss, I., Lallemand, A. Local and global heat transfer coefficients of a stabilised ice slurry in laminar and transitional flows. International Journal of Refrigeration 30, 970–977, 2008.

Fernandez. P., André. V., Rieger. J., Kühnle. A. Nano-emulsion formation by emulsion phase inversion. Colloids and Surfaces A: Physicochemical and Engineering Aspects 251, p. 53–58, 2004.

Fischer. L., Scheid. S. Mischen und homogenisieren - technologien und strategien für ein sicheres Scale-up. SÖFW-Journal 132, p. 74–83, 2006

Fischer. L.J., Von Arx. S., Wechsler. U., Zst. S., Worlitschek. J. Phase change dispersion properties, modelling apparent heat capacity. International Journal of Refrigeration 74, p. 240–253, 2017.

Fleischer. A.S., Chintakrinda. K., Weinstein. R., Bessel. C.A. Transient thermal management using phase change materials with embedded graphite nanofibers for systems with high power requirements. IEEE, p. 561–566, 2008.

Fournaison. L., Guilpart. J. Frigoporteurs monophasiques ou diphasiques ? Revue Générale du froid, Vol. 1001, p. 21-24, 2000.

Fournaison. L., Delahaye. A., Chatti. I., Petitet. J.-P. CO 2 Hydrates in refrigeration processes. Industrial & Engineering Chemistry Research 43, p. 6521–6526, 2004.

Fumoto. K., Kawaji. M., Schalbart. P., Kawanami. T. Long term stability of phase change nano-emulsions. Proceedings of 8th IIR conference of phase change materials and slurries for refrigeration and air conditioning Karlsruhe, Germany, p. 248-255, 2009.

Golemanov. K., Tcholakova. S., Denkov. N. D., CGurkov. T. Selection of surfactants for stable paraffin-in-water dispersions, undergoing solid-liquid transition of the dispersed particles.Langmuir 22, p. 3560-3569, 2006.

Günther. E., Schmid. T., Mehling. H., Hiebler. S., Huang. L. Subcooling in hexadecane emulsions. International Journal of Refrigeration 33, p. 1605–1611, 2010.

Günther. E., Huang. L., Mehling. H., Dötsch. C. Subcooling in PCM emulsions – Part 2: Interpretation in terms of nucleation theory. Thermochimica Acta 522, p. 199–204, 2011.

He. B., Martin. V., Setterwall. F. Phase transition temperature ranges and storage density of paraffin wax phase change materials. Energy 29, p. 1785–1804, 2004.

Ho. C.J., Gao. J. Y. Preparation and thermophysical properties of nanoparticle-in-paraffin emulsion as phase change material. International Communications in Heat and Mass Transfer 36, p. 467–470, 2009.

Hu. X., Zhang. Y. Novel insight and numerical analysis of convective heat transfer enhancement with microencapsulated phase change material slurries: laminar flow in a circular tube with constant heat flux. Int. J. of Heat and Mass Transfer, Vol. 45, p. 3163-3172, 2002.

Huang. L., Petermann. M., Doetsch. C. Evaluation of paraffin/water emulsion as a phase change slurry for cooling applications. Energy 34, p. 1145–1155, 2009.

Huang. L., Doetsch. C., Pollerberg. C. Low temperature paraffin phase change emulsions, International Journal of Refrigeration, Volume 33, Issue 8, p. 1583-1589, 2010a.

Huang. L., Günther. E., Doetsch. C., Mehling. H. Subcooling in PCM emulsions—Part 1: Experimental, Thermochimica Acta, Volume 509, Issues 1–2,p. 93-99, 2010b.

Huang. L., Noeres. P., Petermann. M., Doetsch. C. Experimental study on heat capacity of paraffin/water phase change emulsion. Energy Conversion and Management 51, p. 1264–1269, 2010c.

Huang. L., Petermann. M. An experimental study on rheological behaviours of paraffin/water phase change emulsion. International Journal of Heat and Mass Transfer 83, p. 479–486, 2015.

Huetz. J., Petit. J.P. Notions de transfert thermique par convection. Techniques de l'Ingénieur, Vol. A 1 540, p. 1-47, 1990.

Inaba. H., Morita. S., Nozu. S. Fundamental study of cold heat-storage system of o/w-type emulsion having cold latent-heat-dispersion material. Part 1. Heat Transfer Japanese Research, Volume 23, Issue 3, p. 292-312, 1994

Inaba. H., Morita. S. Flow and cold heat-storage characteristics of phase-change emulsion in a coiled double-tube heat exchanger. Trans. ASME. 117, p. 440–446, 1995.

Inaba. H. New challenge in advanced thermal energy transportation using functionally thermal fluids. International Journal of Thermal Sciences 39, p. 991–1003, 2000.

Kappels. T., Hanu. L., Pollerberg. Rheological investigations of paraffin based phase change slurry using a pipe viscometer. 11th IIR Conference on Phase Change Materials and Slurries for Refrigeration and Air Conditioning, Karlsruhe, Germany. Refrigeration Science and Technology, p. 51-60, 2016.

Kawanami. T., Togashi. K., Fumoto. K., Hirano. S., Zhang. P., Shirai. K., Hirasawa. S. Thermophysical properties and thermal characteristics of phase change emulsion for thermal energy storage media. Energy 117, Part 2, p. 562–568, 2016.

Krugliakov. P. M. Hydrophile-lipophile balance of surfactants and solid particles: physicochemical aspects and applications. In Studies in Interface Science (Elsevier Science B.V), p. 146-266, 2000.

Kumaresan. V., Velraj. R., Das. S. K. The effect of carbon nanotubes in enhancing the thermal transport properties of PCM during solidification. Heat and Mass Transfer 48, p. 1345–1355, 2012.

Li. W., Kin, G., Ma. Y., Dai. L. Conditions for mini-emulsion formation. Oilfield Chem.9, p. 352-356, 1992.

Liu. Y. X., Zhao. C. S., Han. L. Factors affecting the emulsification of paraffin. Paper Chemicals, 4, p. 30-32, 2004.

Lu. W., Tassou. S. A. Experimental study of the thermal characteristics of phase change slurries for active cooling. Applied Energy. Volume 81, Issue 1, p. 366-374, 2012.

McClements, D.J., Dungan, S.R., German, J.B., Simoneau, C., Kinsella, J.E. Droplet Size and Emulsifier Type Affect Crystallization and Melting of Hydrocarbon-in-Water Emulsions. Journal of Food Science 58, p. 1148–1151, 1993.

McClements. D. J. Edible nanoemulsions: fabrication, properties, and functional performance. Soft Matter 7, p. 2297–2316, 2011.

Mehling, H., Cabeza, L. F. Heat and cold storage with PCM: an up to date introduction into basics and applications, Springer, 2008.

Mellari. S., Boumaza. M., Egolf. P. W. Physical modelling, numerical simulations and experimental investigations of Non-Newtonian ice slurry flows. International Journal of Refrigeration 35, p. 1284–1291, 2012.

Mollet. H., Grubenmann. A. (Eds.), Food Formulations, in: Formulation Technology. Wiley-VCH Verlag GmbH, Weinheim, Germany, p. 375–388, 2001.

Morimoto. T., Togashi. K., Kumano. H., Hong. H. Thermophysical properties of phase change emulsions prepared by D-phase emulsification. Energy Conversion and Management 122, p. 215–222, 2016.

Murshed. S. M. S., Leong. K. C., Yang. C. Investigations of thermal conductivity and viscosity of nanofluids. International Journal of Thermal Sciences 47, p. 560–568, 2008.

Myers. D. Surfactant science and technology. (Ed. New Jersey), John Wiley&Sons, Inc.2006 Print, 2006.

Niedermaier. S., Biedenbach. M., Gschwander. S. Characterisation and Enhancement of Phase Change Slurries. Energy Procedia 99, p. 64–71, 2016.

Rosen. M.J. Surfactants and interfacial phenomena. John Wiley & Sons, Inc., Hoboken, NJ, USA, 2004.

Roy. S. K., Avanic. B. L. Laminar forced convection heat transfer with phase change material emulsions. International Communications in Heat and Mass Transfer 24, p. 653–662, 1997.

Salager. J.-L. Surfactants: types and uses. Laboratory of formulation, interfaces, rheology, and processes. Merida, Venezuela: Universidad de los Andes, 2002.

Schalbart. P., Kawaji. M., Fumoto. K. Formation of tetradecane nanoemulsion by low-energy emulsification methods. International Journal of Refrigeration 33, p. 1612–1624, 2010.

Schuchmann. H. P. Emulgiertechnik: Grundlagen, Verfahren und Anwendungen, 3. Auflage. ed. Behr's Verlag DE, Hamburg, 2012.

Schramm. L. L. Emulsions, Foams, and Suspensions: Fundamentals and Applications. Wiley-VCH Verlag GmbH & Co. KGaA, Weinheim, FRG, 2005.

Schroder. J and Gawron. K. Latent heat storage. Energy Research, Vol. 5, p. 103-109, 1981.

Shao. J., Darkwa. J., Kokogiannakis. G. Review of phase change emulsions (PCMEs) and their applications in HVAC systems. Energy and Buildings 94, p. 200–217, 2015.

Shinoda. K., Saito. H. The stability of O/W type emulsions as functions of temperature and the HLB of emulsifiers: the emulsification by PIT-method. Journal of Colloid and Interface Science, 30, p. 258-263, 1969.

Sharma. S. D., Kitano. H., Sagara. K. Phase change materials for low temperature solar thermal applications. Res. Rep. Fac. Eng. Mie Univ, 29, 2004.

Sharma. A., Tyagi. V. V., Chen. C. R., Buddhi. D. Review on thermal energy storage with phase change materials and applications. Renewable and Sustainable Energy Reviews 13, p. 318–345, 2009.

Sohn. C.W., Chen. M. M. Microconvective thermal conductivity in disperse two-phase mixtures as observed in a low velocity couette flow experiment. Journal of Heat Transfer 103, p. 47, 1981.

Stamatiou, E., Kawaji, M. Thermal and flow behaviour of ice slurries in a vertical rectangular channel-part II. Forced convective melting heat transfer. Int. J. of Heat and Mass Transfer, Vol.48, p. 3544-3559, 2005.

Tadros. T. F. Application of rheology assessment and prediction of the long-term physical stability of emulsions. Adv. Colloid Interface 108, p. 227-258, 2004.

Tadros. T. F. Applied surfactants: principles and applications. John Wiley & Sons, 2006.

Tadros. T. F. Emulsion formation, stability, and rheology. In Emulsion Formation and Stability (Ed. Tadros, T. F.), Wiley-VCH Verlag GmbH & Co. KGaA,p. 1–75, 2013.

Tauer. K. Emulsions-Part 1. MPI Colloids and Interfaces, Am Mühlenberg, D-14476 Golm, Germany, 2006.

Taylor. P. Ostwald ripening in emulsions, Adv. Colloid Interface Sci.75, p. 107-163, 1989.

Ure. Z. Slurry ice based cooling systems. Science et technique du froid, p. 172-179, 2000.

Vasile, V., Necula, H., Badea, A., Revellin, R., Bonjour, J., Haberschill, P. Experimental analysis on rheological and heat transfer characteristics of paraffin/water emulsion. 11th IIR Conference on Phase Change Materials and Slurries for Refrigeration and Air Conditioning, May 2016, Karlsruhe, Germany. Refrigeration Science and Technology, 32-40, 2016.

Vasile, V., Necula, H., Badea, A., Revellin, R., Bonjour, J., Haberschill, P. New technology in comfort cooling applications: Experimental study on paraffin in water emulsion., CIEM 2017, 157–161, 2017.

Vasile, V., Necula, H., Badea, A., Revellin, R., Bonjour, J., Haberschill, P. Experimental study of the heat transfer characteristics of a paraffin-in-water emulsion used as a secondary refrigerant. International Journal of Refrigeration, 88, 1–7, 2018.

Vasile, V., Necula, H., Badea, A., Revellin, R., Bonjour, J., Haberschill, P. Investigation of heat transfer and rheology of a phase change material emulsion with a high concentration in surfactant. 12th IIR Conference on Phase Change Materials and Slurries for Refrigeration and Air Conditioning, May 2018, Canada. Refrigeration Science and Technology, 190-197, 2018.

Vilasau. J., Solans. C., Gómez. M. J., Dabrio. J., Mújika-Garai. R., Esquena. J. Stability of oil-in-water paraffin emulsions prepared in a mixed ionic/nonionic surfactant system. Colloids and Surfaces A: Physicochemical and Engineering Aspects 389, p. 222–229, 2011.

Wang. B., Zhang. Y., Sun. D. Preparation and application of wax emulsion. Shandong Chem. Ind. 33, p. 14-17, 2004.

Xu. H., Yang. R., Zhang. Y. P., Lin. J., Wang. X. Thermal physical properties and key influence factors of phase change emulsion. Chinese Science Bulletin, Volume 50, Issue 1, p. 88-93, 2005.

Yu, W., France, D.M., Timofeeva E.V., Singh, D., Routbort J.L. Thermophysical property-related comparison criteria for nanofluids heat transfer enhancement in turbulent flow. Appl. Phys. Lett., 96, pp. 1-3, 2010.

Yu, W., Xie, H. A. Review on nanofluids: preparation, stability mechanisms and applications. Journal of Nanomaterials, p. 1–17, 2012.

Youssef. Z., Delahaye. A., Huang. L., Trinquet. F., Fournaison. L., Pollerberg. C., Doetsch. C. State of the art on phase change material slurries. Energy Conversion and Management 65, p. 120–132, 2013.

Zhao. Z. N., Wu. T., Shi. Y. Q., Li. L. X. An investigation on rheology and heat transfer characteristics for a phase change emulsion. Journal of Engineering Thermophysics 22, p. 589, 2001.

Zhao. Z., Shi. Y., Zhang. Y. Flow and heat transfer characteristics of phase change emulsion in a coiled double-tube heat exchanger. Journal of Engineering Thermophysics 23, p. 730, 2002.

Zhang. X., Fan. Y., Tao. X., Yick. K. Crystallization and prevention of supercooling of microencapsulated n-alkanes. Journal of Colloid and Interface Science 281, p. 299–306, 2005.

Zhang. P., Ma. Z. W. An overview of fundamental studies and applications of phase change material slurries to secondary loop refrigeration and air conditioning systems. Renewable and Sustainable Energy Reviews 16, p. 5021–5058, 2012.

Zhang. X., Niu. J., Zhang. S., Wu. J.-Y. PCM in water emulsions: supercooling reduction effects of nano-additives, viscosity effects of surfactants and stability: PCM in water emulsions: supercooling, viscosity and stability. Advanced Engineering Materials 17, p. 181–188, 2015.

Zhang. X., Wu. J., Niu. J. PCM-in-water emulsion for solar thermal applications: The effects of emulsifiers and emulsification conditions on thermal performance, stability and rheology characteristics. Solar Energy Materials and Solar Cells 147, p. 211–224, 2016.

Zou. D., Feng. Z., Xiao. R., Qin. K., Zhang. J., Song. W., Tu. Q. Preparation and flow characteristic of a novel phase change fluid for latent heat transfer. Solar Energy Materials and Solar Cells 94, p. 2292–2297, 2010.

Zou. D., Xiao. R., Feng. Z. Progress on paraffin emulsion in field of latent heat transportation, New Chem. Mater. 40, p. 39-41, 2012.

FOLIO ADMINISTRATIF

THESE DE L'UNIVERSITE DE LYON OPEREE AU SEIN DE L'INSA LYON

NOM : VASILE
(avec précision du nom de jeune fille, le cas échéant)

DATE de SOUTENANCE : 26 juillet 2019

Prénoms : Virginia

TITRE : Experimental study of the thermal and rheological behaviour of paraffin-in-water emulsions used as a secondary refrigerants

NATURE : Doctorat

Numéro d'ordre : 2019LYSEI056

Ecole doctorale : MEGA (Mécanique, Énergétique, Génie Civil, Acoustique)

Spécialité : Thermique et énergétique

RÉSUME :
Une émulsion à changement de phase (PCME: phase-change matériel émulsion) est un fluide consistant en une émulsion d'un matériau à changement de phase (PCM, phase change matériel), comme de la paraffine, dispersé dans un fluide porteur (phase continue), souvent de l'eau ou une solution aqueuse de surfactant. Les PCME peuvent être envisagés comme fluides à haute performance thermique (frigoporteurs ou caloporteurs) en raison de leur potentiel de transport de chaleur latente (cristallisation ou fusion du PCM).
Cette thèse présente des résultats expérimentaux concernant le comportement thermo-rheologique des différentes versions de PCME (émulsions de paraffine dans différentes solutions aqueuses de surfactant, avec une concentration massique en paraffine égale à 30 %) sur une plage de température de 0 - 20 °C. Les propriétés thermophysiques des émulsions ont été déterminées. Ensuite, une étude expérimentale du transfert de chaleur par convection forcée laminaire a été effectuée. Le coefficient de transfert de chaleur convectif de l'émulsion pendant le refroidissement a été déterminé dans une configuration expérimentale proche de celle pouvant être rencontrée dans des échangeurs thermiques à plaques. La configuration se compose principalement de deux canaux rectangulaires (80 x 6 mm²) de longueurs égale à 1 m. Des corrélations utiles pour évaluer les coefficients d'échange thermique (locaux ou globaux) ont été établies entre les nombres de Nusselt, de Reynolds et de Prandtl. Un banc d'essais spécifique a également été utilisé pour analyser le comportement rhéologique des PCME. Des essais ont été effectués à l'aide d'un viscosimètre à différentes températures. La stabilité des émulsions a été examinée sous diverses charges thermomécaniques. Les expériences ont révélé un comportement rheofluidisant.
L'ensemble de ces résultats montre que les PCME sont des candidats prometteurs pour les applications à la climatisation.

MOTS-CLÉS : Émulsion de paraffine ; Écoulement laminaire; Transfert de chaleur ; Rhéologie ; Corrélation ; Propriétés thermophysiques

Laboratoire (s) de recherche : CETHIL

Directeur de thèse: Jocelyn BONJOUR

Président de jury : George DARIE

Composition du jury : Adrian Badea, Jocelyn Bonjour, Rémi Revellin, Monica Siroux, Ludger Josef Fischer, Rodica Frunzulica, Daniela Popescu, George Darie.